Effect of Side Chains on Organic Donor (D) and Acceptor (A) Complexes and Photophysical Properties of D-A Dyads

EFFECT OF SIDE CHAINS ON ORGANIC DONOR (D) AND ACCEPTOR (A) COMPLEXES AND PHOTOPHYSICAL PROPERTIES OF D-A DYADS

A Dissertation Presented

by

AMARNATH BHEEMARAJU

Submitted to the Graduate School of the
University of Massachusetts Amherst in partial fulfillment
of the requirements for the degree of

DOCTOR OF PHILOSOPHY

September 2011

Chemistry

EFFECT OF SIDE CHAINS ON ORGANIC DONOR (D) AND ACCEPTOR (A) COMPLEXES AND PHOTOPHYSICAL PROPERTIES OF D-A DYADS

A Dissertation Presented

by

AMARNATH BHEEMARAJU

Approved as to style and content by:

_____
D. Venkataraman, Chair

_____
Paul M. Lahti, Member

_____
Ricardo B. Metz, Member

_____
Ryan C. Hayward, Member

_____
Craig T. Martin, Department Head
Chemistry

DEDICATION

For my family

ACKNOWLEDGMENTS

First, I would like to thank my research advisor DV for his guidance. He always encouraged the group to ask questions. Whenever, I bring any result to him, the questions he always asks me are “How do you know” and “What does it tell you”. He always emphasizes the importance of good presentation skills. He is very good in scientific communication, and he has excellent ability to conduct chemistry shows. Second, I thank Travis. I learnt a lot from him regarding synthetic organic chemistry and laboratory techniques.

I thank my committee members, Prof. Paul Lahti, Prof. Ricardo Metz and Prof. Ryan Hayward. They have always been co-operative, and they provided me with good feed back, advice, and suggestions. They are good scientists who are always ready to help. I would like to thank my collaborators, Yu Xi, Serkan, and Murat in Prof. Rotello’s group, and Ben from Prof. Mike Barnes’ group for carrying out additional experiments and providing me data. I would also like to thank Prof. Marc Achermann for participating in many discussions.

I thank my parents, my brother, sister-in-law, sister, and brother-in-law for their constant encouragement and for providing moral support from time to time. It has been good to work with the unique members of DV group. I would like to take this opportunity to thank each and every member especially the graduate students, Serkan, Dip, Hari, Nag, Sravan, Kedar, and Dana of my research group for their suggestions and feedback. Finally, thanks Pavan, Devaiah and all my friends, I appreciate you for your support and encouragement.

ABSTRACT

EFFECT OF SIDE CHAINS ON ORGANIC DONOR (D) AND ACCEPTOR (A) COMPLEXES AND PHOTOPHYSICAL PROPERTIES OF D-A DYADS

SEPTEMBER 2011

AMARNATH BHEEMARAJU, B.Sc., NAGARJUNA UNIVERSITY

M.Sc., NATIONAL UNIVERSITY OF SINGAPORE

Ph.D., UNIVERSITY OF MASSACHUSETTS AMHERST

Directed by: Professor D. Venkataraman

This dissertation aims to understand the effect of incompatible side chains on the complexes of π-conjugated electron-rich donors and electron-deficient acceptors in solution. The role of incompatible side chains were studied in simple mixtures of organic donor and acceptor molecules that form donor-acceptor complexes. The incompatible branched and linear alkane side chains on the acceptor and donor respectively prevented complex formation between naphthalene diimide acceptor and naphthalene ether donor. However, the incompatible hydrocarbon-fluorocarbon and polar-non polar side chain pairs did not affect complex formation between the donor and acceptor. In quaterthiophene-naphthalene diimide dyads, the incompatibility of the side chain on the acceptor with respect to the side chain on the donor do not have any influence on the donor-acceptor complex formation. Irrespective of the attached side chains, all the dyads show charge transfer absorption bands and have similar electron transfer rates. The effect of point of attachment of the acceptor to the donor in the quaterthiophene-flavin dyad is also studied.

TABLE OF CONTENTS

Page

LIST OF TABLES

LIST OF FIGURES

CHAPTER 1

INTRODUCTION

1.1 Strategies for uncommon donor acceptor assemblies

Electron-rich (donor) and electron-poor (acceptor) π-conjugated molecules interact to form complexes[1-3] because of the favorable electrostatic interactions that exist between them.[4] The alternating hetero-stacked assembly of electron-rich and electron-poor molecules is most common in solids[5-7] and solution.[8-10] However, segregated assemblies of donors and acceptors are important for high electrical conductivity in organic molecules[11,12] and for increasing the efficiency of organic photovoltaic cells.[13,14] Several strategies have been used previously to obtain uncommon segregated assemblies in which donor and acceptor entities do not interact to form complexes.

In a strategy used by Torrance *et. al*. an unfavorable donor-acceptor overlap is created by selecting specific donor and acceptor molecules to obtain segregated stacks of donors and acceptors.[12] Becker and co-workers have substituted two benzyl donors to the tetracyano-quinodimethane acceptor instead of simply mixing them and have shown that electron-rich and electron-poor molecules could form segregated structures.[11] Mullen and co-workers used a very different strategy, which relies on the difference in the solubilities of the donor and acceptor components. Hexabenzocoronene donor has higher solubility than perylenebis dicarboximide acceptor in chloroform which results in crystallization of the acceptor before the donor to form segregated donor acceptor morphologies in thin films.[15] Iverson and co-workers report phase separation of specific derivatives of 1,5-dialkoxynapthalene ether donor and 1,4,5,8-naphthalenetetracarboxylic diamide acceptor.[4,5] However, the strategy depends mostly on the processing technique used for

obtaining the assembly. In summary, all the strategies mentioned above work only for specific molecules and might not be useful as a general strategy for obtaining segregated donor acceptor assemblies.

The general strategies of assembling the donors and acceptors into segregated stacks are few. Ghosh and co-workers obtained segregated assemblies of naphthalene diimide and naphthalene ether in solution by attaching complementary hydrogen bond forming side chains to the acceptor and donor.[16] Meijer and co-workers have used complementary hydrogen bond forming donors and acceptors to overcome the favorable donor-acceptor interactions.[17,18]

1.2 Role of incompatible side chains in donor acceptor assemblies

In an ingenious but very simple strategy Venkataraman and co-workers, and Aida and co-workers have shown that incompatible side chains could be used for the segregation of donor and acceptor molecules.[1,19,20] They designed dyads having covalently linked electron-rich donor and electron-poor acceptors with incompatible hydrocarbon-fluorocarbon or polar-non polar side chain on the each end of the dyad (Figure 1.1). A segregated assembly of donors and acceptors was obtained in solid state only when dyads with incompatible side chains are used. The dyads with compatible or no side chains formed solids that contain alternate donor acceptor stacks.

The general strategy proposed by Venkataraman and co-workers, and Aida and co-workers could be visually understood by Figure 1.1. As shown in the figure, donor acceptor dyads with incompatible side chains can pack into two possible arrangements. (1) The donors and acceptors arrange on top of each other in homo-stacks. The stabilization of such assembly not only comes from the favorable van der Waal's

interactions between the similar side chains but also as a result of favorable π-π interactions between the donor and acceptor (Figure 1.1a). (2) The donor and acceptor units interact to form alternate donor acceptor stacks (Figure 1.1b). In such an arrangement although the interaction between the donor and acceptor is favored, the interactions between the side chains are not favored. The preference of one arrangement over the two possible donor acceptor assemblies depends on total energies gained by all the interaction in the dyads i.e. π-π, donor-acceptor, and side chain interactions. The segregated assemblies obtained by Venkataraman and co-workers and Aida and co-workers (Figure 1.1a) indicate that it is energetically favorable for the similar side chains to pack themselves than to pack with incompatible side chains and it results in homostacks of donors and acceptors.

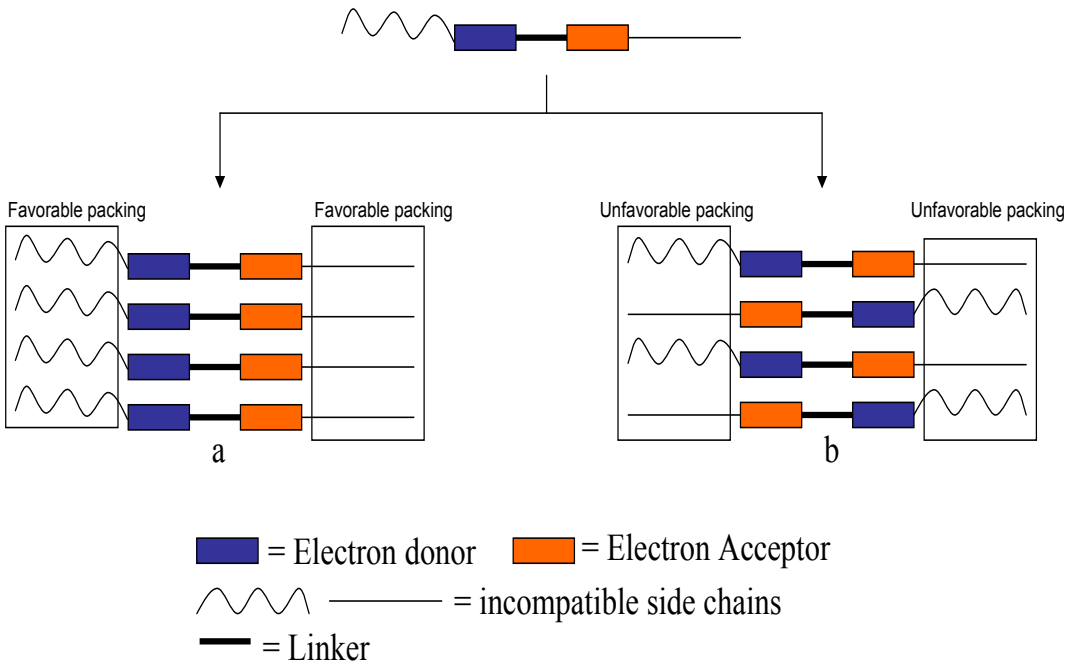

Figure 1.1: A molecular dyad with an electron-deficient part (shown in orange) attached covalently to an electron-rich part (shown in blue) containing dissimilar side chains. (a) Favorable packing of acceptors and donors leads to mixed stacks. (b) Favorable packing of side chains incompatible side chains leads to segregated stacks.

The role of side chains on donor-acceptor assemblies in the solid state is obvious from the work discussed in the earlier part of this chapter. The uncommon segregated assemblies are obtained when electron-rich and electron-poor units of the dyad were attached with incompatible side chains, indicating that favorable donor-acceptor interaction could be overcome by the unfavorable side chain interactions. The role of incompatible side chains on donor acceptor assemblies of dyads is also discussed in detail in chapter 5 of Dr.Benanti's thesis[21].

1.3 Scope and overview of the thesis

One of the important research focuses in the DV group at UMass Amherst is to synthesize and assemble materials that are relevant for organic solar cells. The group is interested in general strategies to control the molecular packing. My dissertation broadly focuses on this aspect of research and specifically explores the utility of incompatible or immiscible side chains as tools for the control of packing of organic semiconductors in solution.

It has been shown previously that incompatible side chains on the donor and acceptor would result in structures where donors and acceptors do not form complexes in the solid state. However, it is not known, how these side chains affect the donor-acceptor interaction in solution. Will the incompatible side chains have similar effect as they have in the solid state? This is the question I would like to answer in my thesis. The studies that lead to answer this question are important because they will enable us to understand the factors that affect the donor-acceptor interactions. Knowledge about factors that leads to changes in the donor acceptor assemblies or those that influence the donor-acceptor interactions is also important for the rational design of donors/acceptors or dyads to

obtain desired organization. Apart from focusing on studies to understand the effect of side chains, my thesis also tries to find if the point of attachment of the acceptor to the donor affects the photophysical properties in a dyad.

Three pairs of side chains have been selected for the studies to identify the role of incompatibility of side chains on the donor-acceptor interactions (Figure 1.2) in solution. Polar and non-polar side chains are selected because Aida and co-workers have proved previously that they affect the favorable donor-acceptor interactions in the solid state.[20] They interact in such a way that polar side chains pack with polar side chains but not with non-polar side chains and hence form a good incompatible side chain pair. Also, these are typically found to form micelles indicating the unfavorable interaction between them.

Hydrocarbon and fluorocarbon pair is selected because they do not mix well and phase segregate at room temperature. It is found that they have unfavorable interactions.[21-23] From our previous research we have shown that fluorocarbon and hydrocarbon (C6) side chains attached to the electron-rich and electron-poor molecules can lead to segregated stacks.[1] Thus, incompatible fluorocarbon and hydrocarbon unfavorable interactions can be attached as side chains to the acceptor and donor molecules to create uncommon structures. We selected branched-linear incompatible side chain pair due to the differences in the geometries between the two, which is supported by the analysis of the crystal structures.

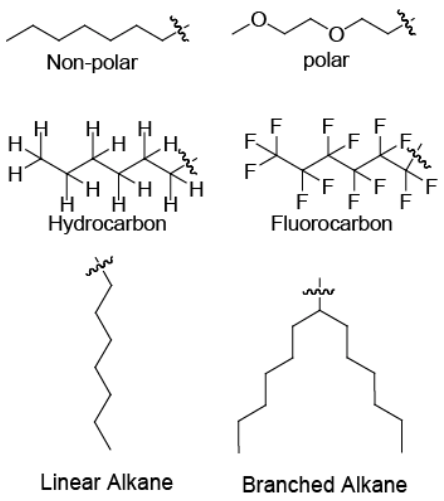

Figure 1.2: Incompatible side chain pairs used for determination of the effect of incompatible side chains on donor acceptor complexes.

The three chapters, chapter 2, chapter 3 and chapter 4 describe my research. The chapter 2 deals with studies on influence of incompatible side chains in simple mixtures of the donor and acceptor organic semiconductors, the second chapter discusses the impact of these side chains on the covalently linked donor acceptor dyads and the last chapter studies how the site of attachment of the acceptor to the donor plays a role in the photophysical properties of covalently linked donor acceptor dyads. A more detailed summary of the chapters is given below.

Chapter 2 of this thesis tries to answer the question of how the geometrically and immiscibly incompatible side chains attached to the electron-rich donor and electron-deficient acceptor affect their packing in solution. Figure 1.3 shows two possible arrangements of how donors and acceptors with incompatible side chains can arrange in solution. In one of the arrangements there is favorable donor acceptor interaction between the acceptors and donors. However, in such arrangement there is an unfavorable interaction between the side chains (Figure 1.3a). In another arrangement, the acceptors and donors pack separately and there is a favorable π-π interaction between the homo-stacks of donor and acceptor, which is complemented by the favorable interactions of the similar side chains (Figure 1.3b). However an intermediate molecular arrangement in

which the conformations of the donors and acceptors avoid the incompatible side chains but simultaneously form a strong donor acceptor complex is also possible.

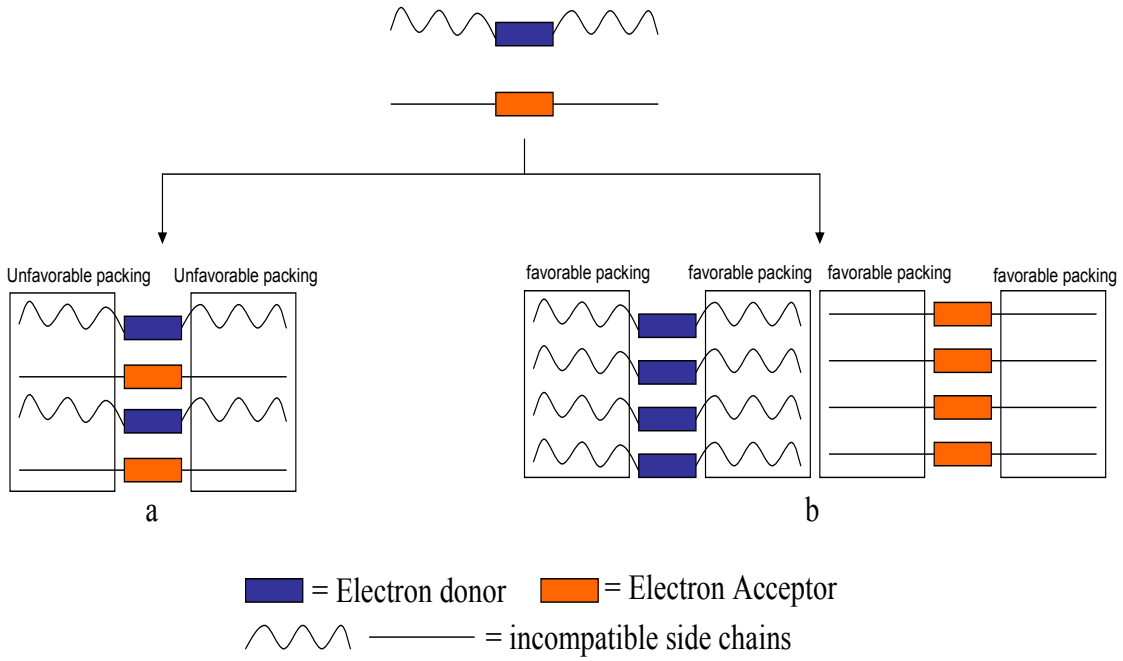

Figure 1.3: The electron-deficient (acceptor) and electron-rich (donor) attached with incompatible side chains. (a) Acceptor donor self-assembly with incompatible side chains together. (b) Segregated columnar acceptor donor assembly with compatible side chains together.

Naphthalene diimide (NDI) acceptor with different side chains was synthesized. Naphthalene ether (NE) with hydrophobic side chains is used as donor. The side chains on the acceptor are selected such that they are either compatible or incompatible with the side chains attached to the donor. The molecular structures of the acceptor NDI and donor NE are shown in Figure 1.4. The effect of side chains was assessed using the differences in the binding constants between the donor and acceptor. The binding constants were determined using NMR titration. It is found that the branched side chain containing acceptor will not form a complex with the naphthalene ether containing linear

side chain. However, with other side chains the incompatibility of the side chains does not play a role in the packing of the acceptor and donor. This result indicates that the electrostatic complementarity determines the binding between the acceptor and donor units, with more electron deficient acceptors forming stronger complexes with the donor.

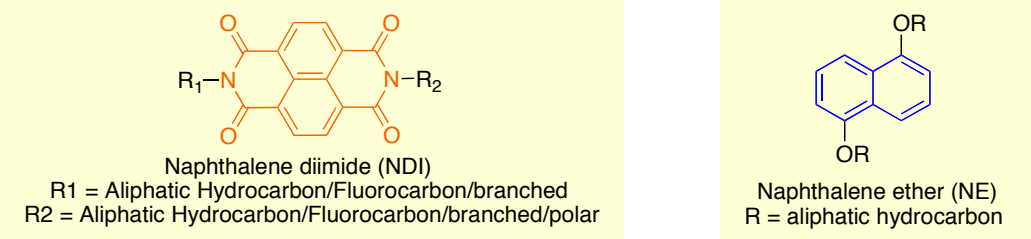

Figure 1.4: Structures of NDI acceptor and NE donor.

In the chapter 2 we discussed the effect of incompatible side chains on the complex formation in mixtures of donors and acceptors. As indicated by the study the incompatible side chains other than the branched side chain do not influence the donor-acceptor favorable interactions that are undesirable for efficient charge migration in organic solar cells. One of the possible reasons for this is the large number of possible packing conformations that acceptor and donor molecules can adopt to avoid side chain interactions but still form alternate donor acceptor complexes. Chapter 3 of this thesis tries to answer the question of how the incompatible side chains attached to the covalently linked electron-rich donor and electron-deficient acceptor affect the donor acceptor complex formation in solution.

In the case of dyads, the donor and acceptor units are covalently linked. The various assemblies that the dyads can take when attached with incompatible side chains were shown earlier in Figure 1.1. In addition to these arrangements, the dyads with flexible linker can fold to form an intramolecular donor acceptor complex.

The model dyads (Figure 1.5) are designed by covalently linking naphthalene diimide acceptor to the quaterthiophene donor through a flexible linker, and the ends of naphthalene diimide and quaterthiophene are attached with incompatible side chains. The absorption spectral studies carried out in chloroform reveals complex formation in all the dyads, irrespective of the side chains. Furthermore, the study points out that electron transfer takes place in these dyads. The rates of electron transfer (ET) are determined by the fluorescence quenching studies. These rates are almost the same for all of the dyads irrespective of the side chains.

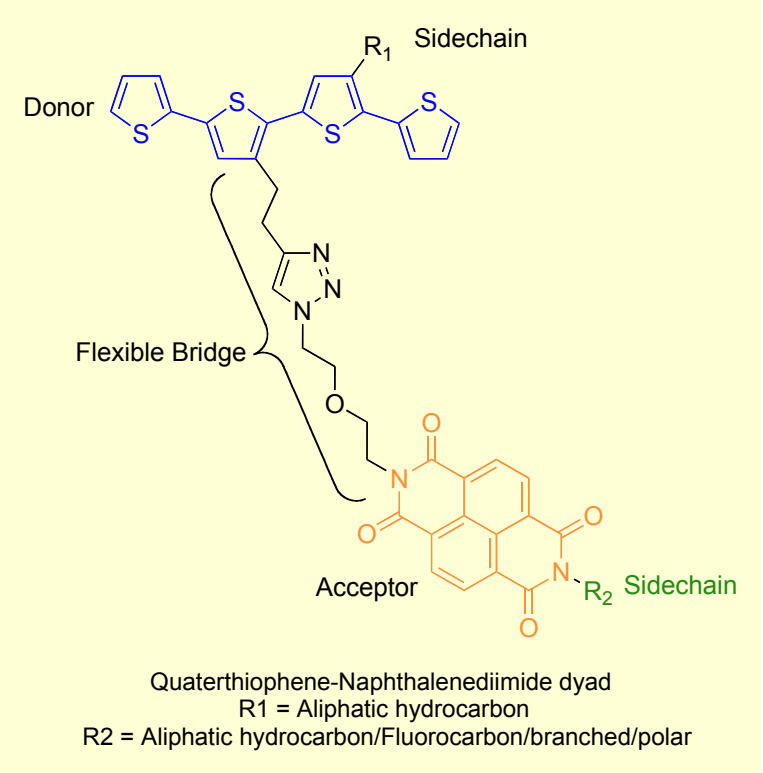

Figure 1.5: Structure of naphthalenediimide-quaterthiophene dyad.

Chapter 4 discusses the synthesis of novel dyads based on flavin acceptor and quaterthiophene donor. Two dyads are designed by attaching the acceptor to the donor

QT molecule at two different positions, namely N3 (Figure 1.6) and N10, through a flexible covalent linker.

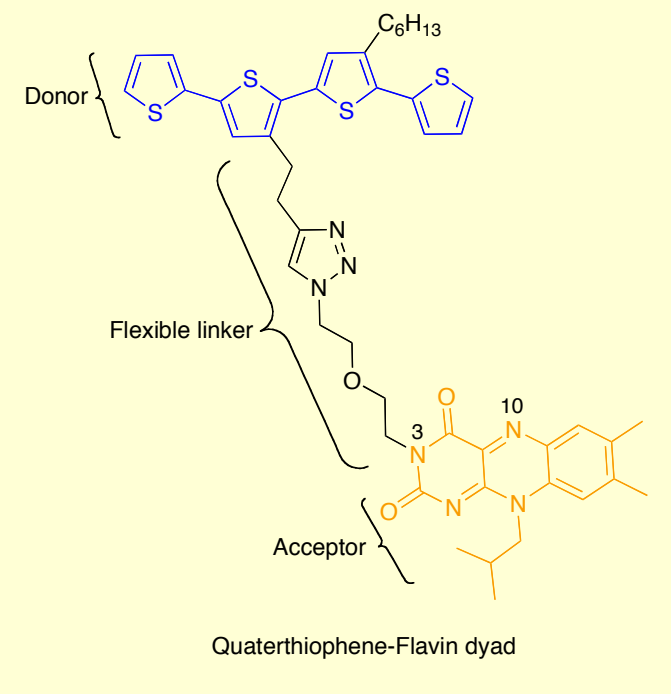

Figure 1.6: Structure of quaterthiophene-flavin dyad

The results from the two flavin-quaterthiophene dyads indicate very high quenching of fluorescence in both. The fluorescence lifetime of the dyads determined using the time-resolved fluorescence decay studies indicated changes in the quenching ability of the dyads with respect to the position of attachment of the acceptor to the donor. The studies indicate the probable role of conformational geometry between the donor and acceptor in the dyads in the electron transfer rates.

1.4 References

1. Benanti, T. L.; Saejueng, P.; Venkataraman, D., "Segregated assemblies in bridged electron-rich and electron-poor pi-conjugated moieties," *Chemical Communications* **2007**, 692-694.

2. Percec, V.; Glodde, M.; Bera, T. K.; Miura, Y.; Shiyanovskaya, I.; Singer, K. D.; Balagurusamy, V. S. K.; Heiney, P. A.; Schnell, I.; Rapp, A.; Spiess, H. W.; Hudson, S. D.; Duan, H., "Self-organization of supramolecular helical dendrimers into complex electronic materials," *Nature* **2002**, *419*, 384-387.

3. Lokey, R. S.; Iverson, B. L., "Synthetic molecules that fold into a pleated secondary structure in solution," *Nature* **1995**, *375*, 303-305.

4. Reczek, J. J.; Villazor, K. R.; Lynch, V.; Swager, T. M.; Iverson, B. L., "Tunable columnar mesophases utilizing C-2 symmetric aromatic donor-acceptor complexes," *Journal of the American Chemical Society* **2006**, *128*, 7995-8002.

5. Alvey, P. M.; Reczek, J. J.; Lynch, V.; Iverson, B. L., "A Systematic Study of Thermochromic Aromatic Donor-Acceptor Materials," *Journal of Organic Chemistry* **2010**, *75*, 7682-7690.

6. Reczek, J. J.; Iverson, B. L., "Using aromatic donor acceptor interactions to affect macromolecular assembly," *Macromolecules* **2006**, *39*, 5601-5603.

7. Koshkakaryan, G.; Klivansky, L. M.; Cao, D.; Snauko, M.; Teat, S. J.; Struppe, J. O.; Liu, Y., "Alternative Donor-Acceptor Stacks from Crown Ethers and Naphthalene Diimide Derivatives: Rapid, Selective Formation from Solution and Solid State Grinding," *Journal of the American Chemical Society* **2009**, *131*, 2078-2079.

8. Cubberley, M. S.; Iverson, B. L., "H-1 NMR investigation of solvent effects in aromatic stacking interactions," *Journal of the American Chemical Society* **2001**, *123*, 7560-7563.

9. Gabriel, G. J.; Iverson, B. L., "Aromatic oligomers that form hetero duplexes in aqueous solution," *Journal of the American Chemical Society* **2002**, *124*, 15174-15175.

10. Bradford, V. J.; Iverson, B. L., "Amyloid-like behavior in abiotic, amphiphilic foldamers," *Journal of the American Chemical Society* **2008**, *130*, 1517-1524.

11. Becker, J. Y.; Bernstein, J.; Bittner, S.; Levi, N.; Shaik, S. S., "Strategic design of organic conductors - structure of a prototypical molecule," *Journal of the American Chemical Society* **1983**, *105*, 4468-4469.

12. Torrance, J. B.; Mayerle, J. J.; Lee, V. Y.; Bechgaard, K., "New class of highly conducting organic materials - charge-transfer salts of the tetrathiafulvalenes with the tetrahalo-para-benzoquinones," *Journal of the American Chemical Society* **1979**, *101*, 4747-4748.

13. Thompson, B. C.; Frechet, J. M. J., "Organic photovoltaics - Polymer-fullerene composite solar cells," *Angew. Chem.-Int. Edit.* **2008**, *47*, 58-77.

14. Venkataraman, D.; Yurt, S.; Venkatraman, B. H.; Gavvalapalli, N., "Role of Molecular Architecture in Organic Photovoltaic Cells," *Journal of Physical Chemistry Letters* **2010**, *1*, 947-958.

15. Schmidt-Mende, L.; Fechtenkotter, A.; Mullen, K.; Moons, E.; Friend, R. H.; MacKenzie, J. D., "Self-organized discotic liquid crystals for high-efficiency organic photovoltaics," *Science* **2001**, *293*, 1119-1122.

16. Molla, M. R.; Das, A.; Ghosh, S., "Self-Sorted Assembly in a Mixture of Donor and Acceptor Chromophores," *Chemistry-a European Journal* **2010**, *16*, 10084-10093.

17. Jonkheijm, P.; Stutzmann, N.; Chen, Z. J.; de Leeuw, D. M.; Meijer, E. W.; Schenning, A.; Wurthner, F., "Control of ambipolar thin film architectures by co-self-assembling oligo(p-phenylenevinylene)s and perylene bisimides," *Journal of the American Chemical Society* **2006**, *128*, 9535-9540.

18. Wurthner, F.; Chen, Z. J.; Hoeben, F. J. M.; Osswald, P.; You, C. C.; Jonkheijm, P.; von Herrikhuyzen, J.; Schenning, A.; van der Schoot, P.; Meijer, E. W.; Beckers, E. H. A.; Meskers, S. C. J.; Janssen, R. A. J., "Supramolecular p-n-heterojunctions by co-self-organization of oligo(p-phenylene vinylene) and perylene bisimide dyes," *Journal of the American Chemical Society* **2004**, *126*, 10611-10618.

19. Li, W. S.; Yamamoto, Y.; Fukushima, T.; Saeki, A.; Seki, S.; Tagawa, S.; Masunaga, H.; Sasaki, S.; Takata, M.; Aida, T., "Amphiphilic molecular design as a rational strategy for tailoring bicontinuous electron donor and acceptor arrays: Photoconductive liquid crystalline oligothiophene-C-60 dyads," *Journal of the American Chemical Society* **2008**, *130*, 8886-8887.

20. Li, W. S.; Saeki, A.; Yamamoto, Y.; Fukushima, T.; Seki, S.; Ishii, N.; Kato, K.; Takata, M.; Aida, T., "Use of Side-Chain Incompatibility for Tailoring Long-Range p/n Heterojunctions: Photoconductive Nanofibers Formed by Self-Assembly of an Amphiphilic Donor-Acceptor Dyad Consisting of Oligothiophene and Perylenediimide," *Chemistry-an Asian Journal* **2010**, *5*, 1566-1572.

21. Benanti, T. L., "Strategies for Directing Aromatic Packing," *Thesis* **2008**.

22. De Luca, G.; Liscio, A.; Melucci, M.; Schnitzler, T.; Pisula, W.; Clark, C. G.; Scolaro, L. M.; Palermo, V.; Mullen, K.; Samori, P., "Phase separation and affinity between a fluorinated perylene diimide dye and an alkyl-substituted hexa-peri-hexabenzocoronene," *Journal of Materials Chemistry* **2010**, *20*, 71-82.

23. Kohlmeier, A.; Nordsieck, A.; Janietz, D., "Tailoring Thermotropic Mesophase Morphologies by Molecular Recognition and Fluorophobic Effect," *Chemistry of Materials* **2009**, *21*, 491-498.

24. Dunitz, J. D., "Organic fluorine: Odd man out," *Chembiochem* **2004**, *5*, 614-621.

CHAPTER 2

EFFECT OF INCOMPATIBLE SIDE CHAINS ON THE AROMATIC DONOR-ACCEPTOR COMPLEX

2.1 Introduction

Organic electron acceptors and donors have favorable charge transfer interactions.[1-6] This favorable interaction has been used extensively for obtaining donor-acceptor complexes in solution[7] and solid phases.[8] Heterostacks of donor and acceptor are obtained in solution by using naphthalene diimide (NDI) acceptor and naphthalene ether (NE) donor.[9-11] The main objective of obtaining them in solution especially in water or buffer is to achieve structures that can potentially mimic the biologically active macromolecules like polypeptides.[12] Similarly, favorable D-A interactions have been used to obtain alternating donor acceptor stacks in solid state. The main motivation behind such study is to obtain ordered structures that will have potential applications in organic electronics especially organic ferroelectrics.[8,13]

Studies on donor-acceptor complexes have resulted in understanding the some of the factors that influences the interactions between them. Detailed studies that indicate the role of solvent polarity on binding ability of well-defined donor-acceptor assemblies that adopt a secondary pleated structure have been carried out. The results reveal that complexation is stronger in polar solvents because of more de-solvation of hydrophobic aromatic units, which results in stronger interaction between the aromatic donor acceptor units. It is also found, however, that the magnitude of donor-acceptor interactions depends on geometry of interacting donor and acceptor and the electrostatic complementarity between them. As expected, the binding constant in the slightly polar

solvent $CDCl_3$ is very low (2±0.5 M^{-1}) compared to that obtained in the more polar solvent D_2O (2045±63 M^{-1}).[10]

Another important factor that may affect the donor-acceptor interaction is the processing method used to assemble them. Iverson *et. al.* studied mixtures of naphthalene diimide acceptors and naphthalene ether donors in solid phase with different side chains.[14.15] The results indicate that heating an equimolar mixture of donor and acceptor to the isotropic temperatures and slowly crystallizing it results in phase-separated donor acceptor assemblies in some specific cases. Furthermore, it is indicated in this study that the color change from red to off-white (due to change in the assembly of donors and acceptors from alternating hetero-stacks to homo-stacks) is rapid with an isopropyl group on naphthalene ether, which causes steric hindrance for formation of the donor-acceptor complex. This study does not, however, shed light on the role of side chains in enhancing or preventing donor-acceptor complexes. In summary, these studies only indicate the importance of processing technique for obtaining solids that consist of alternating or phase separated donor acceptor constituents rather than understanding the role of side chains on donor-acceptor complexes.[14,15]

Ghosh and co-workers attached hydrogen bonding forming side chains on the donor and acceptor units.[17,18] They studied the effect of placement of complimentary hydrogen bonds on the donor acceptor assemblies in solution. Naphthalene diimide and naphthalene ether are di-substituted with amide-functionalized side chains. The distance between the two-amide groups on the naphthalene diimide acceptor is different from the one in naphthalene ether donor. The consequence of such difference is the minimization of complementary hydrogen bonding interactions only when donors and acceptors pack

in homo-stacks but not in the alternate hetero-stack charge transfer complexes. This strategy proves that the hydrogen bonding side chains along with the complementary aromatic π- π interactions can be utilized for tune the donor-acceptor interactions.[16] Similarly Meijer and co-workers study the role of complementary hydrogen bonds on the assembly of donor and acceptor molecules.[17,18]

However, studies on the effect of side chains on the donor-acceptor complexes are very limited. We hypothesized that side chains that are non-compatible/mutually phobic will affect the donor-acceptor complexes and their assemblies. Initially we tested our hypothesis on benzene donor, perfluorobenzene acceptor, hexane, and perfluorohexane side chains. Schweizer and co-workers have calculated gas-phase interaction energies of benzene, hexafluorobenzene, hexane, and perfluorohexane dimers. Additionally they also found the interaction energies of benzene-perflorobenzene, hexane-perfluorobenzene dimers.[19] On assessing the interaction energies we found that it would be more energetically favorable for donors and acceptors to interact with themselves than to form donor-acceptor complexes if hydrocarbon and fluorocarbon side chains are attached to them. Similarly, we proposed that polar-nonpolar and linear-branched side chain pairs could have potential influence on the donor acceptor packing. Our hypothesis was further supported by experimental results. Venkataraman and co-workers have proved that incompatible side chains would impact the favorable donor-acceptor interaction.[1] It was observed from the crystal structures of naphthalenemonoimide acceptor and naphthalene ether donor with incompatible fluorocarbon and hydrocarbon side chains attached to the donor and acceptor units respectively packed differently compared to the ones without side chains.[1] Similarly, Aida and co-workers have shown that the side chains affect the

donor-acceptor interactions in perylenediimide acceptor and quarterthiophene donor dyad.[20] These studies indicate that the role of incompatible side chains on defining the assemblies of donors and acceptors and their influence on the favorable donor-acceptor interactions.

However, all the studies mentioned above are performed to assess the role of incompatible side chains in solid state. Furthermore, they are proved to hold good for donor bridge acceptor dyads only. Thus, it is very interesting to know how this side chains that influence the donor-acceptor favorable interactions in dyads in solid state will affect in simple mixtures in solution. Furthermore, these studies can more generally be applied to any simple donors and acceptors that are not attached covalently and are not restricted conformationally to form the donor-acceptor complex. Additionally, the role of solvents in preventing or allowing the interactions between the side chains can also be understood. In future such studies will help in selecting the right side chains for obtaining strong, weak or no complexes between the donor and acceptor units in solution for obtaining various types of assemblies for various applications. Such studies will help in designing the organic semiconductors whose assemblies could be tuned to obtain morphologies that lead to increase in the efficiency of organic solar cells. Moreover, the use of solution processing techniques to assemble the organic semiconductors will lead to low manufacturing cost for optoelectronic devices.

To answer the question of the role of incompatible side chains on donor-acceptor complexes in solution we have picked simple naphthalene ether donor and naphthalene diimide acceptor that are discussed previously and those that are known to form a good donor acceptor complex. The structure of naphthalene ether and naphthalene diimide are

shown in Figure 2.1. The incompatible side chains that are selected for the study are hydrocarbon-fluorocarbon, polar-nonpolar and branched-linear alkanes. This set of incompatible side chains is selected because of their known role in affecting the donor-acceptor complexation.

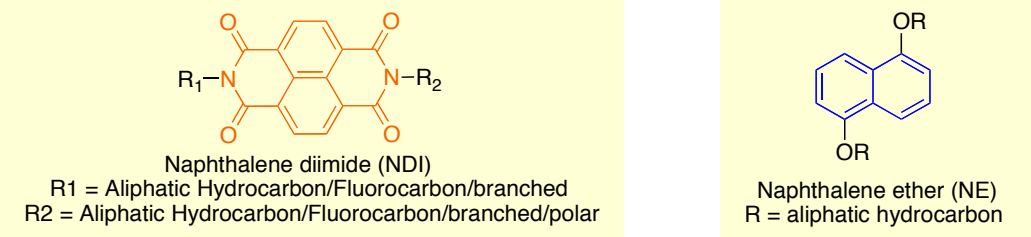

Figure 2.1: NDI and NE with different side chains.

2.2 Synthesis of molecules for the study

The molecules that are synthesized here serve as a model for the studies of the effect of side chains on the donor-acceptor complexes. Electron-rich naphthalene ether (NE) with hydrophobic side chains, and electron-deficient naphthalene diimide (NDI) with incompatible or compatible side chains, to the side chain attached donor are synthesized.

The synthesis of donor (**2**) for the study is started with commercially available 1,5-napthlenediol (1). Dihexylnaphthelene ether, **2** is obtained by reaction of 1,5-napthlenediol with hexyl iodide (Figure 2.2).

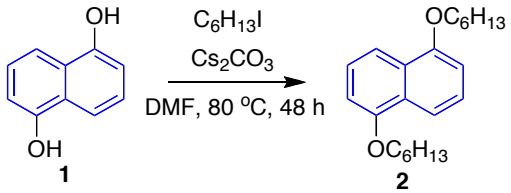

Figure 2.2: Synthesis of donor NE (**2**)

The amines required for the synthesis of different NDI acceptor are obtained. Fluorocarbon ($C_6F_{13}CH_2NH_2$ and $C_7F_{15}CH_2NH_2$) and alkyl ($C_6H_{13}NH_2$) amines are available from commercial sources. Branched alkyl amine (**4**) was synthesized from the branched alkyl ketone (**3**) using the previously reported procedure[21] (Figure 2.3).

Various NDI acceptors with different side chains were synthesized from commercially available starting material naphthalene dianhydride (NDA). For the synthesis of Hc-NDI-Fc, first mono hexyl substituted naphthalene imide; N-hexyl-1,4,5,8-naphthalenetetracarboxylicmonoanhydride (**5**) was prepared following a previously[22] reported procedure (Figure 2.4). There is always little amount of Hc-NDI-Hc, which is formed as a by-product. This mixture containing **5** and Hc-NDI-Hc, was used for the next reaction to synthesize Fc-NDI-Hc without further purification. Mono substituted NDI and fluorocarbon amine ($C_6F_{13}CH_2NH_2$) mixture in chloroform in the presence of imidazole at refluxing temperatures was initially tried for the synthesis of product, Fc-NDI-Hc. But the product could not be obtained by this method. However, good yields of the final product (Fc-NDI-Hc) were obtained by refluxing the mixture of the starting materials dissolved in DMF solvent. The symmetrical NDIs *i.e.* Hc-NDI-Hc, and Fc-NDI-Fc were synthesized in good yields by adding two equivalents of corresponding amines to one equivalent of NDA. But this procedure did not work for the synthesis of br-NDI-br. For this, starting materials in imidazole at high temperatures afforded the product. On the other hand, the asymmetrical NDI (Hc-NDI-OH) is synthesized by equimolar addition of corresponding amines to NDA (Figure 2.5).

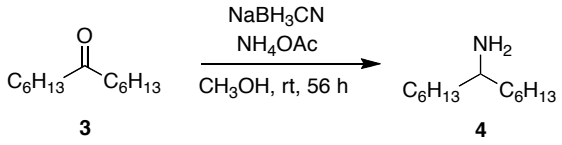

Figure 2.3: Synthesis of hexylheptylamine.

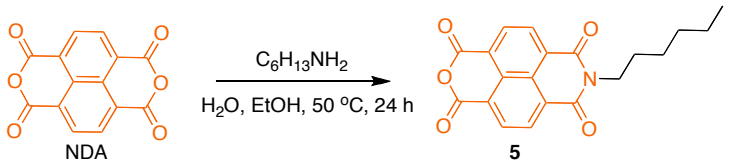

Figure 2.4: Synthesis of N-hexyl-1,4,5,8-naphthalenetetracarboxylicmonoanhydride.

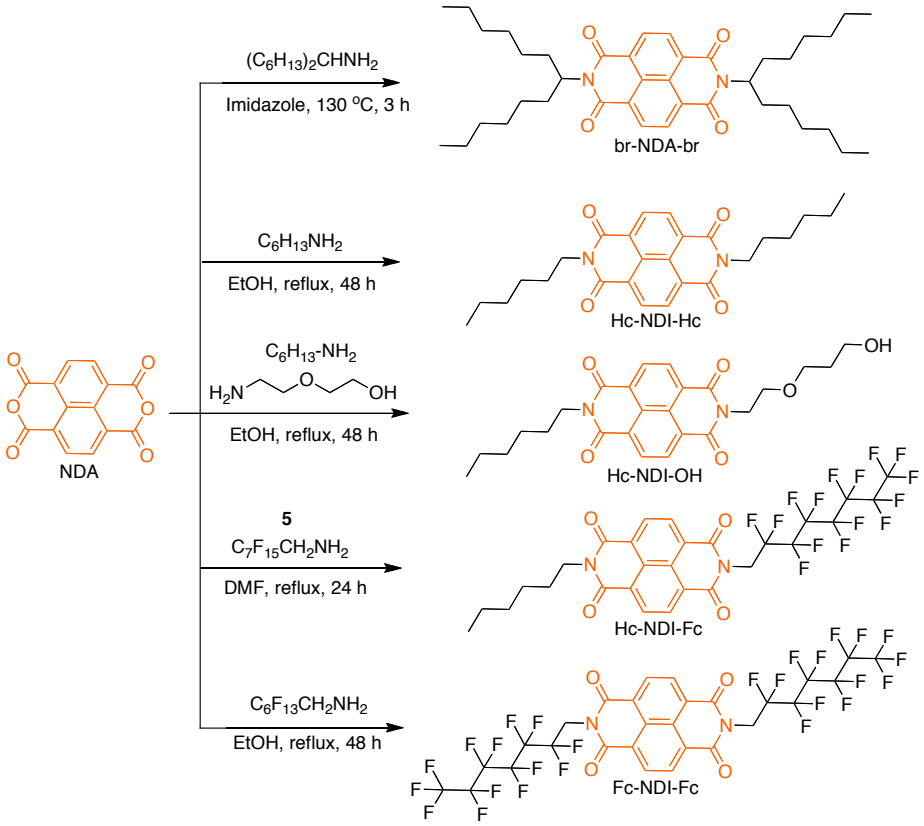

Figure 2.5: Synthesis of NDI acceptor with various side chains.

2.3 Characterization

All the compounds are characterized by using ^{1}H NMR. The peak corresponding to the aromatic NDI protons are usually observed above 8 ppm (Figure 2.6). In the case of NE (**2**) the aromatic NE peaks appear at 6.8, 7.4 and 7.9 ppm (Figure 2.7). The important indications for the presence of the branched alkyl and fluorocarbon side chains on the NDI is the presence of the multiplet peak near 5.1 ppm and triplet peak near 5 ppm, respectively (See A.2 section in appendix).

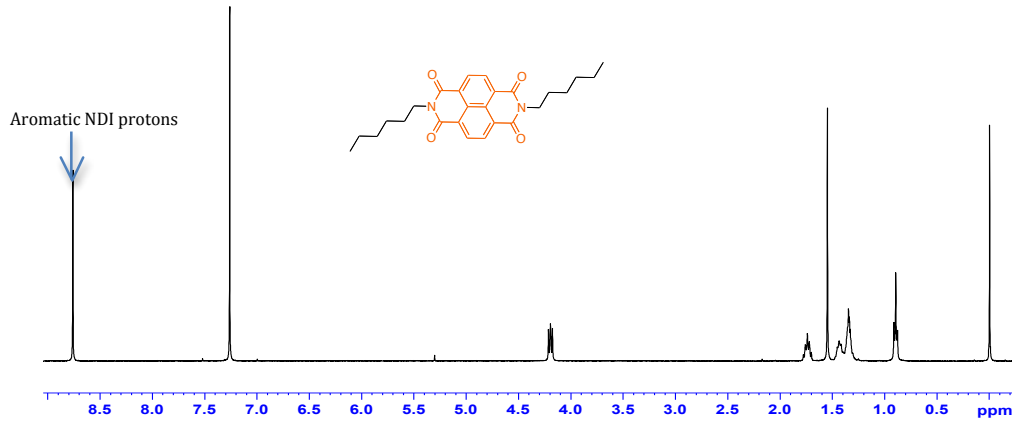

Figure 2.6: ^{1}H NMR of Hc-NDI-Hc in $CDCl_3$.

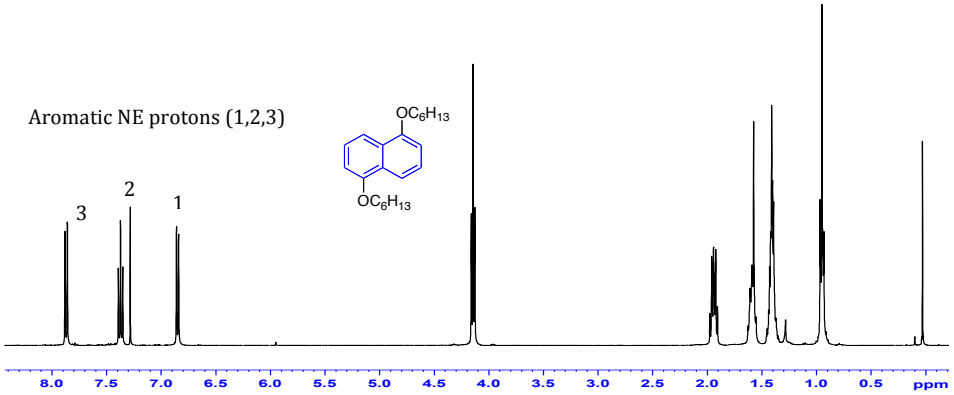

Figure 2.7: ^{1}H NMR of NE (**2**) in $CDCl_3$.

2.4 Absorption characteristics

The absorption spectrum of mixture of Hc-NDI-Hc and NE in dichloromethane is shown in Figure A.1 (See Appendix). It is observed that a new absorption band appears at longer wavelengths and this is not present in absorption spectra of either donor or acceptor alone. This is assigned to a charge transfer band of the donor acceptor complex. The appearance of this band indicates the complex formation between the donor and acceptor units.

2.5 Binding stoichiometry

The important objective of this chapter, as mentioned in the beginning of the chapter, is to find the influence of side chains on the donor-acceptor (DA) complexes. One way to understand this is to determine the binding constants for DA complexes and analyze the results with respect to the side chains on the donor/acceptor units. One way to accurately find the binding constants for donor acceptor complexes is by using NMR titration methods. Though Isothermal calorimetry (ITC) can also be used to find the binding constants of DA complexes, the heat changes are so small that they are undetectable by the instrument and even at very high concentrations of NDI and NE, no signal with acceptable signal to noise ratio could be obtained.

The first step towards finding the binding constants for the NDI-NE complex is to find the binding stoichiometry of the NDI and NE complex. A Jobs' plot is the most commonly used method for this purpose. In this method the sum of the concentrations of NDI and NE are kept constant at 3.75 mM, and the concentration of the NDI and NE are changed for each sample. A total of seven samples were prepared for the study. The exact concentrations used for this experiment are shown in Table 2.1.

Naphthalene diimide (NDI) when mixed with NE in $CDCl_3$ due to the favorable charge transfer interaction a complex is formed. This results in the change of the chemical shift of the free NDI (without NE) aromatic protons, δ_{free} towards upfield (Figure 2.8). This change in the chemical shift of the NDI aromatic protons (δ_{obs}) is monitored and the change in free and observed chemical shifts ($\Delta\delta = \delta_{free} - \delta_{obs}$) is calculated for each of the seven samples used for the study (Table 2.1). A plot of product of mole fraction (MF) of NDI and the change in the chemical shift ($\Delta\delta$) vs. mole fraction of NDI will allow us to determine the stoichiometry of binding. Figure 2.9 shows hypothetical examples of Jobs' plots for 1:1, 1:2 and 2:1 binding stoichiometries. For the 1:1, 1:2 and 2:1 binding the maximum on the y-axis in Figure 2.9 is found at mole fractions 0.5, 0.33 and 0.66 respectively.

Table 2.1: Change in NMR chemical shifts for Jobs' plots of Hc-NDI-Hc : NE.

Sample	[NDI] (mM)	[NE] (mM)	Mole fraction of NDI	δ_{obs} (ppm)	$\Delta\delta = \delta_{free} - \delta_{obs}$ (ppm)
1	3.75	0	1.0	8.7597	0
2	3.0	0.75	0.8	8.7589	0.0008
3	2.5	1.25	0.66	8.7584	0.0013
4	1.88	1.88	0.5	8.7579	0.0016
5	1.25	2.5	0.33	8.7572	0.0025
6	0.75	3.0	0.2	8.7569	0.0028
7	0.42	3.333	0.112	8.7567	0.003

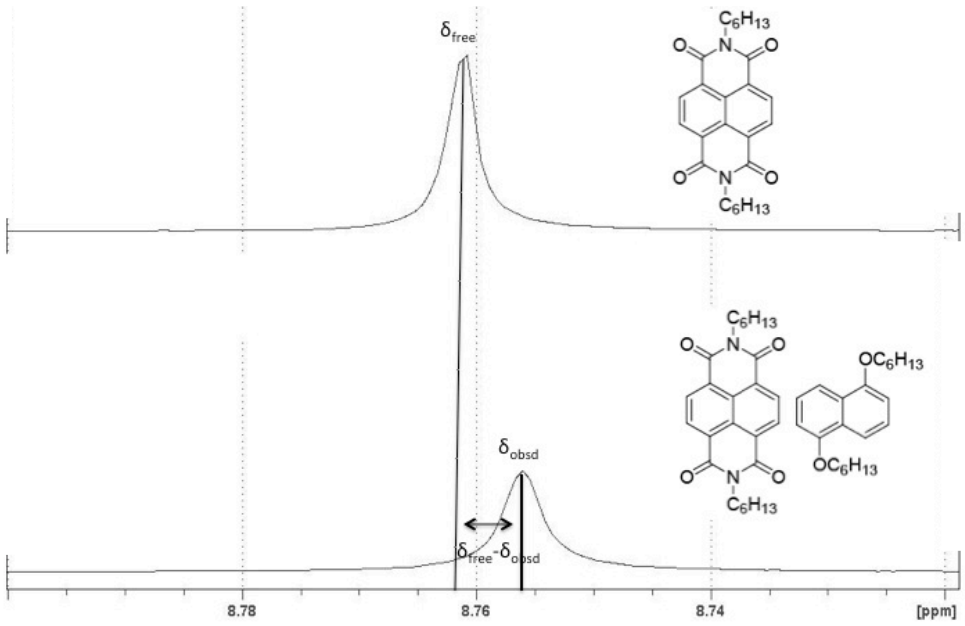

Figure 2.8: The change in chemical shift of NDI aromatic proton on addition of NE.

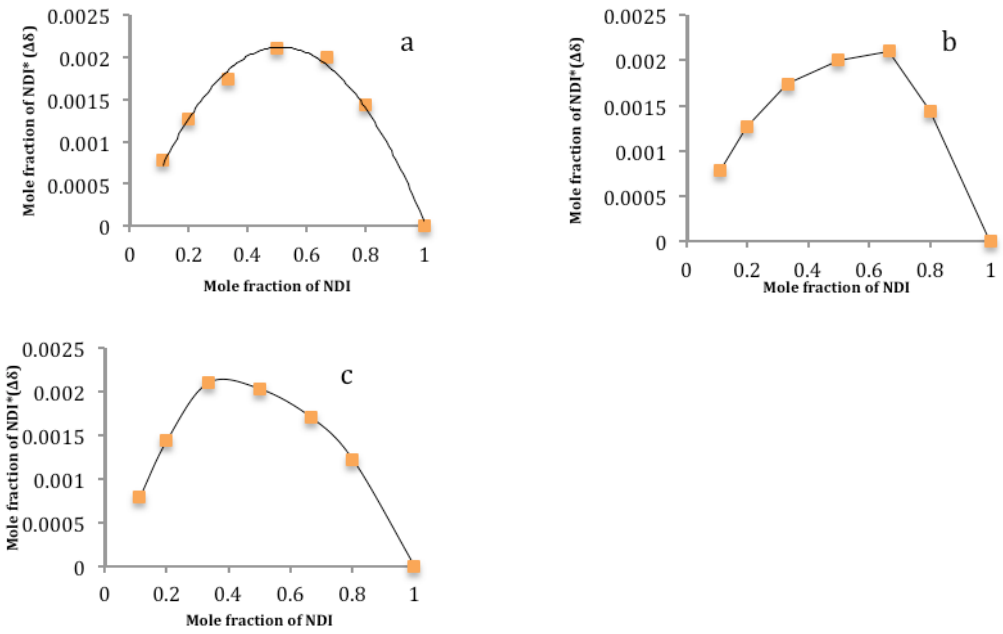

Figure 2.9: Hypothetical Jobs plot for the (a) 1:1, (b) 2:1 (c) 1:2 binding stoichiometries.

The addition of NE to br-NDI-br did not change the chemical shift of free NDI aromatic proton and thus Jobs' plot for this mixture could not be plotted. The Jobs' plot for all other NDIs i.e. Hc-NDI-Hc, Hc-NDI-OH, Hc-NDI-Fc and Fc-NDI-Fc are shown in Figure 2.10.

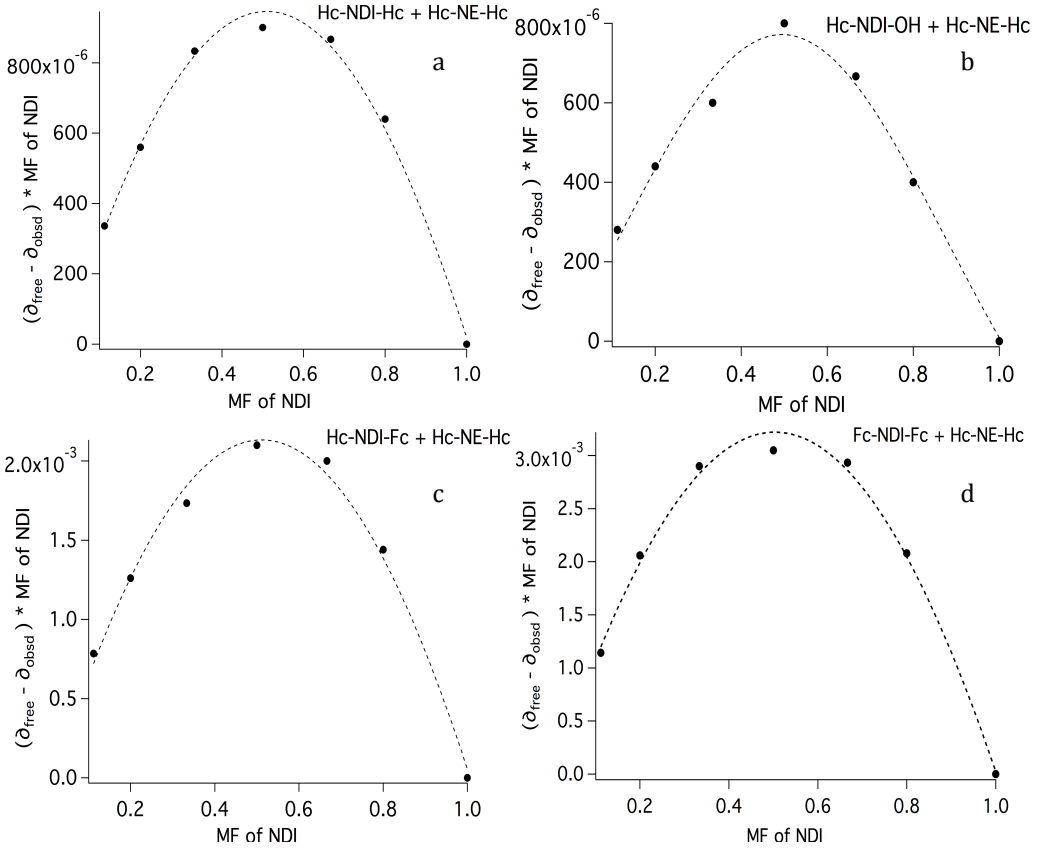

Figure 2.10: Jobs' plots for evaluation of binding stoichiometries for mixtures of NDIs and NE. The Jobs plot for (a) Hc-NDI-Hc : NE, (b) Hc-NDI-OH : NE, (c) Hc-NDI-Fc : NE, (4) Fc-NDI-Fc : NE.

The mole fractions of NDI used in the experiments for Jobs' plot are the same as presented in Table 2.1 for all the various NDIs studied. In all of the mixtures (NDIs and NE) it was observed that the maximum value for the product of Δδ and MF of NDI (y-

axis) is found when the MF of NDI is 0.5 (Figure 2.10). This indicates a 1:1 binding between NDI and NE in the NDI-NE complexes.

2.6 Binding constants

The stoichiometry of binding for the NDI: NE complex is found to be 1:1 for all the different NDIs. The binding constant for 1:1 binding between the donor and acceptor is determined using equation 1.

$$\delta_{free} - \delta_{obsd} = (\partial free - \partial bound) \times \frac{\left\{[D]+[A]+(1/K)-\sqrt{([D]+[A]+(1/K))^2-4[D][A]}\right\}}{2[D]} \quad \ldots. (1)$$

The terms in the equation (1) are listed below.

δ_{free} = chemical shift of free NDI aromatic proton

δ_{obsd} = observed chemical shift of acceptor after it it bound to NE

δ_{bound} = chemical shift of complex

[D] = Initial concentration of donor (mM)

[A] = Initial concentration of acceptor (mM)

K = binding constant (mM)

The method of NMR titrations has been used to find out the binding constant, K. In this method the NDI concentrations of the sample was held constant at 3.75 mM. Seven different samples were prepared by varying concentrations of NE. The actual concentrations of NE used are listed in Table 2.2. The values of Δδ are also shown in Table 2.2.

Table 2.2: Changes in NMR chemical shifts for binding isotherms of Hc-NDI-Hc and NE mixtures.
Concentration of Hc-NDI-Hc kept constant at 3.75 mM for all the samples.

Sample	[NE] (mM)	$\Delta\delta = \delta_{free} - \delta_{obs}$ (ppm)
1	0	0
2	1.88	0.0018
3	3.75	0.0039
4	7.5	0.0083
5	15.0	0.0149
6	30.0	0.0316
7	60.0	0.0623

The ($\Delta\delta$) values are plotted against the concentration of NE to obtain a series of data points. These points are fitted to a non-linear curve using the method of non-linear least squares and by custom written program using Igor software. The values of K are determined by this method. The binding constants are determined by plotting binding isotherms for different NDI: NE mixtures (Figure 2.11).

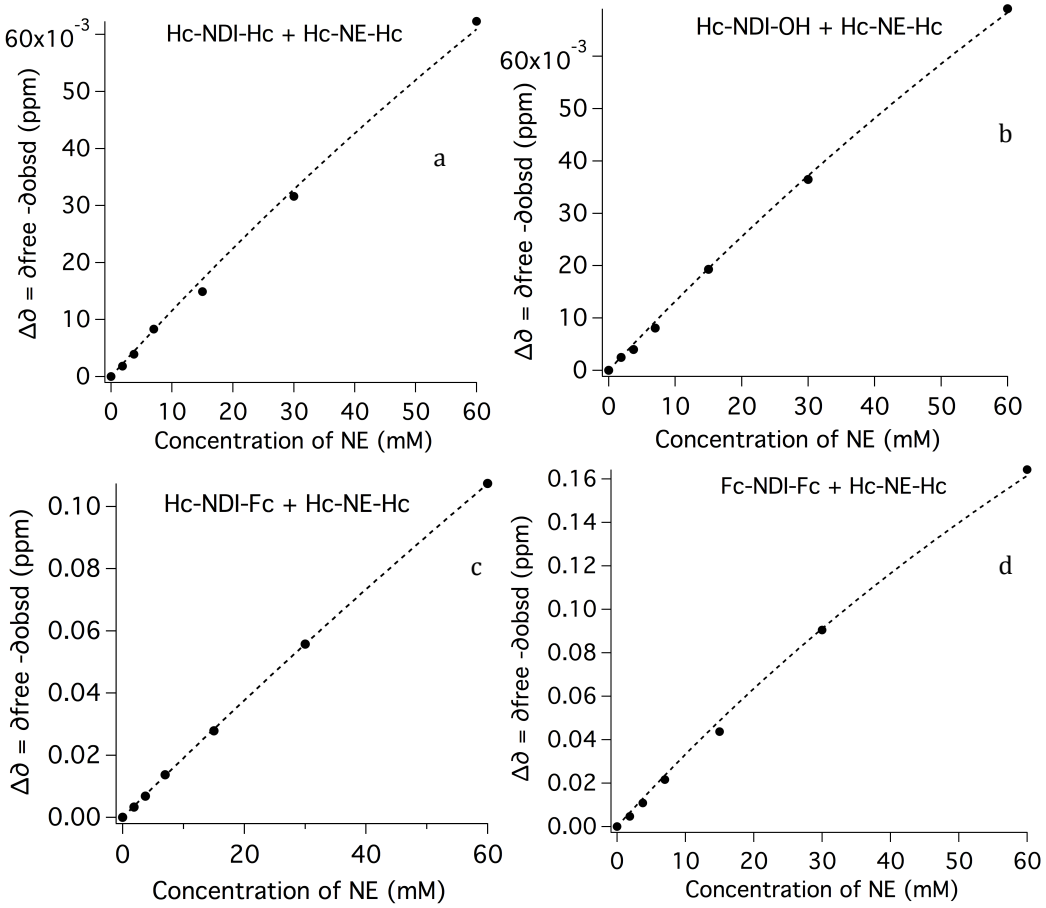

Figure 2.11: Binding isotherms for NDI: NE mixtures (a) Hc-NDI-Hc:NE (b) Hc-NDI-OH:NE (c) Hc-NDI-Fc:NE (d) Fc-NDI-Fc:NE.

The (δ_{free} - δ_{bound}) values in the equation 1, set for Hc-NDI-Hc, Hc-NDI-OH, Hc-NDI-Fc, and Fc-NDI-Fc titrations to obtain a good fit for the data using non-linear curve fitting method are 0.42, 0.42, 0.6, and 0.7 ppm respectively. The binding constants of NDI-NE complexes for Hc-NDI-Hc, Hc-NDI-OH, Hc-NDI-Fc and Fc-NDI-Fc determined by fitting the data in the non-linear curves are listed in Table 2.3. The binding constants were initially obtained in mM^{-1}, which is converted, to M^{-1}.

Table 2.3: Binding constants of NDI:NE complexes.

Compound	K (M^{-1})
Hc-NDI-Hc	2.85 ± 0.054
Hc-NDI-OH	3.27 ± 0.037
Hc-NDI-Fc	3.58 ± 0.056
Fc-NDI-Fc	5.06 ± 0.089

The binding constants (K) obtained form the NMR binding titrations indicate that the binding between the NDI and NE is low. This is very low compared to the K values obtained for the dimeric NDI and NE molecules but these values are consistent with those obtained by Iverson for the monomeric free NDI and NE. The solvents also play an important role in the binding between the NDI and NE. It is found previously that the K is small in less polar solvents and high in more polar solvents. In $CDCl_3$, which is a moderately polar solvent, the K values are expected to be low and are consistent with the previous report.[10] From the results the strength of the binding for the binding for different NDIs with NE is Fc-NDI-Fc > Fc-NDI-Hc > Hc-NDI-OH > Hc-NDI-Hc > br-NDI-br. These values are inconsistent with the initial hypothesis that incompatible side chains could break the interaction between the donor and acceptor units as they do in the solid state.

2.7 Electrochemistry

One of the interesting features that are observed for NDIs with different side chains is that it will affect the electron density. It is found that when NDI is attached with side chain containing electron-withdrawing atoms it becomes more electron-deficient. The presence of fluorocarbon and polar side chains both made the NDI more electron-deficient. This can be observed by analyzing the map of electrostatic surface potentials of the NDIs determined using by AM1 calculations on Spartan software (Figure 2.12). It is known that the reduction potentials decrease as the compounds become more electron-deficient. To check this, the reduction potentials of all the NDIs with different side chains were determined using cyclic voltammetry.

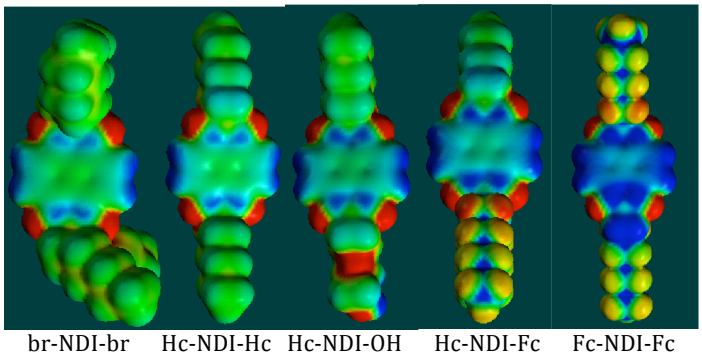

Figure 2.12: Electrostatic surface potentials of various NDIs.

The electrochemical properties of the NDIs (br-NDI-br, Hc-NDI-Hc, Hc-NDI-OH, Hc-NDI-Fc and Fc-NDI-Fc) and NE (**2**) were found by cyclic voltammetry. All samples (2×10^{-3} M) were prepared with tetrabutylammonium perchlorate (0.1 M) as the supporting electrolyte in methylene chloride. All measurements were done on a BAS Epsilon instrument, which has a three-electrode cell with platinum working and counter

electrodes and Ag/Ag^+ reference electrode. The redox potentials were determined versus Ag/Ag^+ reference electrolyte.

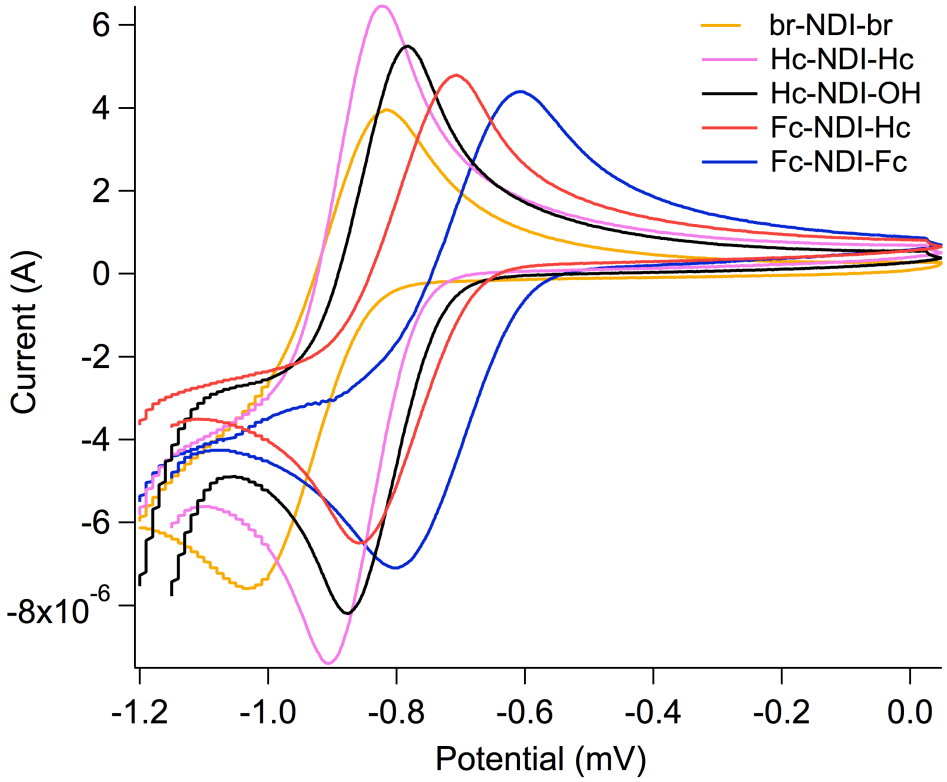

Figure 2.13: Cyclic voltammograms of NDIs. Potentials vs. Ag/Ag^+, Scan speed 100 mVs^{-1}

Table 2.4: Reduction potentials of various NDIs.

Sample	E_{red} (V)
br-NDI-br	-1.01
Hc-NDI-Hc	-0.911
Hc-NDI-OH	-0.887
Hc-NDI-Fc	-0.865
Fc-NDI-Fc	-0.799

The cyclic voltammograms of different NDIs are shown in Figure 2.13. The reduction potentials of NDIs are listed in Table 2.4. All the NDIs were reduced reversibly, indicating the formation of a stable radical anion. The reduction potentials and surface electrostatic potentials of the NDIs indicate that the electron-withdrawing side chains will make the NDI units electron-deficient. This is because of the inductive effect by the side chains.

2.8 Conclusions

The favorable interactions between the NDI acceptors and NE donor could not be broken in solution with the side chains selected for the study though some of this side chains has been used successfully to break this favorable interaction in the other donor-acceptor dyads in solid phase. The reasons for such discrepancy between the results obtained in the previous studies and this study could be because of the following differences. Firstly, the side chains were proved to break the interaction in other donor-acceptor complexes that may not be as strong the complex between the NDI and NE. Secondly, the previous studies were done on molecules that are covalently linked by rigid linkers in most cases and the energy gained due to the pi-pi stacking of homo-stacks is more per molecule than the energy gained by forming the homo-stacks of the monomers. Thirdly, the assemblies were obtained in the solid state and by process of careful crystallization. Fourthly, Aida *et. al*. used long chain and multiple incompatible side chains to break the donor acceptor interactions.[21] The other reasons for the observed differences could be as listed, (1) the NDI and NE are interacting in such a way that the donor acceptor complexes avoid the side chain interactions, thus making the unfavorable

interactions between the incompatible side chain and the favorable interactions between the compatible side chains un-operational. (2) The side chains are solvated by the solvent in which the studies were carried out, thus minimizing interactions between the side chains. (3) The NDI and NE interactions are so strong that the chain length and the number of the incompatible side chains used are not strong enough to break this favorable interaction. It was observed in this study that there is no complex formation between the br-NDI-br and NE. This could be because of the steric hindrance of the branched side chains, which prevent the approach of the planar donor and acceptor units studied here. It was also found that the binding constants decrease as the reduction potential of the NDI increases (more negative). Thus the observed lack of binding between the br-NDI-br and NE could be also because it has the highest reduction potential among all the NDI used.

2.9 Suggestions for future research

The following things could be tried in the future for affecting the favorable donor and acceptor interactions and obtaining the homo stacks of donors and acceptors. (1) The site of attachment of the side chains to the donor or acceptor could be changed in such a way that the unfavorable incompatible side chains interactions become operational. (2) The solvent used for the assembly could be changed so that the side chains can be de-solvated and interaction between them is maximized. (3) The number of aromatic units (NDI and NE) per molecule can be increased by attaching additional aromatic rings or attaching additional NDIs to the acceptor and additional NEs to the donor. This will increase the energy gained by the interaction of the hydrophobic aromatic units and hence lead to more propensity for self-stacking. (4) The length and number of incompatible side chains on the donor and acceptor could be increased to enhance the interactions between

the side chains thus leading the formation of homo-stacks of acceptors and donors. (5) Attachment of side chains on the NDI that do not change the electrostatics, so that the complex formation between the donor and acceptor becomes independent of electrostatics.

2.10 References

1. Benanti, T. L.; Saejueng, P.; Venkataraman, D., "Segregated assemblies in bridged electron-rich and electron-poor pi-conjugated moieties," *Chemical Communications* **2007**, 692-694.

2. Gabriel, G. J.; Sorey, S.; Iverson, B. L., "Altering the folding patterns of naphthyl trimers," *Journal of the American Chemical Society* **2005**, *127*, 2637-2640.

3. Horiuchi, S.; Yamochi, H.; Saito, G.; Sakaguchi, K.; Kusunoki, M., "Nature and origin of stable metallic state in organic charge-transfer complexes of bis(ethylenedioxy)tetrathiafulvalene," *Journal of the American Chemical Society* **1996**, *118*, 8604-8622.

4. Lin, F.; Huang, X. M.; Qu, S. C.; Fang, Z. Y.; Huang, S.; Song, W. T.; Zhu, X.; Liu, Z. F., "Characteristics of charge density waves on the surfaces of quasi-one-dimensional charge-transfer complex layered organic crystals," *Physical Review B* **2011**, *83*.

5. Percec, V.; Glodde, M.; Bera, T. K.; Miura, Y.; Shiyanovskaya, I.; Singer, K. D.; Balagurusamy, V. S. K.; Heiney, P. A.; Schnell, I.; Rapp, A.; Spiess, H. W.; Hudson, S. D.; Duan, H., "Self-organization of supramolecular helical dendrimers into complex electronic materials," *Nature* **2002**, *419*, 384-387.

6. Scott, J. C.; Bozano, L. D., "Nonvolatile memory elements based on organic materials," *Adv. Mater.* **2007**, *19*, 1452-1463.

7. Zych, A. J.; Iverson, B. L., "Conformational modularity of an abiotic secondary-structure motif in aqueous solution," *Helv. Chim. Acta* **2002**, *85*, 3294-3300.

8. Koshkakaryan, G.; Klivansky, L. M.; Cao, D.; Snauko, M.; Teat, S. J.; Struppe, J. O.; Liu, Y., "Alternative Donor-Acceptor Stacks from Crown Ethers and Naphthalene Diimide Derivatives: Rapid, Selective Formation from Solution and Solid State Grinding," *Journal of the American Chemical Society* **2009**, *131*, 2078-2079.

9. Bradford, V. J.; Iverson, B. L., "Amyloid-like behavior in abiotic, amphiphilic foldamers," *Journal of the American Chemical Society* **2008**, *130*, 1517-1524.

10. Cubberley, M. S.; Iverson, B. L., "H-1 NMR investigation of solvent effects in aromatic stacking interactions," *Journal of the American Chemical Society* **2001**, *123*, 7560-7563.

11. Gabriel, G. J.; Iverson, B. L., "Aromatic oligomers that form hetero duplexes in aqueous solution," *Journal of the American Chemical Society* **2002**, *124*, 15174-15175.

12. Lokey, R. S.; Iverson, B. L., "Synthetic molecules that fold into a pleated secondary structure in solution," *Nature* **1995**, *375*, 303-305.

13. Horiuchi, S.; Tokura, Y., "Organic ferroelectrics," *Nature Materials* **2008**, *7*, 357-366.

14. Alvey, P. M.; Reczek, J. J.; Lynch, V.; Iverson, B. L., "A Systematic Study of Thermochromic Aromatic Donor-Acceptor Materials," *Journal of Organic Chemistry* **2010**, *75*, 7682-7690.

15. Reczek, J. J.; Villazor, K. R.; Lynch, V.; Swager, T. M.; Iverson, B. L., "Tunable columnar mesophases utilizing C-2 symmetric aromatic donor-acceptor complexes," *Journal of the American Chemical Society* **2006**, *128*, 7995-8002.

16. Molla, M. R.; Das, A.; Ghosh, S., "Self-Sorted Assembly in a Mixture of Donor and Acceptor Chromophores," *Chemistry-a European Journal* **2010**, *16*, 10084-10093.

17. Hoeben, F. J. M.; Jonkheijm, P.; Meijer, E. W.; Schenning, A., "About supramolecular assemblies of pi-conjugated systems," *Chemical Reviews* **2005**, *105*, 1491-1546.

18. Syamakumari, A.; Schenning, A.; Meijer, E. W., "Synthesis, optical properties, and aggregation behavior of a triad system based on perylene and oligo(p-phenylene vinylene) units," *Chemistry-a European Journal* **2002**, *8*, 3353-3361.

19. Dunitz, J. D.; Gavezzotti, A.; Schweizer, W. B., "Molecular shape and intermolecular liaison: Hydrocarbons and fluorocarbons," *Helv. Chim. Acta* **2003**, *86*, 4073-4092.

20. Li, W. S.; Saeki, A.; Yamamoto, Y.; Fukushima, T.; Seki, S.; Ishii, N.; Kato, K.; Takata, M.; Aida, T., "Use of Side-Chain Incompatibility for Tailoring Long-Range p/n Heterojunctions: Photoconductive Nanofibers Formed by Self-Assembly of an Amphiphilic Donor-Acceptor Dyad Consisting of Oligothiophene and Perylenediimide," *Chemistry-an Asian Journal* **2010**, *5*, 1566-1572.

21. Che, Y. K.; Datar, A.; Balakrishnan, K.; Zang, L., "Ultralong nanobelts self-assembled from an asymmetric perylene tetracarboxylic diimide," *Journal of the American Chemical Society* **2007**, *129*, 7234-7235.

22. Greenfield, S. R.; Svec, W. A.; Gosztola, D.; Wasielewski, M. R., "Multistep photochemical charge separation in rod-like molecules based on aromatic imides and diimides," *Journal of the American Chemical Society* **1996**, *118*, 6767-6777.

CHAPTER 3

EFFECT OF SIDE CHAINS ON DONOR-ACCEPTOR COMPLEX IN QUATER THIOPHENE-NAPHTHALENE DIIMIDE DYADS

3.1 Introduction

In the previous chapter, the role of side chains on the donor-acceptor complexes was studied. Contrary to our hypothesis, it was found that the donor-acceptor binding is not varied even if the side chains on the donor and acceptor are incompatible in nature. The indifference in binding could be because the donor and acceptor are not linked and thus they could adopt any conformation in solutions that avoid the side chain interactions but still form a complex.

In this chapter, we covalently linked the donor and acceptor units to reduce the number of conformations and hence minimize the number of possibilities that donor and acceptor units take to avoid the side chain interactions in solution. We hypothesized that this may enhance the effect of side chains of the donor acceptor dyad and hence may have effect on the donor-acceptor interactions.

The side chains selected for the study are based on the previous literature that suggests the importance of side chains on the donor-acceptor interactions. In our group, Benanti *et. al.* have obtained segregated assembly of donors and acceptors by the use of incompatible aliphatic hydrocarbon-aliphatic fluorocarbon side chains.[1] Naphthalene imide acceptor is linked covalently to naphthalene ether donor to obtain dyads **1-3** (Figure 3.1). Fluorocarbon and hydrocarbon side-chains were attached to naphthalene imide and naphthalene ether units, respectively. The incompatible side chain pair was selected based on the fact that the aliphatic hydrocarbons do not co-crystallize with

aliphatic fluorocarbons due to their mutual phobicity. The mutually phobic hydrocarbon fluorocarbon side chains on the dyads resulted in segregation of donor acceptor units while the same dyads without side chains resulted in the mixing of donor acceptor units as evidenced by the crystal structures. The results indicated the incompatible hydrocarbon fluorocarbon side chains affect the favorable donor-acceptor interactions in the donor-acceptor dyads in the solid state.[1]

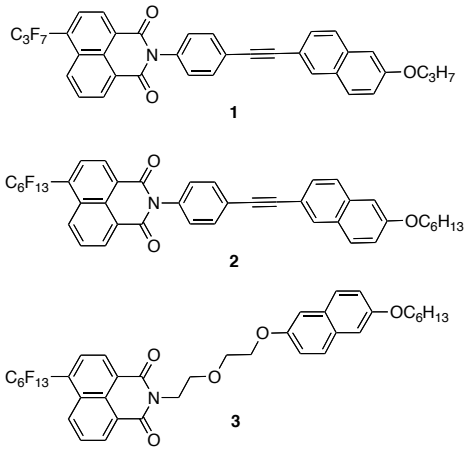

Figure 3.1: NI-NE dyads **1-3**

Similarly, Aida and co-workers proved the role of incompatible amphiphilic, polar and non-polar side chains on the donor-acceptor interactions.[2,3] They synthesized quaterthiophene-C60 and quaterthiophene-perylenediimide dyads with amphiphilic side chains attached to the donor and acceptor units. Segregated continuous stacks of donor and acceptor units were obtained in spite of the fact that the donor and acceptor units tend to stack over each other to form charge transfer complexes. However, these assemblies could be obtained in the solid state by carefully controlling the temperature and solvent composition.[2,3]

To date, there are no previous attempts to study the effect of incompatible side chains on the packing of donor-acceptor units of dyads in solution. If the incompatible side chains produce similar effect as in the solid state then it is possible to tune the donor-acceptor interactions. In addition to the hydrocarbon-fluorocarbon, and polar-non polar side chains we have used geometrically incompatible branched-linear hydrocarbon side chain pair. A tool to control the donor-acceptor interactions in solution is important for obtaining continuous segregated assemblies of donors and acceptors in the solid state. Venkataraman *et. al*., Hoppe *et. al*., and Gunes *et. al*. have pointed out that such assemblies are desirable for the active layer of organic solar cells.[4-6] Additionally, the solution-processable organic solar cells have low fabrication costs.[7]

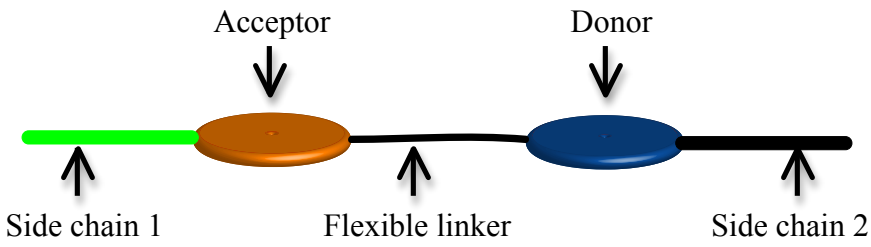

Figure 3.2: Donor-acceptor dyad, side chains 1 and side chain 2 are incompatible.

The molecular model of the dyads used for study of the effect of incompatible side chains on donor-acceptor interactions in solution is shown in Figure 3.2. This chapter also aims to find the photophysical properties of the dyads to understand the differences in quenching dynamics with respect to the side chains. Extensive studies on charge transfer characteristics of several donor-acceptor dyads were studied[8-12], but the photophysical properties of quaterthiophene-naphthalenediimide dyads with flexible linker have not been studied before.

3.2 Synthesis of the dyads

Quarterthiophene (QT) – naphthalene diimide (NDI) dyads are used to serve as a model for the studies of the effect of side chains on the donor-acceptor complexes. Naphthalene diimide is chosen as an acceptor because it was used as an efficient n-type[13-19] organic semiconductor. Quaterthiophene is chosen as thiophene based oligomers[20]/polymer[21] are used as p-type semiconductors in organic solar cells. The donor and acceptor chosen are thus relevant for making organic solar cells. They also serve as model compounds to extrapolate the properties of polymers made with these dyads. All the QT-NDI dyads have the following essential features as shown in Figure 3.3: (1) Electron-rich QT donor covalently attached to the electron-deficient NDI acceptor with a flexible linker. (2) QT with hydrophobic hexyl side-chain. (3) Hydrophobic/Polar/Fluorocarbon or branched side-chain attached to the NDI acceptor.

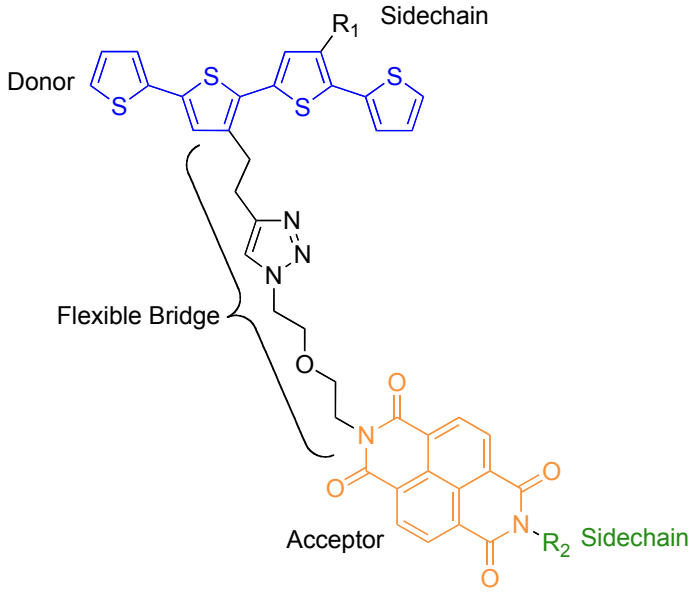

Quaterthiophene-Naphthalenediimide dyad
R1 = Aliphatic hydrocarbon
R2 = Aliphatic hydrocarbon/Fluorocarbon/branched/polar

Figure 3.3: Quaterthiophene-naphthalene diimide (**QT-NDI**) dyad.

The donor part (**14**) of the dyad was synthesized using the scheme shown in Figure 3.4, which was started from a commercially available compound thiophene-3-methanol (**5)**. The compound **6** was obtained by stirred compound **5** in a biphasic mixture of CH_2Cl_2 and concentrated HCl, which resulted in the substitution of the hydroxyl of **5** with a chloro group. The protected terminal alkyne contained in compound **7** was obtained in a very good yield by the reaction of **6** with lithiated 1-triisopropylsilyl (TIPS)-1-propyne. The bromination of compound **7**, with 1 equivalent of NBS in $HOAc/CHCl_3$ medium produced the mono-brominated product, compound **8** in 82% yield. Palladium catalyzed Suzuki coupling was used to synthesize the bithiophene compound (**11**) by the reaction of compound **8** and 4-alkylthiophene-2-boronic ester (**10)**.

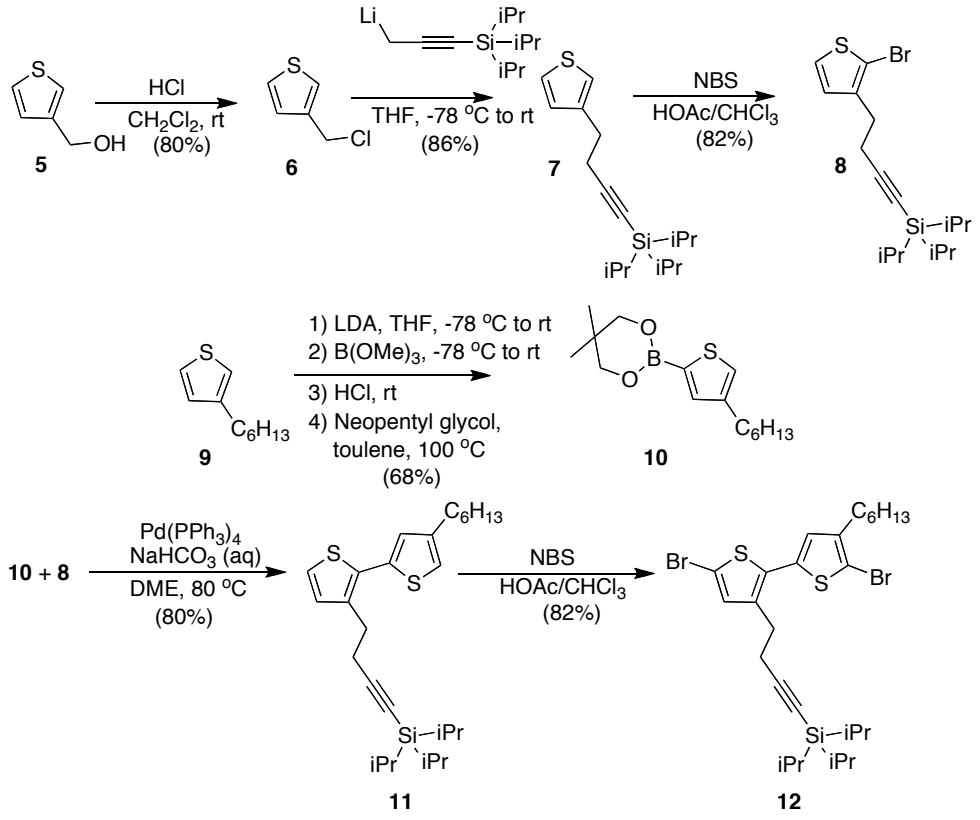

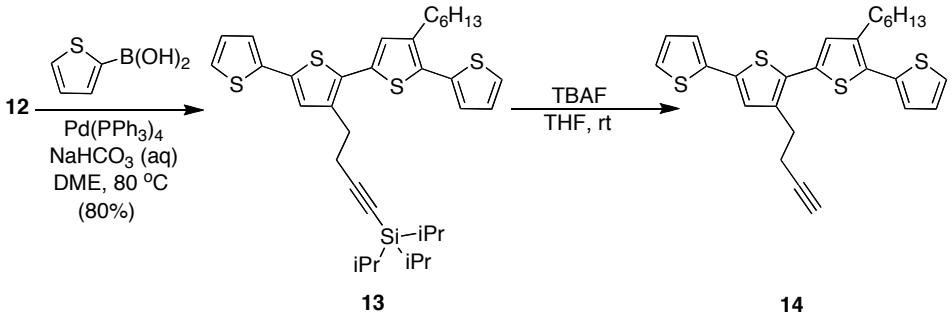

Figure 3.4: Synthesis of **QT** donor**.**

The compound **10** was obtained by subjecting the 3-hexylthiophene (**9**) to LDA (generated in situ) and trimethylborate. The resulting reaction mixture was hydrolyzed to thiophene boronic acid, which can be converted without purification to the desired neopentyl glycol ester (**10**). The reaction of NBS with **11** gave the dibrominated product **12**. The quarterthiophene **13** was obtained by palladium catalyzed Suzuki coupling reaction of the dibrominated compound **12** and 2-thiophene boronic acid. The compound **14** was obtained by the de-protection of the terminal alkyne **13** by reacting with TBAF and was used for the synthesis of dyads without further purification.

The synthesis of acceptors for the dyads is shown in Figure 3.5. Compounds **16a-16d** were synthesized by refluxing commercially available napthalene dicarboxylicanhydride **15** with equimolar mixtures of 2-(2-aminoethoxy)ethanol and the corresponding amine ($R\text{-}NH_2$) using procedures reported in the literature. All the amines used for the synthesis of **16a-16d** are commercially available except the branched amine, $(C_6H_{13})_2CHNH_2$, which was prepared from $(C_6H_{13})_2CO$ using previously reported synthetic protocol (Compound **4** in Chapter 2). The alcohol at the terminus on the NDI side chain was first mesylated and corresponding azides **17a-17d** were obtained by the reaction of the mesylate with sodium azide.

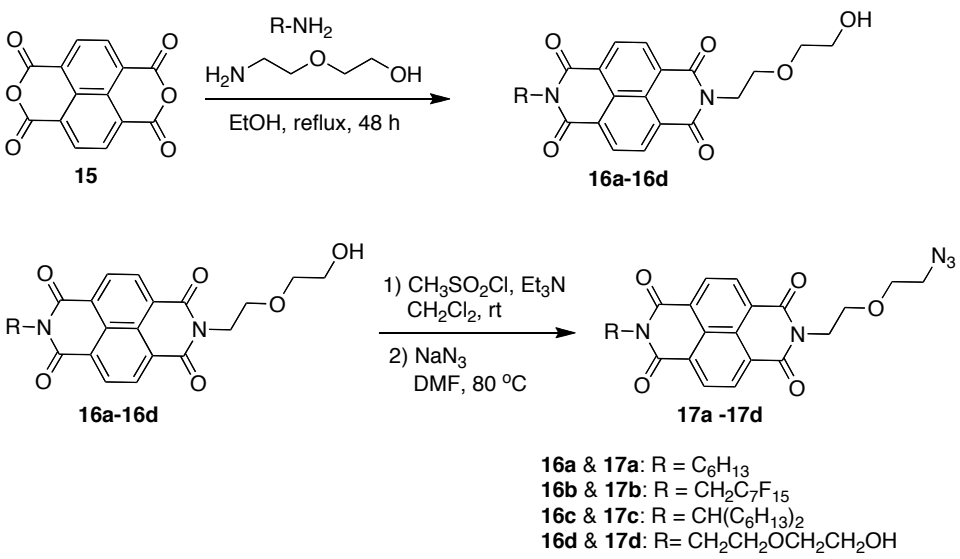

Figure 3.5: Synthesis of NDI acceptors with various side chains.

The dyads **1-4** were synthesized through the copper-catalyzed 1,3-Huisgen cycloaddition between quaterthiophene **14** and **17a-17d**. In addition to the dyads, we also synthesized a control quaterthiophene molecule **18**, to probe the effect of the presence of napthalene diimide by copper-catalyzed 1,3-Huisgen cycloaddition between quaterthiophene **14** and Hexylazide (Figure 3.6).

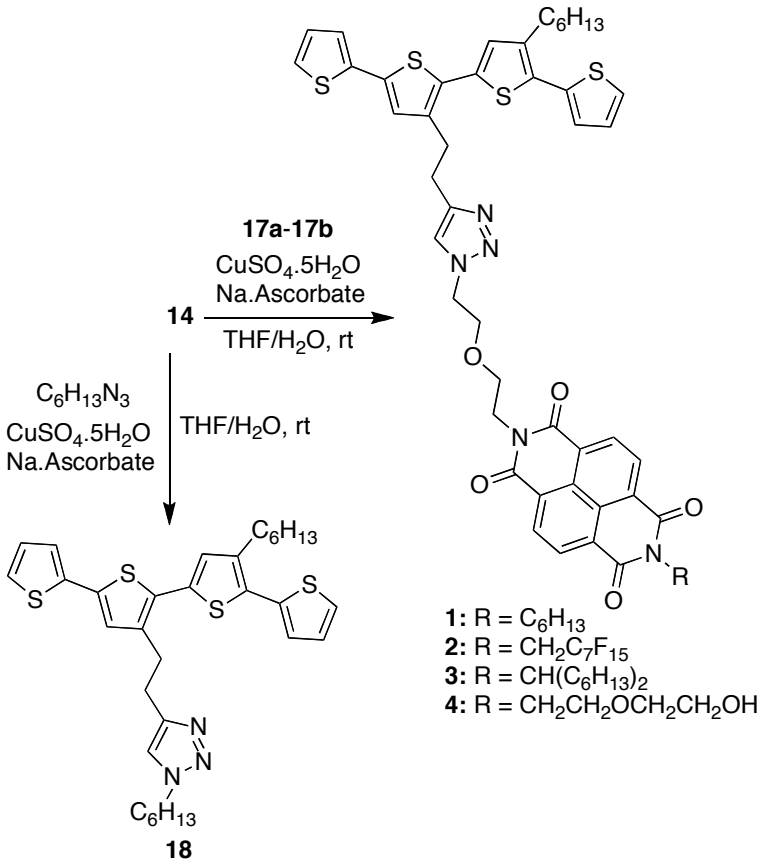

Figure 3.6: Synthesis of QT-NDI dyads (**1**-**4**) and control donor molecule (**18**).

3.3 Characterization

All the compounds were characterized by using ^{1}H and ^{13}C NMR. Figure 3.7 shows the ^{1}H NMR spectra of dyad **1** in $CDCl_3$. Furthermore, they were confirmed by the mass spectroscopy. The peak after 8 ppm corresponds to the aromatic NDI protons of the dyads. The eight aromatic QT peaks appears at 7.36, 7.29, 7.21, 7.12, 7.07, 7.04, 7.01 and 6.88 ppm. The important indications for the covalent linkage between the QT and NDI units are the presence of triazole proton that is observed at 6.77 ppm and the absence of the alkyne proton of compound **14**.

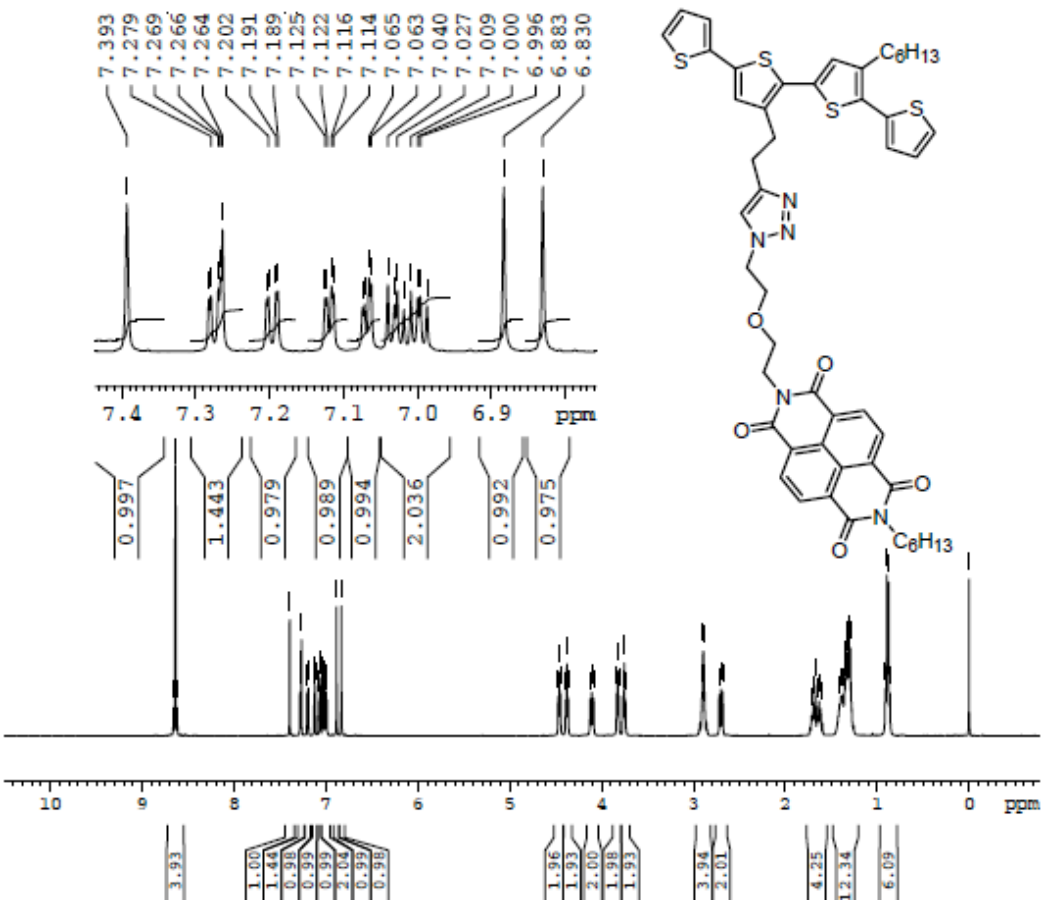

Figure 3.7: ^{1}H NMR of dyad **1** in $CDCl_3$

The absorption characteristics, orbital energies, and the quenching dynamics of the dyads will provide the information regarding the donor acceptor complexes of the dyads. These characteristics were studied and will be discussed in detail in the following sections.

3.4 Absorption characteristics

Absorption measurements: The UV-visible absorption spectra of the compounds were measured on a Shimadzu UV 2600PC spectrometer. All solutions were prepared in chloroform.

Figure 3.8 shows a representative UV-Vis spectra for the dyad (**1**) and its components, the acceptor (**16a**) and donor (**13**). The absorption spectra of the dyad between 300 and 500 nm resembles the spectra obtained by the superposition of the absorption spectra of the constituents, **16a** and **13** with sharp vibronic peaks of the naphthalene diimide and the broad absorption band of the quarternary thiophene.

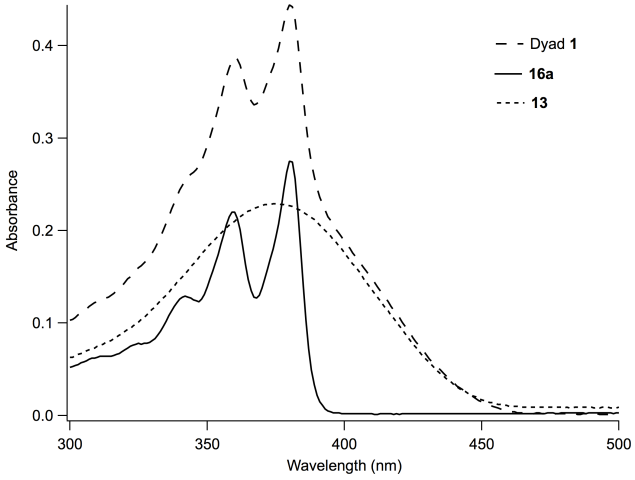

Figure 3.8: UV-Vis absorption spectra of dyad **1** and its components, acceptor (**16a**) and donor (**13**) at concentration = 10^{-3} M.

Dyads **1-4** also have a broad absorption around 500-600 nm, presumably from the charge transfer interaction of the donor with the acceptor (Figure 3.9). The two typical charecteristics of the charge transfer interaction are (1) the presence of an absorption peak that is not present in either donor or acceptor units, and (2) absorption band at long wavelengths. These characteristics for the charge transfer interaction between the donor QT and acceptor NDI are fulfilled in the Dyads **1-4** as shown in Figure 3.10.

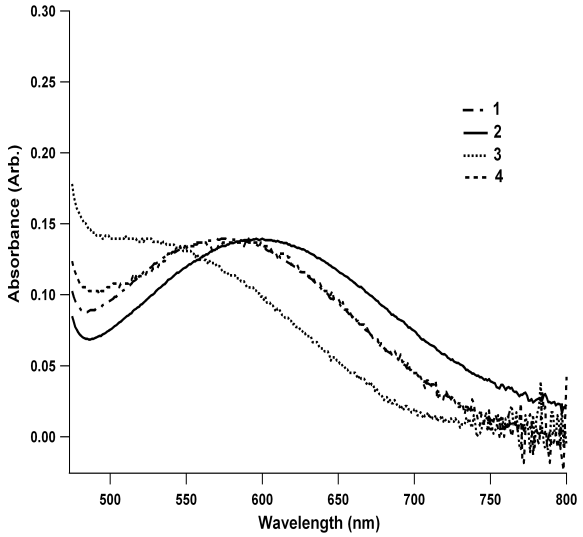

Figure 3.9: Absorption spectra of dyads **1**-**4** in chloroform showing the absorption attributable to quaterthiophene-napthalene diimide charge-transfer interaction.

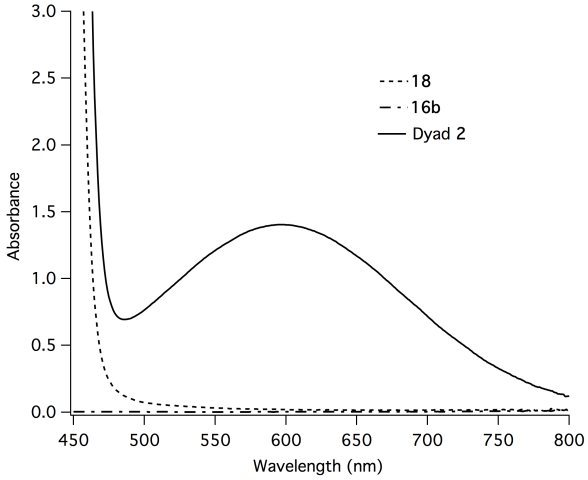

Figure 3.10: Absorption spectra of dyad **2**, acceptor **16b**, and donor **18**.

Another important charecteristic of the charge-transfer interaction is the sensitivity of the absorption band to solvent polarity. Figure 3.11 shows the absoption spectra of Dyad 2 in chloroform, dichlolоromethane and acetonitrile. The change in the λ_{max} is observed with change in the polarity of the solvent supporting the presence of charge transfer interaction between the acceptor and donor in dyads.

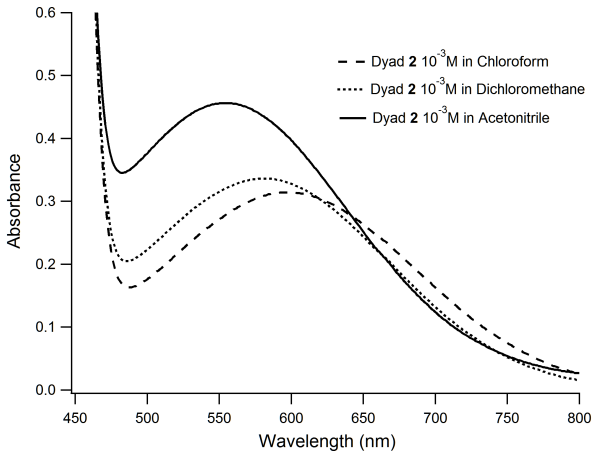

Figure 3.11: Absorption spectra of dyad **2** in chloroform, dichloromethane, and acetonitrile.

The charge transfer interaction observed in the dyads may be due to intramolecular or intermolecular interaction between the donor and acceptor. To test this the intensity of the charge transfer peak is observed for the dyads **2** with increasing concentration (Figure 3.12). It is observed that the intensity of this peak changes linearly with concentration in accordance with the Beer-Lambert law (Figure 3.13). These observations are consistent with an intramolecular donor-acceptor interaction instead of intermolecular donor-acceptor interaction.

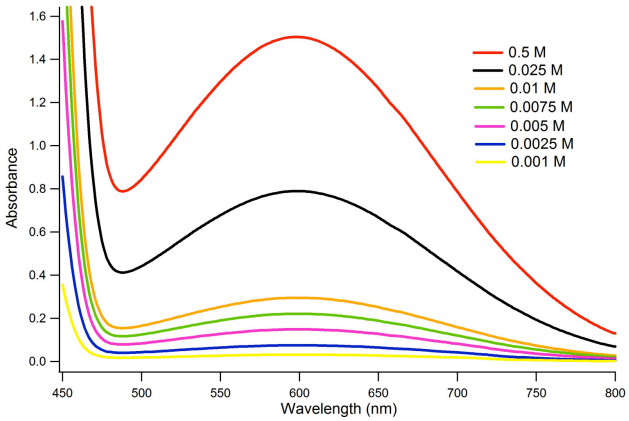

Figure 3.12: The absorption spectra of dyad **2** at various concentrations in chloroform.

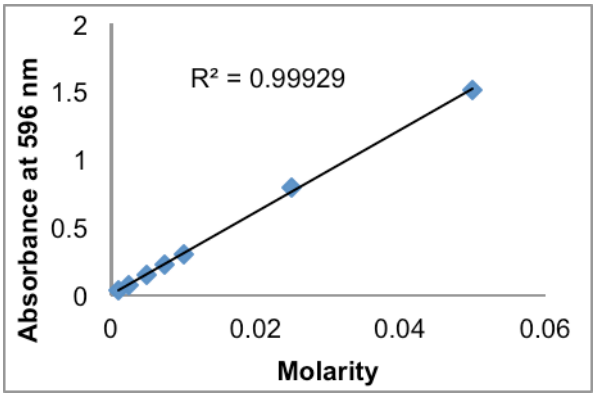

Figure 3.13: Beer-Lambert's plot for charge transfer band of dyad **2**.

3.5 Fluorescence spectroscopy

Fluorescence spectra were obtained on the same setup used for the measurement of time-resolved fluorescence measurements. All solutions were prepared in chloroform. Figure 3.14 shows a representative emission spectra for the donor (**13**) and absorption spectra of the acceptor (**16a**). The emission spectra of **13** was obtained by exciting **13** at λ= 405 nm; the acceptor does not have absorbance at this wavelength. From Figure 3.14, it can be ascertained that there is zero overlap between the emission spectra of the donor and the absorbance spectra of the acceptor.

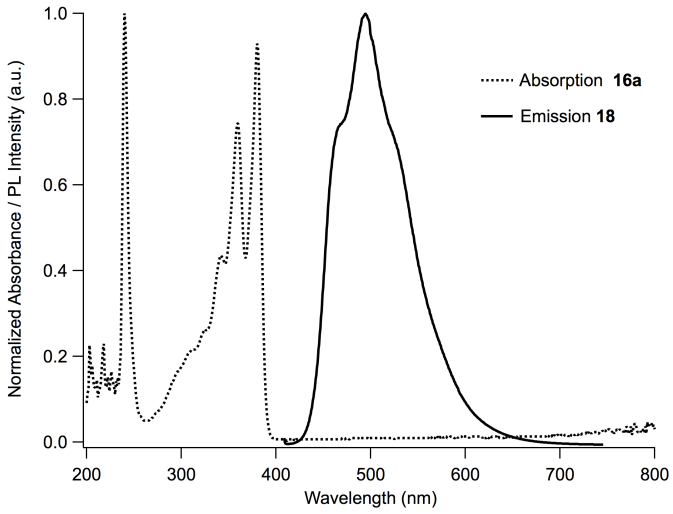

Figure 3.14: Absorption spectra of acceptor (**16a**) and emission spectra of donor (**18**).

We observed the presence of the charge-transfer band in all the dyads **1**-**4**. This indicated the formation of the charge transfer complex between the donor and the acceptor. However, we also observed slight difference in the λ_{max} indicating that the side-chains may have an effect in the formation of the complex. Thus, to find out if these subtle changes would affect the photophysical properties especially on the energy or electron transfer kinetics we have carried out fluorescence quenching studies on the dyads.

Figure 3.15 shows representative emission spectra illustrating the quenching of donor fluorescence upon attachment to the acceptors (**17a-d**), compared to the donor alone (**13**). In all the dyads the photoluminiscence intensity dropped significantly compared to the donor alone. In dyads (**3** and **4**) the intensity dropped to 15.5%, in **2** to 18.6 % and in **1** it decreased to 16.4%.

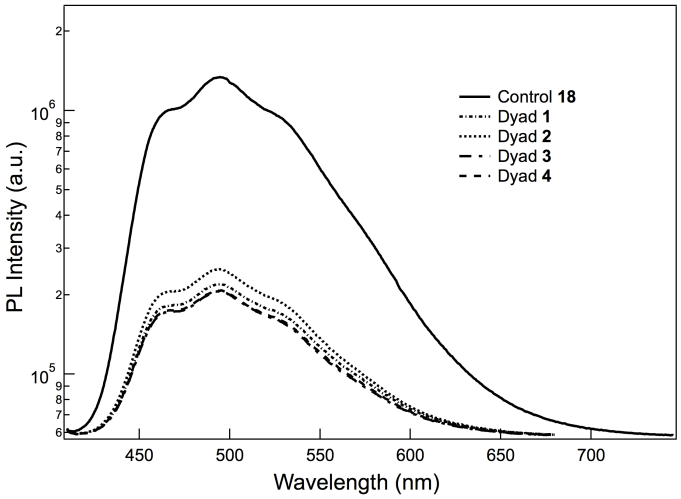

Figure 3.15: Fluorescence spectra of the donor (**18**) and dyads (**1-4**). The concentration for all the compounds was 1 x 10^{-4} M in chloroform and the excitation wavelength was 405 nm.

3.6 Electrochemistry

The electrochemical properties were determined by cyclic voltammetry on a BAS Epsilon system. The setup consisted of three-electrode cell with Pt as working and as counter electrodes; and Ag/Ag^+ reference electrode. Samples were prepared in methylene chloride (c = 2 x 10^{-3} M) with tetrabutylammonium perchlorate (0.1 M) as the supporting electrolyte. The reduction and oxidation potentials were determined versus a ferrocene-ferricenium (Fc/Fc^+) standard. The working and auxiliary electrodes were cleaned after each run.

We measured the oxidation and reduction potentials of the acceptors (**16a-c, 17d**), donor (**13**), and dyads (**1-4**) using cyclic voltammetry (CV). The measured potentials were calibrated with the standard ferrocene-ferricenium (Fc/Fc^+). The HOMO levels and LUMO levels were obtained from the oxidation and reduction potentials. The optical band gap of acceptors and donor were determined from the UV-Vis absorption spectra.

Figure 3.16 shows the cyclic voltammograms of dyad **1**, donor **13** and acceptor **16a**. All the dyads were characterized by two waves corresponding to the oxidation of quaterthiophene and to the reduction of naphthalene diimide.

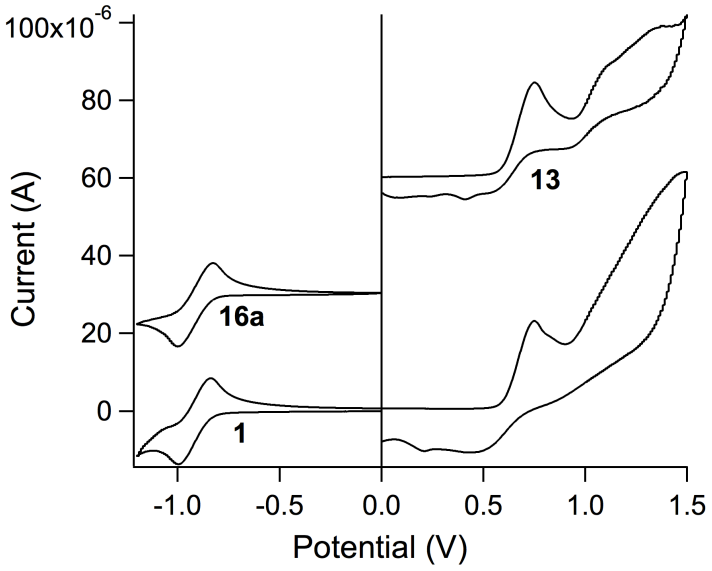

Figure 3.16: The cyclic voltammogramm of the dyad (**1**), acceptor (**16a**) and donor (**13**) determined in dichloromethane in presence of 0.1 M TBAP.

The oxidation of quaterthiophene donor (**13**) was found to be quasi-reversible. Reduction peak of NDI was reversible that indicated the formation of a stable radical anion. LUMO values of **16a-c**, **17d** are reported in Table 3.**1**. The HOMO energy levels could not be determined at the operating voltages used for our experiments. Thus these values were derived from optical band gaps and the LUMO values from CV.

The energy levels of the LUMO of the donor and LUMOs of the acceptors are situated such that it is energetically favorable for the electron transfer from the donor to the acceptor. The difference in energy between the LUMOs is found to be highest in the case of dyad **2**.

Table 3.1: Molecular orbital energies of the dyads and the components quaterthiophene and naphthalene diimide moieties.

Compound	E_{red}	E_{ox}	LUMO (eV)	HOMO (eV)	ΔE_{opt}
16a	-1.08		-3.72	-6.91 [a]	3.19
16b	-1.00		-3.80	-7.01 [a]	3.21
16c	-1.09		-3.73	-6.88 [a]	3.15
17d	-1.05		-3.78	-6.93 [a]	3.15
13		0.53			
1	-1.09	0.54			
2	-1.02	0.52		-	
3	-1.11	0.53			
4	-1.09	0.53			

Sample concentration 2 x 10^{-3}M in Dichloromethane-TBAP (0.1 M) vs Ag/Ag+ reference electrode, scan speed = 100 mVs-1, For irreversible redox process, E_0 found at $I_0=I_p$ x 0.855. E_{ox} and E_{red} are reported vs. Fc/Fc+ standard. Values of HOMO and LUMO were based on Fc/Fc+ being -4.8 eV. ΔE_{opt} are optical band gap found determined from the energy at lowest energy excitation [a] Values determined using the energies of frontier orbitals and $\Delta E_{opt.}$[22]

From the Table 3.1, it can be observed that, the E_{ox} and E_{red} values of the individual donors, and acceptors almost remain same in the dyads. This probably indicates that the complexed dyad that was observed as charge transfer band in the optical absorption spectroscopy is below the limit of detection of the cyclic voltammetry.

3.7 Time resolved fluorescence

We measured the time-resolved quenching decay dynamics using time-correlated single-photon-counting to investigate the exciton dynamics of the dyads in more detail. The samples were excited using 405 nm pulsed diode laser with a repetition rate of 40MHz and pulse width of 50 ps, which only excited the quaterthiophene moiety. The collected fluorescence was dispersed by a spectrograph/ monochromator. A CCD camera recorded the steady-state fluorescence. The time-resolved fluorescence (TRFL) at

emission peak of 490nm was detected with an avalanche photodiode (APD, id Quantique id100-50) for photon counting, and the APD output was analysed by a time-correlated single photon counting (TCSPC) board (PicoQuant PicoHarp 300). The instrument response function (IRF) has a full width at half-maximum of ~50 ps. By fitting the TRFL decay curves with a single exponential decay, we obtained the lifetimes of excited states for donor QT and dyads with different side-chains.

Figure 3.17 shows the photoluminescence (PL) dynamics of donor (**18**) and dyad **1** on excitation of donor at 405 nm in chloroform. The analysis of the PL emission was done at 490 nm, close to the emission maximum of the donor molecules. The photoluminescence dynamics at other wavelengths within the donor emission spectrum show very similar decay. We observed that the dyad PL decay rate was faster than PL quenching of the donor alone. The decay curves show a single-exponential decay indicating a single pathway for quenching process, i.e. unimolecular quenching. The occurence of bimolecular intermolecular quenching could be excluded as the concentration of the solutions used were very low (10^{-4} M), and also based on the fact that the quenching rate is independent of concentration of the dyad.

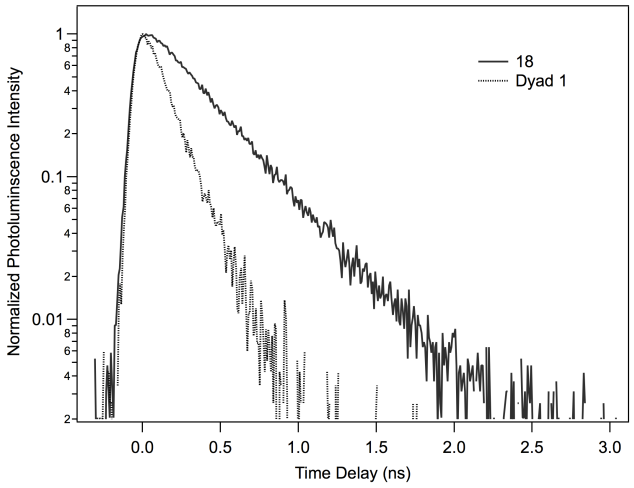

Figure 3.17: Fluorescence decay of donor in dyad (**1**) and donor (**13**). Concentrations of 18 and 1 are 1 x 10^{-4} M in chloroform. Excitation wavelength 405 nm and emission observed at 490 nm.

The exciton lifetime (τ) of donor was found to be 366 ps. In contrast, when dyads **1**-**4** are excited at the same wavelength, the lifetimes were observed to be 165, 172, 157, and 163 ps respectively.

The rapid quenching of donor fluorescence observed could be either due to the photoinduced energy transfer or electron transfer. A close examination of the UV-Vis and emission spectra of the individual donor and acceptor shows that there is no overlap of the donor emission and absorption of acceptor. This indicates that photoinduced energy transfer from donor to the acceptor can be clearly excluded. Thus, the changes that were observed in the fluorescence intensity of dyads can be unambigously assigned to an efficient photoinduced electron transfer (PET) from the donor to the acceptor. Furthermore, the results from CV also indicates the possibility of electron transfer.

The rate constant for electron transfer (k_{ET}) was determined from lifetimes using equation (2).

$$k_{ET} = 1/\tau_{dyad} - 1/\tau_{donor} \quad (2)$$

Results from fluorescence quenching studies are presented in Table 3.2. There is no appreciable change in the electron transfer rates among the four dyads (**1**-**4**) and were consistently measured.

Table 3.2: Lifetimes and electron transfer rates of dyads **1**-**4** and donor.

Compound	τ (ps)	k_{ET} (10^9s)
1	165	3.33
2	172	3.08
3	153	3.80
4	167	3.26
18	366	-

Charge transfer complex bands at longer wavelengths were seen in all the dyads studied. Such changes typically indicate interaction between the donor and acceptor units of the dyads. Fujitsuka *et. al*. have reported that the electron transfer in donor-bridge-acceptor dyads with flexible linker occurs in the folded conformation.[23] It can be fairly assumed that in the dyads (**1**-**4**) also, the electron transfer takes place in the folded conformation of the DBA dyad molecules, where the quaterthiophene donor and NDI acceptor weakly interact with each other as observed from the absorption spectra.

The dyads (**1**-**4**) are chosen such that the side-chain attached to the acceptor NDI unit is either compatible or incompatible (chemical/geometrically) in nature to the side-chain attached to the donor. In dyad **1**, the interaction between the hydrocarbon-

hydrocarbon side-chains on donor and acceptor is favorable. In contrast, the dyads **2-4** have incompatible side-chains on the donor and acceptor units. In the folded conformation of the dyad, **1** should have more favorable interactions between the side-chains than between the acceptor and donor units in **2-4** which have incompatible side-chains, provided the solvent does not weaken those interactions. Thus it can be assumed that the electron transfer rates should vary among the dyads. This assumption is consistent with the previous observation that bulky subsitutents on donor-acceptor complexes will alter the nature of interacton between the donor and acceptors and that the quenching rates will differ with respect to the distance and geometry between the acceptor and donor units of the rigid dyads.

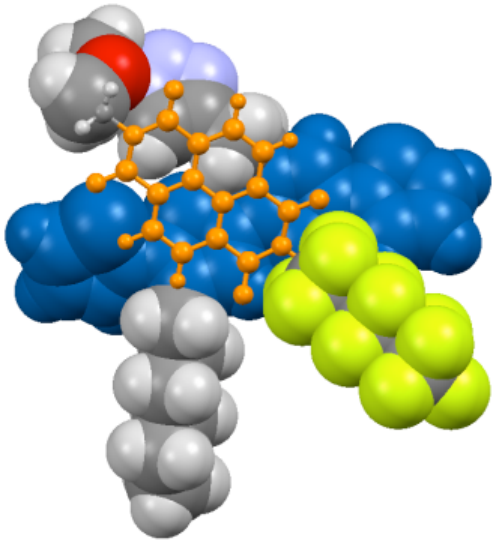

Figure 3.18: A calculated conformation for dyad **2** indicating that although there is interaction between the quaterthiophene (blue) and naphthalene diimide (orange) units, there is no interaction between the hydrocarbon and fluorocarbon side chains.

Our finding that electron transfer rates were independent of the nature of the side-chains is therefore unexpected. The indifferences in ET rates in these dyads indicate that the interactions (favorable or non-favorable) between the side chains are very minimal

and the donor and acceptor moieties can adopt conformation in which the side chain are far apart and their interactions are minimal. For example, in dyad **2**, which has hydrocarbon and fluorocarbon side-chains, a calculated energy minimized folded conformation indicates that although there is an interaction between the quaterthiophene and naphthalene diimide moieties, there is minimal interaction between the side-chains (Figure 3.18).

3.8 Conclusions

We have observed a strong donor fluorescence quenching in the dyads based on quaterthiophene donor and naphthalene diimide acceptor with different side chains. The UV-Vis and emission spectra of the acceptor and donor do not overlap indicating the possibility of electron transfer rather than energy transfer. The time resolved fluorescence data indicates rapid decay rates in all dyads indicating electron transfer from the donor to the acceptor moiety. The energy levels of the LUMOs of the donor and the acceptor are situated to favour the electron transfer from donor to the acceptor. The electron transfer rates of the all the dyads are found to be same, indicating that incompatible side-chains attached to the acceptors do not affect the electron transfer rates in the dyads.

We believe that the solvent molecules are weakening the unfavourable side chain interactions, and the donor and acceptor can adopt an orientation that avoids side chain interactions. We hope that this study will stimulate future research into pathways to control the electron transfer rates and charge recombination rates based on subtle changes in the structures of the dyads and polymers with covalently linked acceptor donor units.

3.9 Suggestions for future research

Future investigations should be focused on varying the factors that lead to stronger unfavorable interactions between the side-chains and to obtain segregated assemblies of donors and acceptors in solution. The following things could be tried. (1) The solvent could be changed so that the side chains can be de-solvated and interactions between side chains are maximum. (2) The length and number of incompatible side chains on the donor and acceptor could be increased to enhance the interactions between the side chains. (4) The donor and acceptor could be attached by using a rigid linker to prevent the intramolecular complexation between the donor and acceptor units.

3.10 References

1. Benanti, T. L.; Saejueng, P.; Venkataraman, D., "Segregated assemblies in bridged electron-rich and electron-poor pi-conjugated moieties," *Chemical Communications* **2007**, 692-694.

2. Li, W. S.; Saeki, A.; Yamamoto, Y.; Fukushima, T.; Seki, S.; Ishii, N.; Kato, K.; Takata, M.; Aida, T., "Use of Side-Chain Incompatibility for Tailoring Long-Range p/n Heterojunctions: Photoconductive Nanofibers Formed by Self-Assembly of an Amphiphilic Donor-Acceptor Dyad Consisting of Oligothiophene and Perylenediimide," *Chemistry-an Asian Journal* **2010**, *5*, 1566-1572.

3. Li, W. S.; Yamamoto, Y.; Fukushima, T.; Saeki, A.; Seki, S.; Tagawa, S.; Masunaga, H.; Sasaki, S.; Takata, M.; Aida, T., "Amphiphilic molecular design as a rational strategy for tailoring bicontinuous electron donor and acceptor arrays: Photoconductive liquid crystalline oligothiophene-C-60 dyads," *Journal of the American Chemical Society* **2008**, *130*, 8886-8887.

4. Gunes, S.; Neugebauer, H.; Sariciftci, N. S., "Conjugated polymer-based organic solar cells," *Chem. Rev.* **2007**, *107*, 1324-1338.

5. Hoppe, H.; Sariciftci, N. S., "Morphology of polymer/fullerene bulk heterojunction solar cells," *J. Mater. Chem.* **2006**, *16*, 45-61.

6. Venkataraman, D.; Yurt, S.; Venkatraman, B. H.; Gavvalapalli, N., "Role of Molecular Architecture in Organic Photovoltaic Cells," *Journal of Physical Chemistry Letters* **2010**, *1*, 947-958.

7. Griffini, G.; Douglas, J. D.; Piliego, C.; Holcombe, T. W.; Turri, S.; Frechet, J. M. J.; Mynar, J. L., "Long-Term Thermal Stability of High-Efficiency Polymer Solar Cells Based on Photocrosslinkable Donor-Acceptor Conjugated Polymers," *Adv. Mater.* **2011**, *23*, 1660-1664.

8. Guldi, D. M., "Fullerene-porphyrin architectures; photosynthetic antenna and reaction center models," *Chem. Soc. Rev.* **2002**, *31*, 22-36.

9. Collin, J. P.; Guillerez, S.; Sauvage, J. P.; Barigelletti, F.; Decola, L.; Flamigni, L.; Balzani, V., "Photoinduced processes in dyads and triads containing a ruthenium

(II) bis(terpyridine) photosensitizer covalently linked to electron-donor and acceptor groups," *Inorg. Chem.* **1991**, *30*, 4230-4238.

10. Imahori, H.; Guldi, D. M.; Tamaki, K.; Yoshida, Y.; Luo, C. P.; Sakata, Y.; Fukuzumi, S., "Charge separation in a novel artificial photosynthetic reaction center lives 380 ms," *J. Am. Chem. Soc.* **2001**, *123*, 6617-6628.

11. Imahori, H.; Tamaki, K.; Guldi, D. M.; Luo, C. P.; Fujitsuka, M.; Ito, O.; Sakata, Y.; Fukuzumi, S., "Modulating charge separation and charge recombination dynamics in porphyrin fullerene linked dyads and triads: Marcus-normal versus inverted region," *J. Am. Chem. Soc.* **2001**, *123*, 2607-2617.

12. Kuciauskas, D.; Lin, S.; Seely, G. R.; Moore, A. L.; Moore, T. A.; Gust, D.; Drovetskaya, T.; Reed, C. A.; Boyd, P. D. W., "Energy and photoinduced electron transfer in porphyrin-fullerene dyads," *J. Phys. Chem.* **1996**, *100*, 15926-15932.

13. Gawrys, P.; Boudinet, D.; Zagorska, M.; Djurado, D.; Verilhac, J. M.; Horowitz, G.; Pecaud, J.; Pouget, S.; Pron, A., "Solution processible naphthalene and perylene bisimides: Synthesis, electrochemical characterization and application to organic field effect transistors (OFETs) fabrication," *Synth. Met.* **2009**, *159*, 1478-1485.

14. Kruger, H.; Janietz, S.; Sainova, D.; Dobreva, D.; Koch, N.; Vollmer, A., "Hybrid supramolecular naphthalene diimide-thiophene structures and their application in polymer electronics," *Adv. Funct. Mater.* **2007**, *17*, 3715-3723.

15. Lee, Y. L.; Hsu, H. L.; Chen, S. Y.; Yew, T. R., "Solution-processed naphthalene diimide derivatives as n-type semiconductor materials," *Journal of Physical Chemistry C* **2008**, *112*, 1694-1699.

16. See, K. C.; Landis, C.; Sarjeant, A.; Katz, H. E., "Easily synthesized naphthalene tetracarboxylic diimide semiconductors with high electron mobility in air," *Chem. Mater.* **2008**, *20*, 3609-3616.

17. Shao, H.; Nguyen, T.; Romano, N. C.; Modarelli, D. A.; Parquette, J. R., "Self-Assembly of 1-D n-Type Nanostructures Based on Naphthalene Diimide-Appended Dipeptides," *J. Am. Chem. Soc.* **2009**, *131*, 16374-16376.

18. Shukla, D.; Nelson, S. F.; Freeman, D. C.; Rajeswaran, M.; Ahearn, W. G.; Meyer, D. M.; Carey, J. T., "Thin-Film Morphology Control in Naphthalene-Diimide-Based Semiconductors: High Mobility n-Type Semiconductor for Organic Thin-Film Transistors," *Chem. Mater.* **2008**, *20*, 7486-7491.

19. Singh, T. B.; Erten, S.; Gunes, S.; Zafer, C.; Turkmen, G.; Kuban, B.; Teoman, Y.; Sariciftci, N. S.; Icli, S., "Soluble derivatives of perylene and naphthalene diimide for n-channel organic field-effect transistors," *Org. Electron.* **2006**, *7*, 480-489.

20. Liu, P.; Li, Q.; Huang, M. S.; Pan, W. Z.; Deng, W. J., "High open circuit voltage organic photovoltaic cells based on oligothiophene derivatives," *Appl. Phys. Lett.* **2006**, *89,* 213501-1-213501-3.

21. Sirringhaus, H.; Brown, P. J.; Friend, R. H.; Nielsen, M. M.; Bechgaard, K.; Langeveld-Voss, B. M. W.; Spiering, A. J. H.; Janssen, R. A. J.; Meijer, E. W.; Herwig, P.; de Leeuw, D. M., "Two-dimensional charge transport in self-organized, high-mobility conjugated polymers," *Nature* **1999**, *401*, 685-688.

22. Cremer, J.; Mena-Osteritz, E. M.; Pschierer, N. G.; Mullen, K.; Bauerle, P., "Dye-functionalized head-to-tail coupled oligo(3-hexylthiophenes) - perylene-oligothiophene dyads for photovoltaic applications," *Org. Biomol. Chem.* **2005**, *3*, 985-995.

23. Fujitsuka, M.; Harada, K.; Sugimoto, A.; Majima, T., "Excitation Energy Dependence of Photoinduced Processes in Pentathiophene-Perylene Bisimide Dyads with a Flexible Linker," *Journal of Physical Chemistry A* **2008**, *112*, 10193-10199.

CHAPTER 4

PHOTOPHYSICAL PROPERTIES OF QUATERTHIOPHENE-FLAVIN DYADS

4.1 Introduction

The photoinduced electron transfer from electron rich donor to the electron poor acceptor is an essential process in the conversion of light to electricity in organic solar cells.[1-6] A better design of molecular electronic devices could be possible by controlling the electron transfer on a molecular scale.[7] Several model donor-acceptor systems have been studied to understand the factors that can be tuned to control the electron transfer. The distance[8] and geometry[9] between the donor and acceptor in dyads were changed to understand how they contribute to the electron transfer rate. The linker that connects the donor and acceptor in dyads is often a rigid covalent linker.[8,10-12] Although there is extensive research about the electron transfer in model systems with rigid linkers there is lack of understanding on how a flexible linker with acceptor attached at different positions to the donor affects the photophysical properties of the dyads.

In this chapter, we study the effect of point of linkage of acceptor to the donor on the photophysical properties of the dyad by designing a model system containing a donor that is attached with a flexible covalent linker to the acceptor at different positions (Figure 4.1). Quaterthiophene and flavin are used as acceptor and donor entities, respectively, in the dyads.

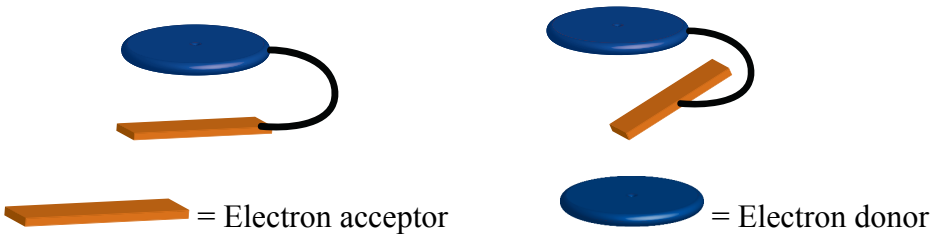

Figure 4.1: Molecular design of the dyads.

Quaterthiophene is chosen because thiophene based oligomers[13]/polymers[14-16] are used as a good p-type semiconductors in organic solar cells. We have chosen flavin as the acceptor for the dyads due to the following reasons: (1) it is reported that flavin has small reorganization energy (λ) of electron transfer. A small λ value will favor the forward electron transfer but hinders the back electron transfer[3], which is a desirable feature for increasing the efficiency of solar cells.[1] (2) Flavin has proven to be a good electron acceptor when attached to N,N-dimethylaniline (DMA) donor. A dyad made with flavin DMA exhibited a very long lifetime.[3] (3) Flavin cofactor is an important coenzyme in biological redox reactions[17] and electron transport.[3,18] (4) It is a good photoreceptor in biological systems.[19] (4) Flavin has a high absorptivity in the visible region. (6) The linker can be attached at either the 3 or the 10 position of the flavin molecule making it possible to design dyads shown in Figure 4.1 for the intended study. (7) Despite the importance of flavin as a good electron acceptor, a dyad based on flavin acceptor and visible light absorbing donor such as oligothiophene has never been published. (8) The redox properties of flavins can be changed by varying the functionality at the C(7) position of the flavin derivatives.[20] It follows, that if flavin is used in the dyads, the redox properties and the band gap of dyads could be changed and hence the charge transfer characteristics.

4.2 Synthesis of molecules

The quaterthiophene (QT) – Flavin (Fl) dyads (**N3 QT-Fl** & **N10 QT-Fl**) are synthesized to study the effect of point of linkage of the acceptor to the donor, and to study their photophysical properties. The two dyads shown in Figure 4.2 have the following features: (1) The donor part is quaterthiophene (**QT**) with hydrophobic hexyl side chain (Figure 4.3). (2) The acceptor part is flavin (**N3 Fl** and **N10 Fl**). (3) The point of attachment of acceptor to the donor is different in the two dyads. (4) Donor and acceptor are connected by a covalent flexible linker.

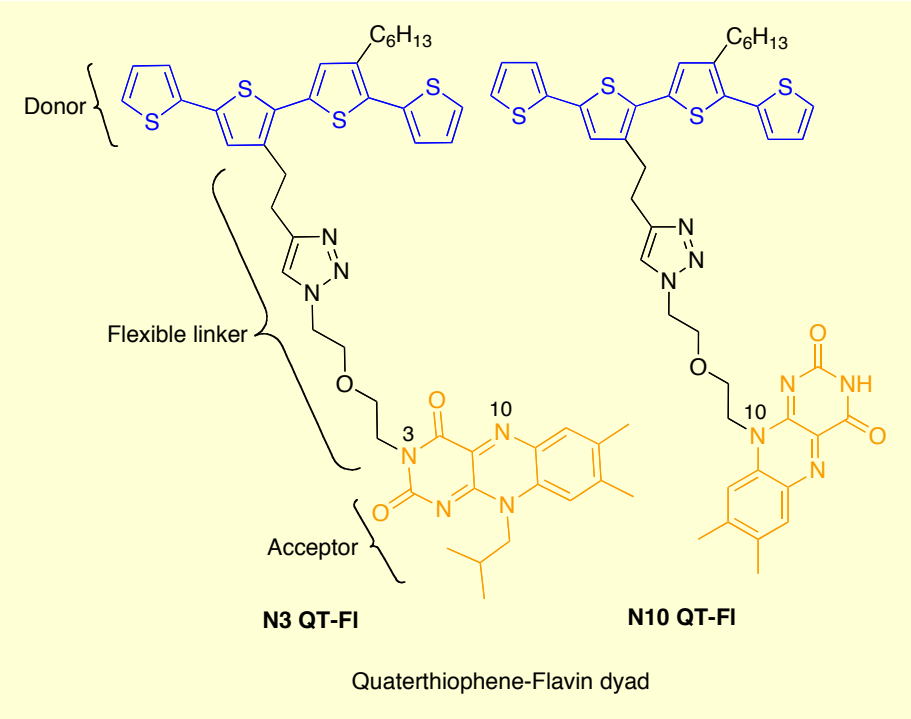

Figure 4.2: Quaterthiophene-flavin (**QT-Fl**) dyads.

The synthesis of the donor part for the dyads was discussed in the chapter 3 of this thesis (See synthesis of compound **13** in section 3.2 of chapter 3).

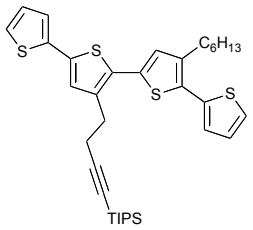

Figure 4.3: Structure of QT donor.

The scheme for the synthesis of the azide linker (**4**) that is used as a covalent linker to attach the donor and acceptor parts of the dyads is shown in Figure 4.4. The synthesis of **4** starts with 2-(2-chloroethoxy)ethanol (**1**), which is converted to an azide (**2**) by reaction with sodium azide. The compound **2** is mesylated to obtain **3.** The reaction of compound **3** with lithium bromide replaces the mesylate with a bromo group to obtain compound **4** in 92% yield**.** Professor Vince Rotello's, group at UMass Amherst made the compound **4**.

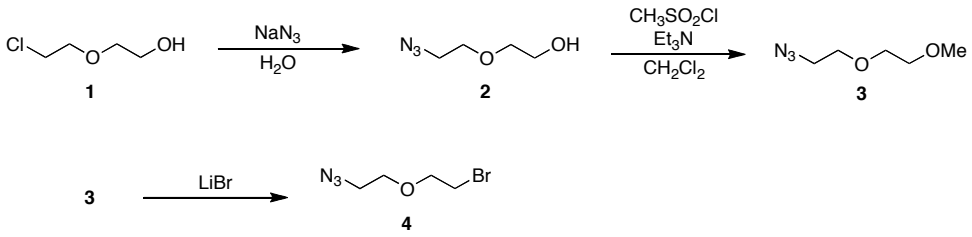

Figure 4.4: Synthesis of bromo-ethoxyethane azide (**4**).

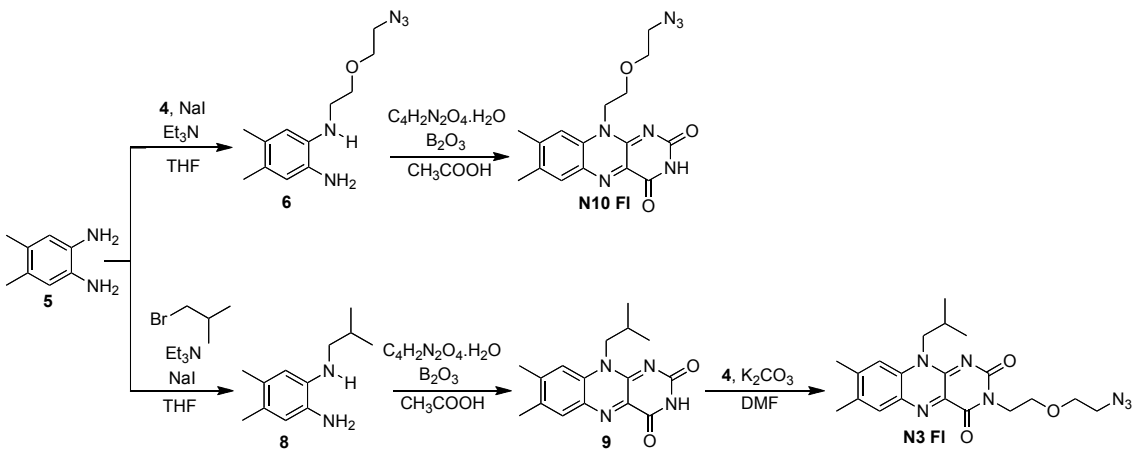

Figure 4.5: Synthesis of flavin acceptors.

The synthesis of the acceptors for the dyads was carried out by the Rotello's group at UMass Amherst, following the scheme shown in Figure 4.5. The starting material for the synthesis of both acceptors (**N3 Fl** and **N10 Fl**) is 4, 5-dimethyl-1, 2-phenylene diamine (**5**). Compound **5** was reacted with **4** in presence of sodium iodide to obtain mono-substituted diamine (**6**). The reaction of **6** with alloxan monohydrate and boron oxide afforded desired acceptor (**N10 Fl**) for the **N10 QT-Fl** dyad. For the synthesis of **N3 Fl** acceptor the compound **5** was first reacted with 1-bromo-2-methylpropane and sodium iodide to obtain mono-substituted diamine product **8**. The reaction of **8** with alloxan monohydrate and boron oxide gave product **9**, which was subsequently converted to the acceptor **N3 Fl** by reaction with **4** in presence of potassium carbonate.

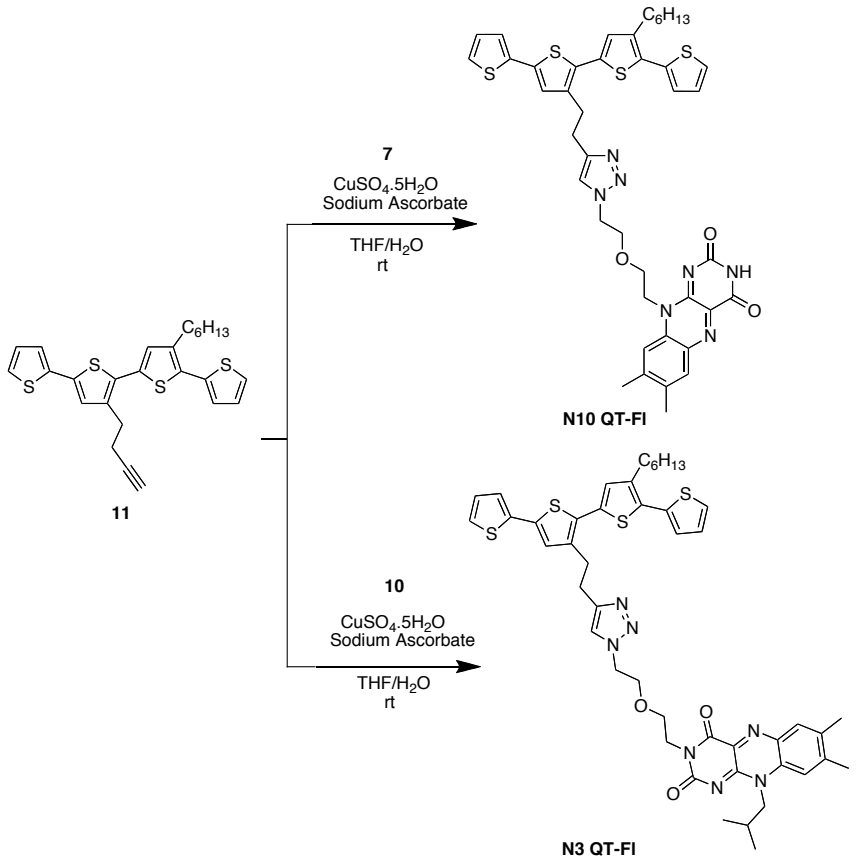

Figure 4.6: Synthesis of **QT-Fl** dyads (**N3 QT-Fl** & **N10 QT-Fl**).

The dyads were synthesized through the copper-catalyzed 1,3-Huisgen cycloaddition according to the scheme shown in Figure 4.6. The reaction between deprotected quaterthiophene **14** (See synthesis of compound **14** in section 3.2 of chapter 3) and **N3 Fl** gave **N3 QT-Fl**. Likewise, the reaction between **14** and **N10 Fl** afforded **N10 QT-Fl** dyad.

4.3 Characterization

All the compounds are characterized by using ^{1}H and ^{13}C NMR. Figure 4.7 shows the ^{1}H NMR spectra of dyad **N3 QT-Fl** in $CDCl_3$. The dyads have the peak corresponding to the aromatic flavin protons at 7.49 and 7.94 ppm. The eight aromatic **QT** peaks appear at 7.29, 7.25, 7.20, 7.13, 7.10, 7.05, 7.01 and 6.91 ppm. The important

indications for the covalent linkage between the donor and acceptor units are the presence of trizole proton that is observed at 6.89 ppm and the absence of the absence of the alkyne proton of compound **14**.

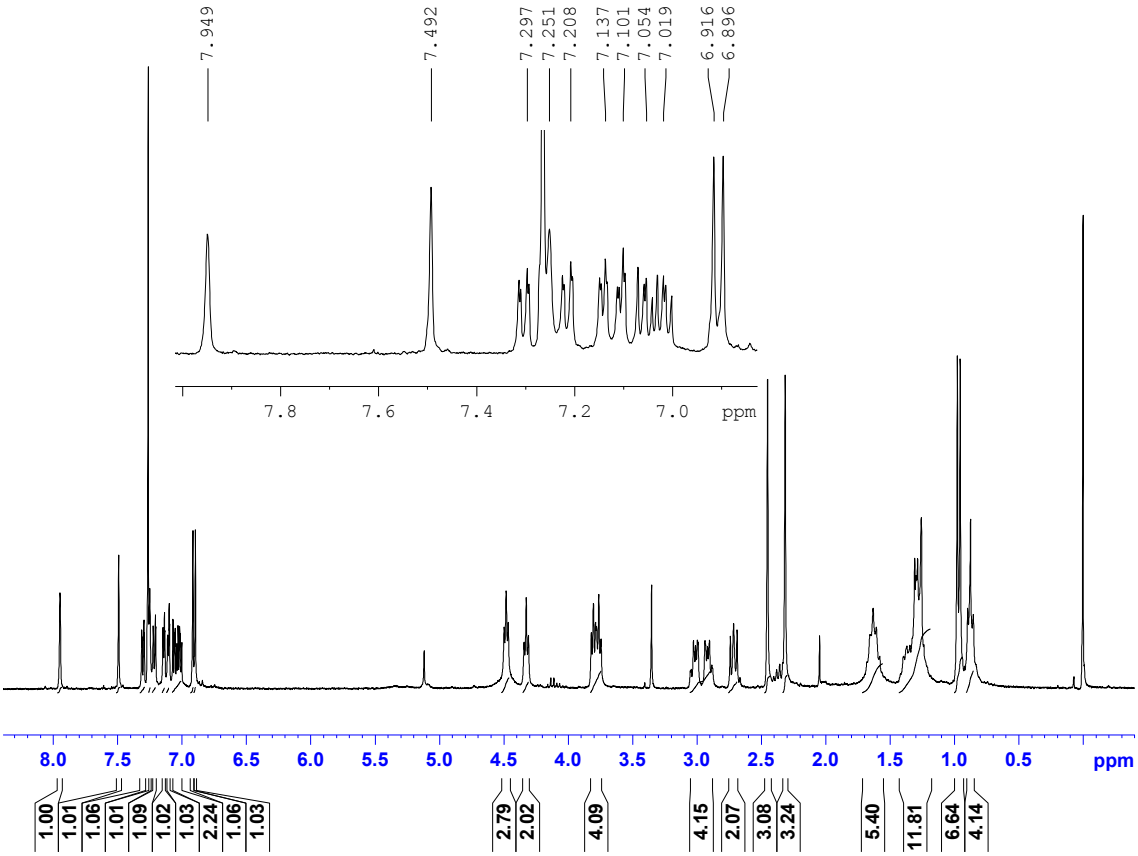

Figure 4.7: ^{1}H NMR of dyad **N3 QT-Fl** in $CDCl_3$.

The absorption characteristics, emission spectroscopy, and the quenching dynamics of the dyads will provide the information regarding the photophysical properties. The effect of point of linkage of acceptor to the donor in dyads on the photophysical properties is also discussed in this chapter.

4.4 Absorption characteristics

Absorption measurements: The UV-visible absorption spectra of the compounds were measured on a Hewlett Packard, 8452A, Diode array spectrophotometer. All solutions were prepared in dichloromethane.

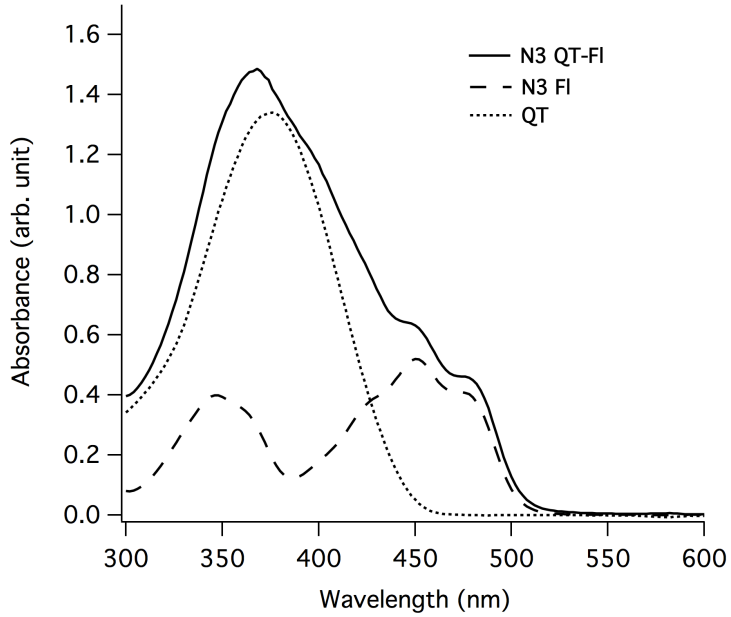

Figure 4.8: UV-Vis absorption spectra of dyad **N3 QT-Fl** and its components, acceptor (**N3 Fl**) and donor (**QT**).

Figure 4.8 shows representative UV-Vis spectra for the dyad (**N3 QT-Fl**) and its components, the acceptor (**N3 Fl**) and donor (**QT**). Flavin has two broad absorption peaks, 310-380 nm and 410-510 nm. Similarly, a broad absorption band of the quarternary thiophene is found between 300 nm to 450 nm. The absorption spectra of the dyad is a simply the sum of the individual absorption spectra of the constituents, **N3 Fl** acceptor and **QT** donor.

The absorption spectra of the dyads (**N3 QT-Fl**) do not have any extra absorption peak other than those from the donor and acceptors, indicating that there is no electronic

interaction between the donor and the acceptor at the concentrations used. However, if there a charge transfer band hidden in the absorption spectra it can not be ascertained by the UV-Vis spectra obtained here.

4.5 Fluorescence spectroscopy

Fluorescence spectra were measured using a Photon Technology International, Inc., spectrometer. All solutions were prepared in dichloromethane. Figure 4.9 shows absorption and emission spectra for the donor (**QT**) and the acceptor (**N3 Fl**). The emission spectra of the donor and acceptor were obtained by exciting them at wavelengths close to their absorption maxima. The overlap of the emission of the donor and absorption spectra of the acceptor indicates the presence or absence of Forster resonance energy transfer (FRET) from donor unit to the acceptor unit in a dyad. Figure 4.9, indicates the possiblity of the FRET as there is a overlap between the emission spectra of the donor and the absorbance spectra of the acceptor (**N3 Fl)**. However, the energy transfer process does not exclude the possibility of electron transfer from donor to the acceptor.

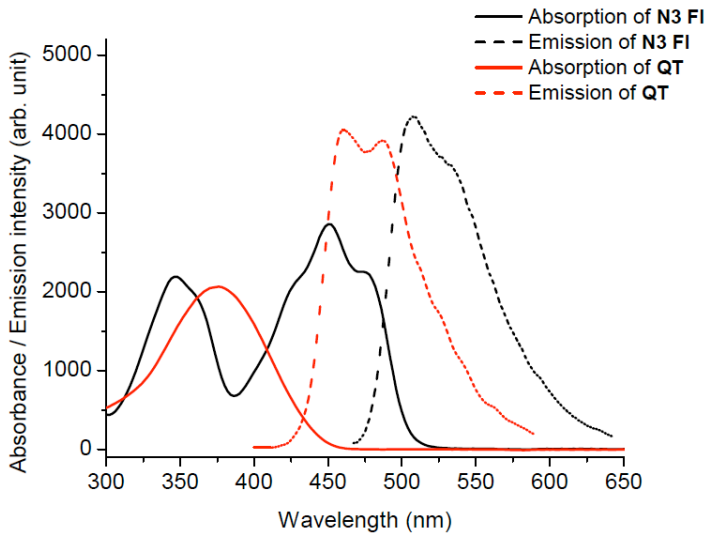

Figure 4.9: Absorption spectra of acceptor (**N3 Fl**) and emission spectra of donor (QT).

In addition to the analysis of the absorption and emission spectra of the acceptor and donor, the emission characteristics of the dyads were recorded. The Figure 4.10 shows (1) the emission spectra of the **N3 QT-Fl** dyad excited at 386 nm (the wavelength close to the maximum absorption of the donor and the least absorption of acceptor) and 450 nm (the wavelength where flavin acceptor has maximum absorption and donor quaterthiophene has least absorption), and (2) The emission spectra of the donor and acceptor excited at 386 nm and 450 nm respectively. A significant drop in emission intensity of the dyad was observed upon excitation at wavelength close to the absorption maxima of either donor or acceptor. A calculated quenching efficiency of 97% was observed when **N3 QT-Fl** was excited at 386 nm. The quenching observed in the dyad could be either due to energy transfer or to electron transfer from the donor to the acceptor. However, if quenching is due to energy transfer there should an increase in the emission intensity of the acceptor upon excitation of the donor. Nevertheless, there is no significant increase in the emission of the donor, indicating that the quenching may be

due to electron transfer from the donor to the acceptor. Another interesting observation is the drop in fluorescence intensity of the dyad even when excited at the absorption maxima of the acceptor indicating the possibility of the energy or electron transfer process. The feasibility of electron or energy transfer processes can be ascertained by calculating the energies of frontier orbitals of the donor, acceptors and dyads.

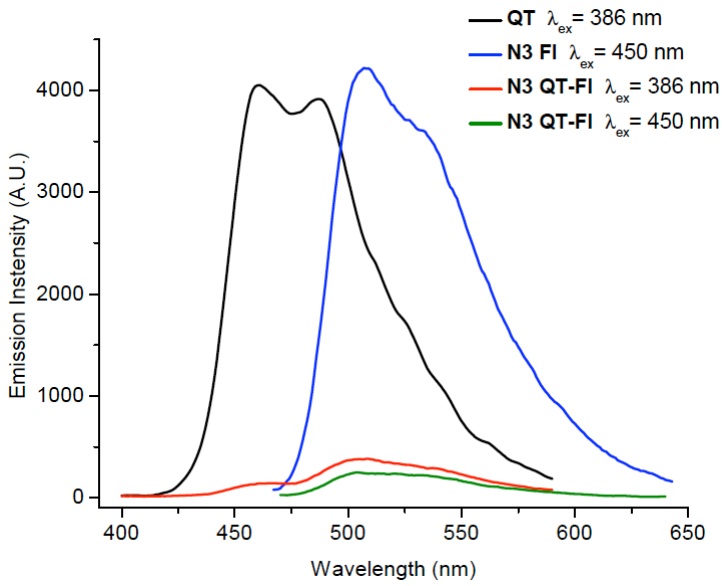

Figure 4.10: Fluorescence spectra of the donor (**QT**), acceptor (**N3 Fl**) and dyads (**N3 QT-Fl** and **N10 QT-Fl**).

4.6 Electrochemistry

The electrochemical properties of flavins, quaterthiophene and dyads were measured using Cypress System Potentiostat, which consists of a three-electrode cell with reference, working and auxiliary electrodes. A silver wire acted as a pseudo reference electrode in this set up.

The measured potentials were calibrated with the standard ferrocene-ferricenium (Fc/Fc^{+}). The HOMO and LUMO levels were obtained from the oxidation and reduction

potentials. The optical band gaps of acceptors and donor were determined from the UV-Vis absorption spectra.

The oxidation behavior of quaterthiophene donor was similar to that seen in chapter 3. The acceptor showed two reduction peaks. The first peak potential was used to determine the LUMO. The energy levels of the HOMO & LUMO values of **QT**, and **N3 Fl** are shown in the figure and were determined using the same procedure detailed previously (see Chapter 3).

It is clear from figure 4.11 that the energy levels of the LUMOs of the donor and acceptors are situated such that it is energetically favorable for the electron transfer from the donor to the acceptor.

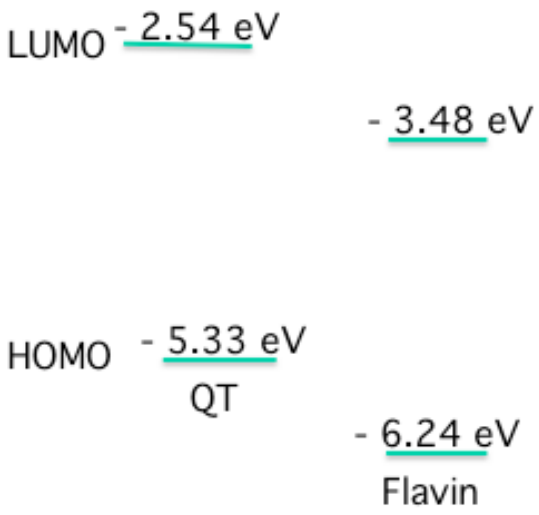

Figure 4.11: Frontier orbital energy levels of the donor and acceptor in dyads.

4.7 Time resolved Fluorescence

The instrumentation and the method of data analysis for the time-resolved fluorescence decay experiments are described in section 3.7 of in this thesis. All the samples are prepared in dichloromethane.

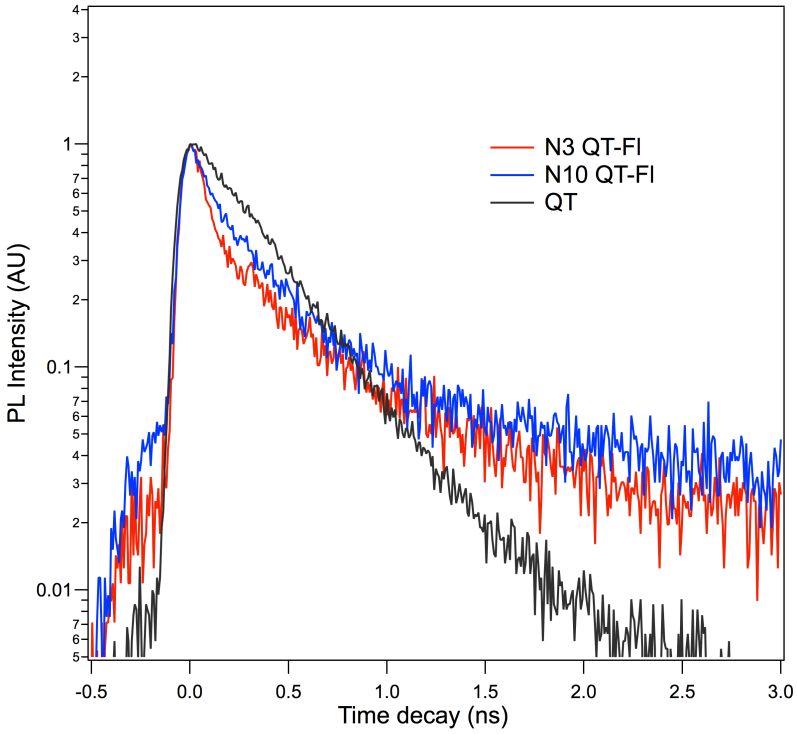

Figure 4.12: Time resolved fluorescence decay of donor in dyad (**N3 QT-Fl**) and donor (**QT**) alone. Excitation wavelength 405 nm and emission observed at 480 nm.

Figure 4.12 shows the photoluminescence (PL) decay of the donor (**QT**) and dyads (**N3 QT-Fl** & **N10 QT-Fl**) on excitation at 405 nm. The excitation at 405 nm excites both the donor and acceptor units. The analysis of the PL emission was done at 480 nm, close to the emission maximum of the **QT** donor. The dyads have bi-exponential decay. The higher quenching rate component in the bi-exponential could be due to the decay of **QT** and has lower lifetime compared to the donor alone. The lifetimes of **QT**,

N10 QT-Fl, and **N3 QT-Fl** are 366 ps, 133 ps and 50 ps respectively. The lower lifetimes of the **QT** donor part of the dyads indicates faster decay of the excited state. The reason for such faster decay may be because of the electron transfer from the donor to the acceptor unit in dyads in addition to the charge recombination that intrinsically occurs in the donor. The decay curves for the dyads shows a bi-exponetial decay indicating two different pathways for quenching process. However the quenching of **QT** was single-exponential suggesting a single pathway for quenching. A complete understanding of the pathways responsible for the quenching is expected in the future as the transient absorption measurement of these compounds is underway. The observed differences in the lifetimes of the dyads may be because of the conformational differences between the two dyads. Wasielewski in his review has pointed that the conformation between the donor and the acceptor in a dyad affect the rate of electron transfer and hence the lifetimes.[9]

To know the differences in the equillibrium conformation of the dyads, calculations were performed using Spartan software.

(a)

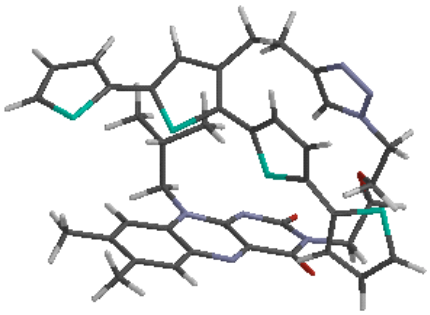

(b)

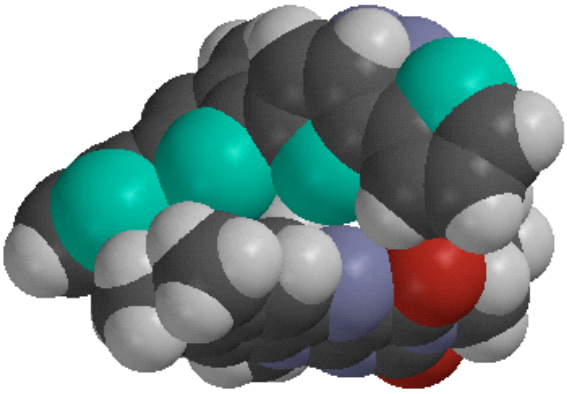

Figure 4.13: Calculated equilibrium conformation for the dyad **N3 QT-Fl** indicating the folded confirmation of the quaterthiophene and flavin units. (a) Tube model. (b) Space filling model.

The figure 4.13 shows the the equillibrium conformer for the **N3 QT-Fl** dyad The method used for these calculations is molecular mechanics with MMFF force field. From the figure it can be seen that all four quaterthiophenes are close to the flavin unit and it has a folded conformation.

(a)

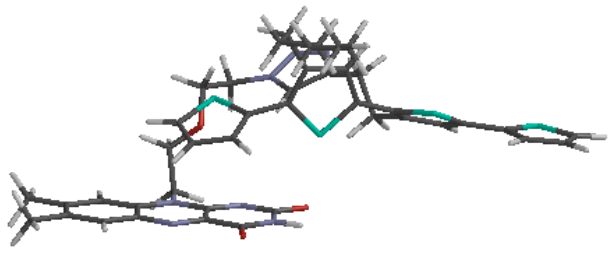

(b)

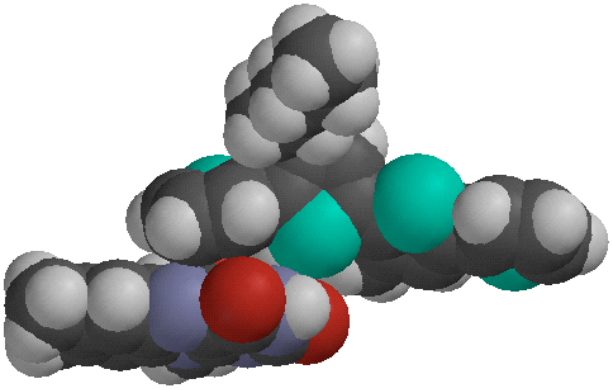

Figure 4.14: Calculated equilibrium conformer for the **N10 QT-Fl** dyad. (a) Tube model. (b) space filling model.

The equillibrium conformer for the **N10 QT-Fl** is also found to be a folded conformer but the difference is that only two of the four thiophene units are in close proximity to the acceptor (Figure 4.14). I reason that this difference in the strucutre of the two conformers leads to the observed changes in the lifetimes. A schematic photoinduced process that might be happening in the dyads is shown in Figure 4.15.

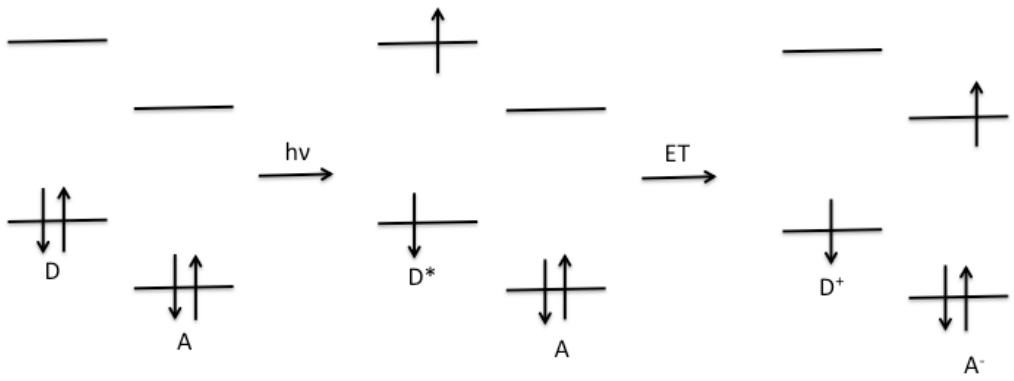

Figure 4.15: Schematic representation of the process that may be happening upon excitation of the donor in the dyads.

We analyzed if the excitation at 405 nm has excited the acceptor unit of the dyads by analyzing the emission of the acceptor.

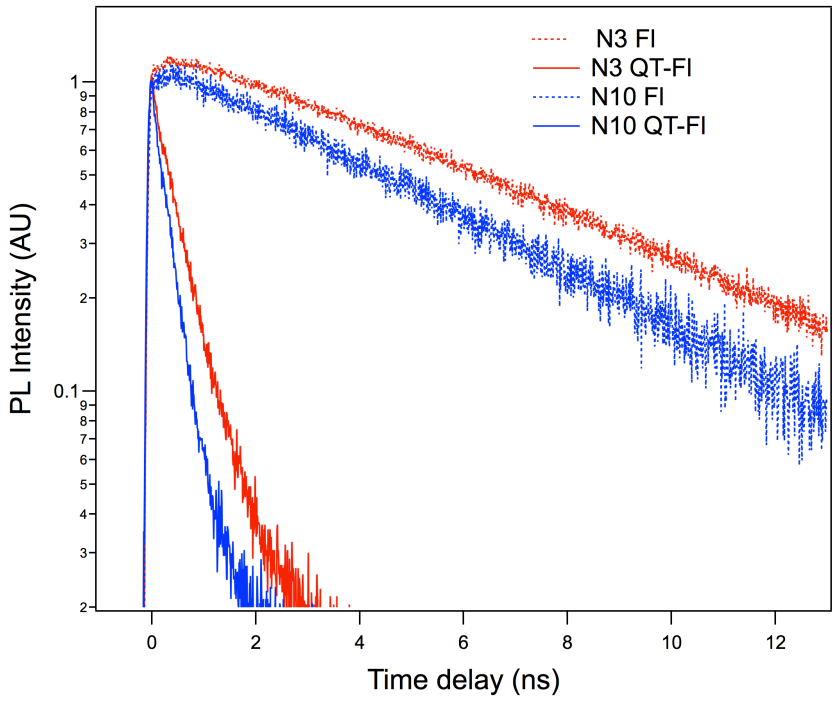

Figure 4.16: Fluorescence decay of donor in dyad (**N3 QT-Fl**) and acceptors (**N3 Fl** and **N10 Fl**). Excitation wavelength 405 nm and emission observed at 550 nm.

To probe the emission decay of the acceptor in the dyads the PL quenching at the wavelength close to the emission maximum of the acceptor was observed. Figure 4.16 shows the drop of emission intensity of the acceptors (**N3 Fl** and **N10 Fl**) and dyads (**N3 QT-Fl** & **N10 QT-Fl**) on excitation at 405 nm. As mentioned previously, at this wavelength both acceptor and donor are excited. The analysis of the PL emission was done at 550 nm, the wavelength where the emission is primarily from acceptors. Similar to the previous observation, higher quenching rates and lower lifetimes were observed for the dyads compared to the flavin acceptors. The lifetimes of **N3 Fl**, **N10 Fl**, **N3 QT-Fl**, and **N10 QT-Fl** are 7.2 ns, 5.5 ns, 478 ps and 332 ps respectively. The **N3 Fl** is found have higher lifetime than **N10 Fl**. The differences in the lifetimes may be due to the differences in the structures of the two acceptors. The higher fluorescence quenching rates observed for the dyads may be due to the electron transfer from the donor to the acceptor unit or energy transfer from acceptor to the donor moiety in addition to the self-quenching of fluorescence that intrinsically occurs on excitation of acceptor. However, the band gaps of the donor and acceptor are situated such that the energy transfer from the acceptor to the donor is not feasible. Contrary to what has been observed previously where the quenching is more in **N3 QT-Fl** dyad than the **N10 QT-Fl** dyad, here we observed lower lifetime for **N3 QT-Fl** than the **N10 QT-Fl** dyad. We reason out that such difference is due to the difference in the self-quenching of acceptors, which predominates than the differences in the rate of electron transfer, if any. Based on the results obtained, the photophysical processes that may be occurring in the dyads upon excitation of flavin are shown in Figure 4.17.

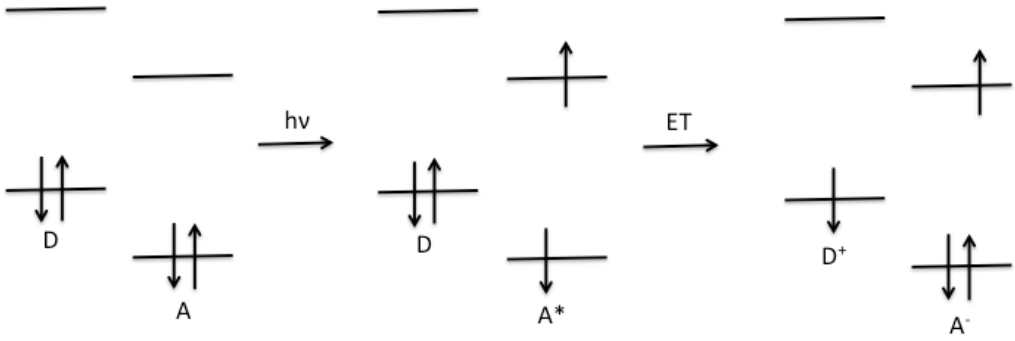

Figure 4.17: Schematic representation of the process that may be happening upon excitation of the acceptor in the dyads.

In summary, we have found that the absorption of the dyads is a linear combination of the absorption from the donor and acceptor units. Furthermore, it is found that there is a good overlap of the absorption spectra of the donor and acceptor moieties. The overlap of the emission of donor and absorption spectra of acceptor unit indicates the possibility of energy transfer. However, when dyads are excited at the absorption maxima of the donor, there is no spontaneous increase in the emission of the acceptor with the decrease in the emission of the donor. This indicates that probably energy transfer is not the primary photophysical process that is happening in this dyad but rather it is electron transfer. Additionally, the energies of the frontier orbitals of the dyads indicate the feasibility of electron transfer from the donor to the acceptor. The rapid quenching of the fluorescence of the dyads on excitation of the donor entity indicates the electron transfer from donor to the acceptor. The slight differences that are observed in the two dyads could be because of the changes in the conformations. It is consistent with the previous observation made for the changes in the electron transfer rates with respect to conformation. This study shows that the equilibrium conformers and the point of

attachment of the acceptor to the donor in the flexible linker donor acceptor dyads can influence the quenching rates.

4.8 Conclusions

We have observed a strong donor fluorescence quenching in the dyads based on quaterthiophene donor and flavin acceptor. The time resolved fluorescence data indicates rapid decay rates in these dyads indicating electron transfer from the donor to the acceptor moiety. The UV-Vis and emission spectra of the acceptor and donor overlap indicating the possibility of energy transfer. The energy levels of the LUMOs of the donor and the acceptor and the lack of increase in fluorescence upon excitation of donor in dyads indicates that the strong quenching of fluorescence in dyads is probably due to electron transfer from the donor to the acceptor. The change in the quenching rates indicates changes in electron transfer rates with respect to the changes in the confirmation. The close proximity of the donor to the acceptor in **N3 QT-Fl** dyad case may be the reason for the higher quenching rates observed than for the **N10 QT-Fl** dyad.

4.9 Suggestions for future research

The detailed information regarding the photophysical pathways could be studied using transient absorption measurements. Efforts in the future should be put to self-assembling the dyads by selecting suitable solvents and by attaching incompatible side chains into segregated structures. Further, the application of these dyads for organic solar cell should be accessed.

4.10 References

1. Coakley, K. M.; McGehee, M. D., "Conjugated polymer photovoltaic cells," *Chemistry of Materials* **2004**, *16*, 4533-4542.

2. Kraabel, B.; Lee, C. H.; Mcbranch, D.; Moses, D.; Sariciftci, N. S.; Heeger, A. J., "Ultrafast Photoinduced Electron-Transfer in Conducting Polymer Buckminsterfullerene Composites," *Chem Phys Lett* **1993**, *213*, 389-394.

3. Murakami, M.; Ohkubo, K.; Fukuzumi, S., "Inter- and intramolecular photoinduced electron transfer of flavin derivatives with extremely small reorganization energies," *Chemistry* **2010**, *16*, 7820-32.

4. Sariciftci, N. S.; Smilowitz, L.; Heeger, A. J.; Wudl, F., "Photoinduced Electron-Transfer from a Conducting Polymer to Buckminsterfullerene," *Science* **1992**, *258*, 1474-1476.

5. Vivo, P.; Alekseev, A. S.; Kaunisto, K.; Pekkola, O.; Tolkki, A.; Chukharev, V.; Efimov, A.; Ihalainen, P.; Peltonen, J.; Lemmetyinen, H., "Photoinduced electron transfer in thin films of porphyrin-fullerene dyad and perylenetetracarboxidiimide," *Phys Chem Chem Phys* **2010**, *12*, 12525-12532.

6. Zenkevich, E.; von Borczyskowski, C.; Shulga, A.; Bachilo, S.; Rempel, U.; Willert, A., "Porphyrin self-assembling complexes in thin polymeric films: Stability, spectral properties, and photoinduced electron transfer dynamics.," *Abstr Pap Am Chem S* **2000**, *219*, U529-U529.

7. McDonald, N. A.; Subramani, C.; Caldwell, S. T.; Zainalabdeen, N. Y.; Cooke, G.; Rotello, V. M., "Simultaneous hydrogen bonding and [pi]-stacking interactions between flavin/porphyrin host-guest systems," *Tetrahedron Letters* **2011**, *52*, 2107-2110.

8. Closs, G. L.; Miller, J. R., "Intramolecular long-distance electron-transfer in organic-molecules," *Science* **1988**, *240*, 440-447.

9. Wasielewski, M. R., "Photoinduced electron-transfer in supramolecular systems for artificial photosynthesis," *Chemical Reviews* **1992**, *92*, 435-461.

10. Kulkarni, A. P.; Wu, P. T.; Kwon, T. W.; Jenekhe, S. A., "Phenothiazine-phenylquinoline donor-acceptor molecules: Effects of structural isomerism on charge transfer photophysics and electroluminescence," *Journal of Physical Chemistry B* **2005**, *109*, 19584-19594.

11. Kanato, H.; Takimiya, K.; Otsubo, T.; Aso, Y.; Nakamura, T.; Araki, Y.; Ito, O., "Synthesis and photophysical properties of ferrocene-oligothiophene-fullerene triads," *Journal of Organic Chemistry* **2004**, *69*, 7183-7189.

12. Hayes, R. T.; Wasielewski, M. R.; Gosztola, D., "Ultrafast photoswitched charge transmission through the bridge molecule in a donor-bridge-acceptor system," *J Am Chem Soc* **2000**, *122*, 5563-5567.

13. Liu, P.; Li, Q.; Huang, M. S.; Pan, W. Z.; Deng, W. J., "High open circuit voltage organic photovoltaic cells based on oligothiophene derivatives," *Applied Physics Letters* **2006**, *89*. 213501-1-213501-3.

14. Benanti, T. L.; Kalaydjian, A.; Venkataraman, D., "Protocols for Efficient Postpolymerization Functionalization of Regioregular Polythiophenes," *Macromolecules* **2008**, *41*, 8312-8315.

15. Tzabari, L.; Tessler, N., "Shockley-Read-Hall recombination in P3HT:PCBM solar cells as observed under ultralow light intensities," *Journal of Applied Physics* **2011**, *109*, 064501-1-064501-5.

16. Rauh, D.; Wagenpfahl, A.; Deibel, C.; Dyakonov, V., "Relation of open circuit voltage to charge carrier density in organic bulk heterojunction solar cells," *Applied Physics Letters* **2011**, *98*, 133301-1-133301-3.

17. Breinlinger, E. C.; Keenan, C. J.; Rotello, V. M., "Modulation of flavin recognition and redox properties through donor atom-pi interactions," *J Am Chem Soc* **1998**, *120*, 8606-8609.

18. Li, G. F.; Glusac, K. D., "The Role of Adenine in Fast Excited-State Deactivation of FAD: a Femtosecond Mid-IR Transient Absorption Study," *Journal of Physical Chemistry B* **2009**, *113*, 9059-9061.

19. Li, G. F.; Glusac, K. D., "Light-triggered proton and electron transfer in flavin cofactors," *Journal of Physical Chemistry A* **2008**, *112*, 4573-4583.

20. Caldwell, S. T.; Farrugia, L. J.; Hewage, S. G.; Kryvokhyzha, N.; Rotello, V. M.; Cooke, G., "Model systems for flavoenzyme activity: an investigation of the role functionality attached to the C(7) position of the flavin unit has on redox and molecular recognition properties," *Chem Commun* **2009**, 1350-1352.

APPENDIX

EXPERIMENTAL

A.1 General Procedures

All chemicals were purchased from commercial sources (Acros, Aldrich, Alfa Aesar, TCI, and Strem) and used without further purification, unless otherwise noted. THF was distilled from sodium-benzophenone ketyl. NBS was recrystallized from water. *n*-BuLi was nominally 1.6 M in hexanes, but was titrated against diphenylacetic acid prior to use. Common solvents were purchased from EMD (through VWR). Routine monitoring of reactions was carried out on glass-supported EMD silica gel 60 F_{254} TLC plates. Flash chromatography was performed using silica gel from Sorbent Technologies (Standard Grade, 60 Å, 32-63 μm). All ^{1}H and ^{13}C NMR spectra were recorded on a Bruker Avance 400 spectrometer. ^{19}F NMR spectra were recorded on a Bruker DPX300 spectrometer. Chemical shifts and coupling constants (*J*) are reported in parts per million (δ) and Hertz, respectively. Mass spectral data were obtained at the University of Massachusetts Mass Spectrometry Facility, which is supported, in part, by the National Science Foundation.

A.2 Synthesis

The detailed procedure for the synthesis of compounds **14**, **17a**, and **17b** dyads 1 and 2 and their characterization using NMR and mass spectrometry can be found in Dr.Travis L.Benanti's Thesis (our group alumni).

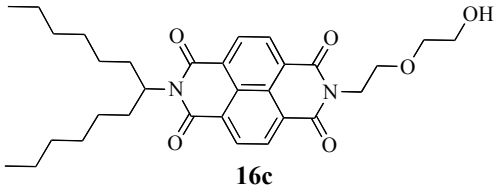

16c

Compound (16c). To a stirred solution of naphthalene-1,4,5,8-tetracarboxylic dianhydride (**15**, 1.0 g, 3.72 mmol) in absolute ethanol (200 mL), was added n-hexylheptylamine (0.74 mL, 3.72 mmol, prepared from previously reported method) and 2-(2- aminoethoxy)ethanol (0.37 mL, 3.72 mmol). The reaction mixture was refluxed for 12 hours and then cooled in an ice bath. The resulting pink precipitate was filtered off and purified by silica gel chromatography (50:50 Hexane/Ethyl acetate) to yield **9c** (399 mg, 20%) as a light pink solid. ^{1}H NMR (400 MHz, $CDCl_3$) δ 8.76 (m, 4H), 5.15 (m, 1H), 4.48 (t, *J* = 5.5, 2H), 3.87 (t, *J* = 5.5, 2H), 3.66 (m, 4H), 2.07-2.35 (m, 3H), 1.85 (m, 2H), 1.06-1.45 (m, 16H), 0.82 (t, *J* = 6.8, 6H). ^{13}C NMR (75 MHz, $CDCl_3$) δ 163.35, 131.30, 127.0, 126.83, 126.30, 72.39, 68.30, 61.93, 55.39, 40.07, 32.39, 31.82, 29.25, 26.98, 22.67, 14.15. MS (FAB+) *m/z* 537 [M+H]+.

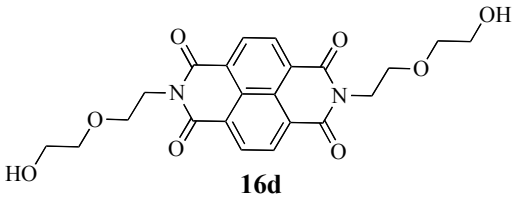

16d

Compound (16d). To a stirred solution of naphthalene-1,4,5,8-tetracarboxylic dianhydride (**15**, 3.0 g, 11.10 mmol) in absolute ethanol (100 mL), was added 2-(2-aminoethoxy)ethanol (2.70 mL, 27.09 mmol). The reaction mixture was refluxed for 24 hours and then cooled in an ice bath. The resulting precipitate was filtered off and purified by silica gel chromatography (70:30 acetone/$CH2Cl_2$) to yield **9c** (3.92 g, 80%)

as a pink solid. ^{1}H NMR (400 MHz, DMSO) δ 8.63 (s, 4H), 4.57 (s, 2H), 4.25 (t, *J* = 6.3, 4H), 3.69 (t, *J* = 6.4, 4H), 3.48 (m, 8H). ^{13}C NMR (75 MHz, DMSO) δ 162.32, 130.39, 125.89, 125.71, 72.13, 66.76, 60.21. MS (FAB+) *m/z* 443 [M+H]+.

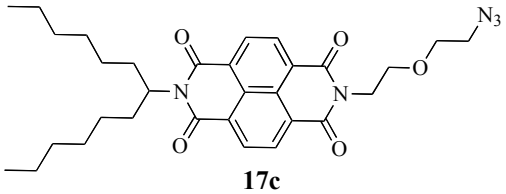

17c

Compound (17c). Under a nitrogen atmosphere, triethylamine (0.52 mL, 3.70 mmol) was added to a stirred solution of **16c** (0.5 g, 0.93 mmol) in methylene chloride (50 mL). The solution was cooled to 0 °C and methanesulfonyl chloride (0.21 mL, 2.70 mmol) was added dropwise. The reaction mixture was warmed to rt and stirred for 3 hours before being quenched with an equal volume of water. The layers were separated and the aqueous layer was extracted with CH_2Cl_2 (2x). The combined organics were washed with sat'd $NaHCO_3$ (2x) and water (1x), dried over Na_2SO_4, filtered, and concentrated *in vacuo* to yield 0.6 g of mesylate, which was carried forward without further purification. The mesylate was dissolved in dry DMF (20 mL) and sodium azide (189 mg, 2.91 mmol) was added. The mixture was purged with N_2 and heated to 80 °C. After stirring overnight, the reaction was cooled to rt and diluted with water (100 mL). The resulting solution was extracted with EtOAc (4x). The combined extracts were washed with water (4x) and sat'd NaCl solution (1x), dried over Na_2SO_4, filtered, and concentrated *in vacuo*. The resulting precipitate was filtered off and purified by silica gel chromatography (50:50 Ethyl acetate/Hexane) to yield **9c** (3.92 g, 80%) as a pink solid. (0.5 g, 92%) as pink powder. ^{1}H NMR (400 MHz, $CDCl_3$) δ 8.75 (m, 4H), 5.15 (m, 1H), 4.49 (t, *J* = 5.6, 2H), 3.88 (t, *J* = 5.6, 2H), 3.71 (t, *J* = 5.0, 2H), 3.32 (t, *J* = 4.9, 2H), 2.07-

2.35 (m, 2H), 1.85 (m, 2H), 1.09-1.40 (m, 16H), 0.82 (t, 6H). ^{13}C NMR (75 MHz, DMSO) δ 163.2, 131.19, 126.97, 126.84, 126.42, 69.94, 68.06, 55.36, 50.81, 39.72, 32.40, 31.83, 29.27, 26.99, 22.68, 14.15; MS (FAB+) *m/z* 562 [M+H]+.

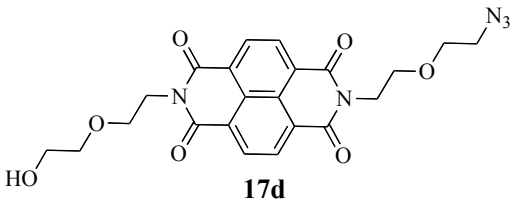

17d

Compound (17d). Under a nitrogen atmosphere, triethylamine (2.38 mL, 16.95 mmol) was added to a stirred solution of **16d** (2.5 g, 5.65 mmol) in DMF (50 mL). The solution was cooled to 0 °C and methanesulfonyl chloride (0.43 mL, 5.65 mmol) was added dropwise. The reaction mixture was warmed to rt and stirred for 3 hours. The DMF was rotary evaporated, water was added and resulting reaction mixture was extracted with ethyl acetate. The organic layer was washed with sat'd $NaHCO_3$ (2x) and water (1x), dried over Na_2SO_4, filtered, and concentrated *in vacuo* to yield 1.0 g of orange color mesylate, which was carried forward without further purification. The mesylate (0.88g, 1.69 mmol) was dissolved in dry DMF (20 mL) and sodium azide (329 mg, 5.07 mmol) was added. The mixture was purged with N_2 and heated to 80 °C. After stirring for 48h, the reaction was cooled to rt and DMF was rotary evaporated, The resulting solid was diluted with water (100 mL) and extracted with EtOAc (4x). The combined extracts were washed with water (4x) and sat'd NaCl solution (1x), dried over Na_2SO_4, filtered, and concentrated *in vacuo*. The obtained solid was run through silica gel column with Ethyl acetate to obtain **10d** (0.71 g, 91%) as light pink color solid. ^{1}H NMR (400 MHz, $CDCl_3$) δ 8.76 (s, 4H), 4.48 (q, J = 5.6, 4H), 3.88 (td, J = 5.6, 2.0, 4H), 3.62-3.75 (m, 6H), 3.31 (t, J = 5.1, 2H), 2.26 (t, J = 5.7, 1H). ^{13}C NMR (75 MHz, $CDCl_3$) 163.24, 163.03, 131.25,

131.17, 126.88, 126.84, 126.80, 126.57, 72.37, 69.96, 68.31, 68.02, 61.94, 50.79, 40.10, 39.76; MS (FAB+) *m/z* 468 [M+H]+.

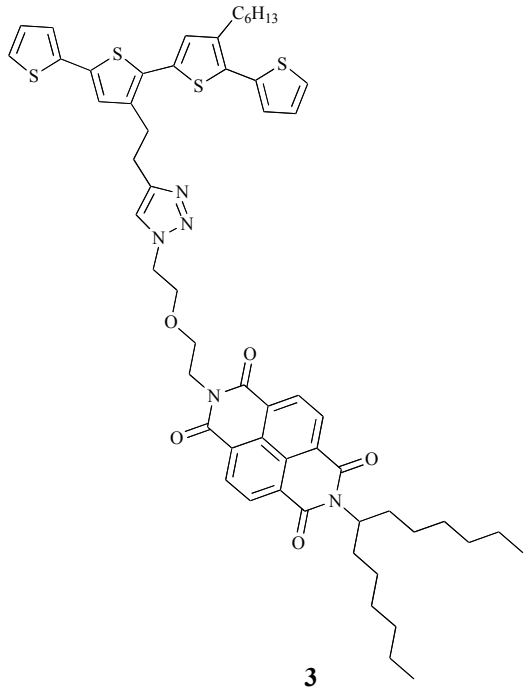

3

Compound (3): The crude alkyne **14** and azide **17c** (260 mg, 0.46 mmol) were dispersed in THF/H_2O (5 mL each). To the stirred mixture was added $CuSO_4 \cdot 5H_2O$ (30.0 mg, 0.12 mmol) and sodium ascorbate (50.0 mg, 0.252 mmol). The heterogeneous mixture was stirred for 48 hours at rt and then partitioned between EtOAc and water. The layers were separated and the aqueous layer was extracted with EtOAc (2x). The combined organics were washed with water (2x) and sat'd NaCl solution (1x), dried over Na_2SO_4, filtered, and concentrated *in vacuo*. Purification of the residue by silica gel chromatography (75:25 ethyl acetate/Hexane) yielded **3** (283 mg, 60%) as a green solid. ^{1}H NMR (400 MHz, $CDCl_3$) δ 8.67 (m, 4H), 7.44 (s, 1H), 7.25, (m, 1H), 7.18 (dd, *J* = 5.1, 1.0, 1H), 7.11 (dd, *J* = 3.6, 1.1, 1H), 7.08 (dd, *J* = 3.6, 1.1, 1H), 7.02 (dd, *J* = 5.1, 3.6, 1H), 6.98 (dd, *J* = 5.1, 3.6, 1H), 6.91 (s, 2H), 5.14 (m, 1H), 4.43 (t, *J* = 5.0, 2H), 4.37 (t, *J*

= 5.4, 2H), 3.81 (t, *J* = 5.0, 2H), 3.72 (t, *J* = 5.46, 2H), 3.00-3.17 (m, 4H), 2.70 (t, J = 8.0, 2H), 2.19 (m, 2H), 1.62 (m, 4H), 1.13-1.42 (m, 22H), 0.86 (t, J = 6.8, 3H), 0.81 (t, *J* = 6.8, 6H). ^{13}C NMR (75 MHz, $CDCl_3$) δ 163.07, 146.99, 140.14, 138.49, 137.11, 135.78, 135.24, 133.42, 131.13, 130.79, 130.37, 128.81, 128.03, 127.54, 126.96, 126.78, 126.53, 126.20, 125.99, 125.51, 124.60, 123.75, 122.53, 69.27, 69.36, 55.35, 50.25, 39.79, 32.38, 31.85, 31.76, 30.69, 29.40, 29.27, 27.02, 26.56, 22.75, 22.69, 14.22, 14.16. HRMS (FAB+) calcd for $C_{57}H_{65}N_5O_5S_4$: 1027.3869.; calcd for $C_{57}H_{66}N_5O_5S_4$: 1028.3902, found 1028.3947 $[M]^+$, 1029.3977 $[M+H]^+$

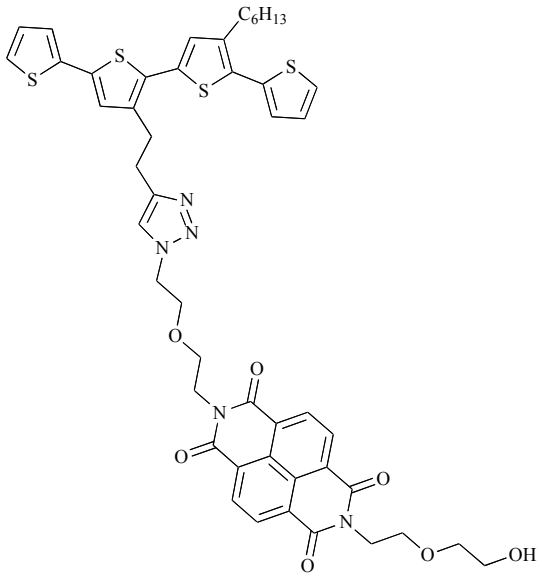

4

Compound (4): The crude alkyne **7** and azide **10d** (126 mg, 0.279 mmol) were dispersed in THF/H_2O (5 mL each). To the stirred mixture was added $CuSO_4 \cdot 5H_2O$ (34 mg, 0.136 mmol) and sodium ascorbate (39 mg, 0.196 mmol). The heterogeneous mixture was stirred for 48 hours at rt and then partitioned between EtOAc and water. The layers were separated and the aqueous layer was extracted with EtOAc (2x). The combined organics were washed with water (2x) and sat'd NaCl solution (1x), dried over

Na_2SO_4, filtered, and concentrated *in vacuo*. Purification of the residue by silica gel chromatography (2:8 acetone/Ethyl acetate) yielded **4** (118 mg, 40%) as a green solid. ^{1}H NMR (400 MHz, $CDCl_3$) δ 8.65 (m, 4H), 7.38 (s, 1H), 7.28, (dd, *J* = 5.1, 1.2, 1H), 7.20 (d, *J* = 5.0, 1H), 7.13 (dd, *J* = 3.6, 1.2, 1H), 7.07 (dd, *J* = 5.0, 3.6, 1H), 7.03 (dd, *J* = 5.1, 3.6, 1H), 7.00 (dd, J = 5.0, 3.6, 1H), 6.89 (s, 1H), 6.83 (S, 1H), 4.46 (t, *J* = 4.92, 2H), 4.34-4.42 (m, 4H), 3.79-3.86 (m, 4H), 3.75 (t, *J* = 5.0, 2H), 3.59-3.3.71 (m, 4H), 2.89 (m, 4H), 2.70 (T, J = 7.7, 2H), 2.24 (m, 1H), 1.63 (m, 2H), 1.37 (t, J = 6.4, 2H), 1.20-1.34 (m, 4H), 0.87 (t, *J* = 6.2, 3H). ^{13}C NMR (75 MHz, $CDCl_3$) δ 163.04, 162.95, 146.94, 140.15, 138.29, 137.06, 135.75, 135.27, 133.35, 131.16, 130.75, 130.32, 128.08, 127.61, 126.86, 126.64, 126.50, 126.34, 126.00, 125.58, 124.71, 123.83, 122.34, 72.37, 69.29, 68.42, 68.30, 61.96, 50.31, 42.18, 40.07, 39.95, 31.78, 30.71, 29.44, 29.21, 26.46, 22.78, 14.25 HRMS (FAB+) calcd for $C_{48}H_{47}N_5O_7S_4$ 933.2358; calcd for $C_{48}H_{48}N_5O_7S_4$ 934.2392 found 934.2437 $[M]^{+\cdot}$; 935.2466 $[M+H]^+$

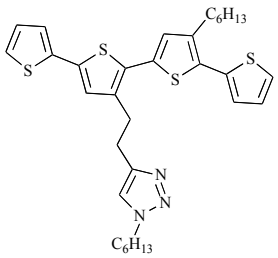

14

Compound (18): The crude alkyne **14** and hexylazide (165 mg, 1.27 mmol) synthesized by a previously reported procedure[1] were dispersed in THF/H_2O (5 mL each). To the stirred mixture was added $CuSO_4 \cdot 5H_2O$ (23 mg, 0.092 mmol) and sodium ascorbate (63.2 mg, 0.353 mmol). The heterogeneous mixture was stirred for 24 hours at rt and then partitioned between EtOAc and water. The layers were separated and the aqueous layer was extracted with EtOAc (2x). The combined organics were washed with

water (2x) and sat'd NaCl solution (1x), dried over Na_2SO_4, filtered, and concentrated *in vacuo*. Purification of the residue by silica gel chromatography (45:55 Ethyl Acetate/Hexane) yielded **4** (532 mg, 87%) as a yellow solid. ^{1}H NMR (400 MHz, $CDCl_3$) 7.31 (dd, J = 5.22, 1.1, 1H), 7.20, (dd, *J* = 5.2, 1.1, 1H), 7.14 (dd, *J* = 3.7, 1.1, 1H), 7.12 (m, 2H), 7.06 (dd, *J* = 5.2, 3.6, 1H), 7.01 (dd, *J* = 5.2, 3.6, 1H), 6.96 (s, 1H), 6.91 (s, 1H), 4.26 (t, *J* = 7.2, 2H), 3.13 (m, 4H), 2.73 (t, J = 7.7, 2H), 1.81 (p, J = 7.2, 2H), 1.64 (m, 2H), 1.34-1.42 (m, 2H), 1.27-1.34 (m, 4H), 1.21-1.27 (m, 4H), 0.81-0.92 (m, 6H). ^{13}C NMR (75 MHz, $CDCl_3$) δ 146.88, 140.21, 138.53, 137.13, 135.80, 135.37, 133.48, 130.86, 130.40, 128.83, 128.04, 127.60, 126.60, 126.09, 125.59, 124.64, 123.78, 120.97, 50.34, 31.78, 31.28, 30.74, 30.47, 29.39, 29.26, 26.62, 26.29, 22.76, 22.52, 14.23, 14.10. HRMS (FAB+) calcd for $C_{32}H_{39}N_3S_4$: 593.2027; calcd for $C_{32}H_{40}N_3S_4$: 594.2060, found 594.2105 [M], 595.2134 [M+H]$^{\cdot}$

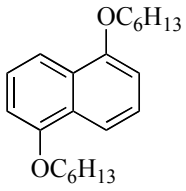

NE

Compound (NE): 1,5-dihydroxynapthalene (3.20 g, 20 mmol), 1-iodohexane (2.95 ml, 40 mmol) and cesium carbonate (6.84 g, 20 mmol) were dispersed in DMF (50 mL). The reaction mixture was stirred for 48 hours at 80 ^{O}C and then DMF is rotovaped. The resulting solid was dissolved in small amount of ethyl acetate and purified by silica gel chromatography (1:99 = EtOAc: Hexane) to obtain NE (4.92 g, 75%) as a green solid.

^{1}H NMR (400 MHz, $CDCl_3$) δ 7.84 (d, *J* = 8.4, 2H), 7.34 (t, *J* = 8.0, 2H), 6.82 (d, *J* = 7.6, 2H), 4.14 (t, *J* = 6.5, 4H), 1.94 (m, 4H), 1.59 (m, 4H), 1.4 (m, 8H), 0.94 (t, *J* = 7.0, 6H).

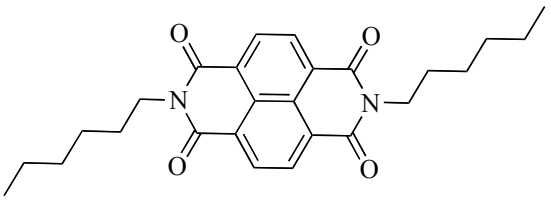

Hc-NDI-Hc

Compound (Hc-NDI-Hc): To a stirred solution of naphthalene-1,4,5,8-tetracarboxylic dianhydride (**15**, 1.61 g, 6.00 mmol) in ethanol (60 mL), was added, and 1-hexylamine (1.61 mL, 12.20 mmol). The reaction mixture was refluxed for 48 hours and then cooled to rt. The solvent was removed *in vacuo* and the residue was dispersed in ice cold EtOH. The pink insoluble material was filtered off, rinsed with cold EtOH, and purified by silica gel chromatography (2:8 Acetone/dichloromethane) to afford **Hc-NDI-Hc** (2.34 g, 90%) as a pink solid. ^{1}H NMR (400 MHz, $CDCl_3$) δ 8.76 (s, 4H), 4.19 (t, *J* = 7.66, 4H), 1.74 (m, 4H), 1.43 (m, 4H), 1.34 (m, 8H), 0.89 (t, *J* = 7.18, 6H).

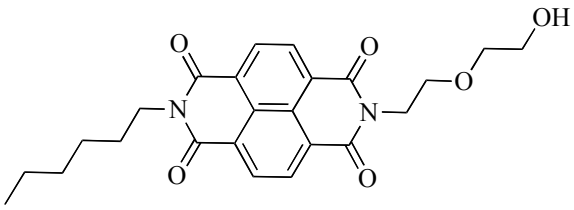

Hc-NDI-OH

Compound (Hc-NDI-OH): The synthesis of Hc-NDI-OH has been described previously in our group's alumni Dr.Travis Benanti's thesis.

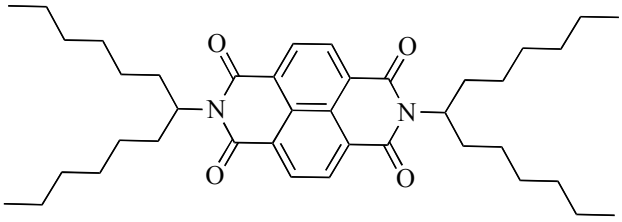

br-NDI-br

Compound (br-NDI-br): The synthesis of br-NDI-br was according to the previous reported procedure. A mixture of naphthalene-1,4,5,8-tetracarboxylic dianhydride (**15**, 0.72 g, 2.68 mmol), n-hexylheptylamine (1.35 g, 6.80 mmol), and imidazole (4.34 g, 63.78 mmol) was vaccumed and argon purged. The reaction mixture was heated and stirred at 130 ^{O}C for 3 h. After cooling to rt, 100 mL of ethanol and 300 mL of 2M HCl were added and stirred for 12 h which resulted in formation of red precipitate that flouts on the solution. This is filtered off and washed several times with water and dried under vaccum for 1 h. The resulting solid was dissolved in chloroform and the solvent is rotovaped to obtain pink red solid that is purified using silica gel chromatography (1:9 = Ethyl acetate: Hexane) to obtain desired product br-NDI-br as pinkish red color solid (1.52 g, 90%) ^{1}H NMR (400 MHz, $CDCl_3$) δ 8.72 (m, 4H), 5.15 (m, 2H), 2.20 (m, 4H), 1.84 (m, 4H), 1.29 (m, 12H), 1.20 (m, 20H), 0.81 (t, *J* = 6.69, 12H).

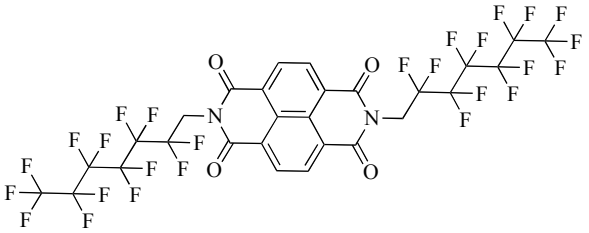

Fc-NDI-Fc

Compound (Fc-NDI-Fc): To a stirred solution of naphthalene-1,4,5,8-tetracarboxylic dianhydride (**15**, 0.26 g, 1.00 mmol) in ethanol (60 mL), HCl salt of perfluoroheptylamine (0.96 g, 2.50 mmol) (just amine will also work) and sodium bicarbonate (0.23 g, 2.75 mmol) was added. The reaction mixture was refluxed for 48 hours and then cooled to rt. The solvent was removed *in vacuo* and the resulting solid was purified by silica gel chromatography (Dichloromethane) to afford **Fc-NDI-Fc** (0.65 g, 70%) as a white solid. ^{1}H NMR (400 MHz, $CDCl_3$) δ 8.87 (s, 4H), 5.04 (t, J = 15.72, 4H).

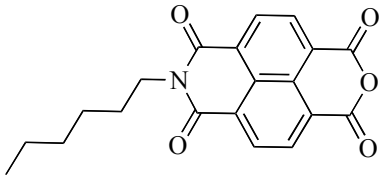

Monohexyl-napthaleneimide

Compound (Monohexyl-napthaleneimide): To a stirred solution of naphthalene-1,4,5,8-tetracarboxylic dianhydride (**15**, 3.0 g, 11.18 mmol) in water-ethanol mixture (20 mL of each), n-hexylamine (4.74 mL, 35.88 mmol) was added. The reaction mixture was stirred at 50 ^{O}C for 24 h and then cooled to rt to obtain white-pink precipitate. A little amount of HCl was added to this to adjust the pH of the reaction mixture to 1, and the resultant mixture was stirred at rt for 1h to obtain precipitate. The

precipitate was filtered off and refluxed in acetic acid (50 mL) for 1 h. The resulting mixture was cooled to rt, and extracted with DCM. The organic layer is rotovaped and dispersed in ethanol to obtain a suspension that is filtered off and washed with ethanol, hexane and a little amount of ether to obtain the desired product with little amount of dihexylnaphthalenedimide (1:12 = dihexylnapthalenediimide: monohexyl-naphthaleneimide). ^{1}H NMR (400 MHz, $CDCl_3$) δ 8.82 (m, 4H), 8.77 (s, 0.17H), 4.21 (t, J = 7.4, 2H), 1.75 (m, 2H), 1.44 (m, 2H), 1.36 (m, 4H), 0.91 (t, J = 6.9, 3H).

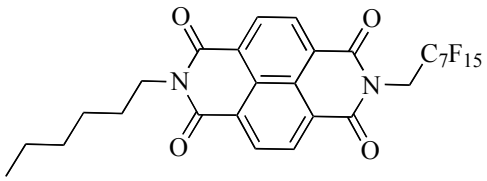

Hc-NDI-Fc

Compound (Hc-NDI-Fc): To a stirred solution of monohexyl-naphthaleneimide (0.29 g, 0.83 mmol) in DMF (20 mL), petadecafluorooctylamine (0.32 g, 0.82 mmol), and Imidazole (0.03 g, 0.41 mmol) are added. The reaction mixture was refluxed for 24 hours and then cooled to rt. The solvent was removed *in vacuo* and acetone is added to the mixture. The resulting precipitate was filtered off and discarded. The filtrate is rotovaped and purified by silica gel chromatography (Dichloromethane) to obtain the desired product Hc-ND-Fc (0.48 g, 80 %) as a white color powder. ^{1}H NMR (400 MHz, $CDCl_3$) δ 8.81 (m, 4H), 5.03 (t, J = 15.6, 2H), 4.20 (t, J = 7.6, 2H), 1.75 (m, 2H), 1.44 (m, 2H), 1.34 (m, 4H). 0.9 (t, , J = 7.02, 3H).

A.3 Absorption Spectra

The absorption spectra of mixture of Hc-NDI-Hc and NE in dichloromethane are shown in Figure A.1.

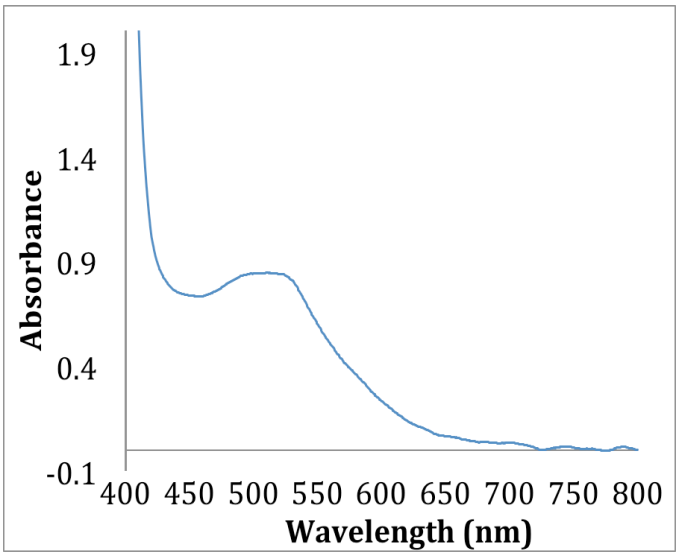

Figure A.1: The absorption spectra of mixture of Hc-NDI-Hc and NE in dichloromethane (Concentration = 0.1 M).

BIBLIOGRAPHY

1. Benanti, T. L.; Saejueng, P.; Venkataraman, D., "Segregated assemblies in bridged electron-rich and electron-poor pi-conjugated moieties," *Chemical Communications* **2007**, 692-694.

2. Lokey, R. S.; Iverson, B. L., "Synthetic molecules that fold into a pleated secondary structure in solution," *Nature* **1995**, *375*, 303-305.

3. Alvey, P. M.; Reczek, J. J.; Lynch, V.; Iverson, B. L., "A Systematic Study of Thermochromic Aromatic Donor-Acceptor Materials," *Journal of Organic Chemistry* **2010**, *75*, 7682-7690.

4. Reczek, J. J.; Iverson, B. L., "Using aromatic donor acceptor interactions to affect macromolecular assembly," *Macromolecules* **2006**, *39*, 5601-5603.

5. Koshkakaryan, G.; Klivansky, L. M.; Cao, D.; Snauko, M.; Teat, S. J.; Struppe, J. O.; Liu, Y., "Alternative Donor-Acceptor Stacks from Crown Ethers and Naphthalene Diimide Derivatives: Rapid, Selective Formation from Solution and Solid State Grinding," *Journal of the American Chemical Society* **2009**, *131*, 2078-2079.

6. Gabriel, G. J.; Iverson, B. L., "Aromatic oligomers that form hetero duplexes in aqueous solution," *Journal of the American Chemical Society* **2002**, *124*, 15174-15175.

7. Bradford, V. J.; Iverson, B. L., "Amyloid-like behavior in abiotic, amphiphilic foldamers," *Journal of the American Chemical Society* **2008**, *130*, 1517-1524.

8. Becker, J. Y.; Bernstein, J.; Bittner, S.; Levi, N.; Shaik, S. S., "Strategic design of organic conductors - structure of a prototypical molecule," *Journal of the American Chemical Society* **1983**, *105*, 4468-4469.

9. Torrance, J. B.; Mayerle, J. J.; Lee, V. Y.; Bechgaard, K., "New class of highly conducting organic materials - charge-transfer salts of the tetrathiafulvalenes with the tetrahalo-para-benzoquinones," *Journal of the American Chemical Society* **1979**, *101*, 4747-4748.

10. Thompson, B. C.; Frechet, J. M. J., "Organic photovoltaics - Polymer-fullerene composite solar cells," *Angew. Chem.-Int. Edit.* **2008**, *47*, 58-77.

11. Venkataraman, D.; Yurt, S.; Venkatraman, B. H.; Gavvalapalli, N., "Role of Molecular Architecture in Organic Photovoltaic Cells," *Journal of Physical Chemistry Letters* **2010**, *1*, 947-958.

12. Schmidt-Mende, L.; Fechtenkotter, A.; Mullen, K.; Moons, E.; Friend, R. H.; MacKenzie, J. D., "Self-organized discotic liquid crystals for high-efficiency organic photovoltaics," *Science* **2001**, *293*, 1119-1122.

13. Molla, M. R.; Das, A.; Ghosh, S., "Self-Sorted Assembly in a Mixture of Donor and Acceptor Chromophores," *Chemistry-a European Journal* **2010**, *16*, 10084-10093.

14. Jonkheijm, P.; Stutzmann, N.; Chen, Z. J.; de Leeuw, D. M.; Meijer, E. W.; Schenning, A.; Wurthner, F., "Control of ambipolar thin film architectures by co-self-assembling oligo(p-phenylenevinylene)s and perylene bisimides," *Journal of the American Chemical Society* **2006**, *128*, 9535-9540.

15. Wurthner, F.; Chen, Z. J.; Hoeben, F. J. M.; Osswald, P.; You, C. C.; Jonkheijm, P.; von Herrikhuyzen, J.; Schenning, A.; van der Schoot, P.; Meijer, E. W.; Beckers, E. H. A.; Meskers, S. C. J.; Janssen, R. A. J., "Supramolecular p-n-heterojunctions by co-self-organization of oligo(p-phenylene vinylene) and perylene bisimide dyes," *Journal of the American Chemical Society* **2004**, *126*, 10611-10618.

16. Li, W. S.; Yamamoto, Y.; Fukushima, T.; Saeki, A.; Seki, S.; Tagawa, S.; Masunaga, H.; Sasaki, S.; Takata, M.; Aida, T., "Amphiphilic molecular design as a rational strategy for tailoring bicontinuous electron donor and acceptor arrays: Photoconductive liquid crystalline oligothiophene-C-60 dyads," *Journal of the American Chemical Society* **2008**, *130*, 8886-8887.

17. Li, W. S.; Saeki, A.; Yamamoto, Y.; Fukushima, T.; Seki, S.; Ishii, N.; Kato, K.; Takata, M.; Aida, T., "Use of Side-Chain Incompatibility for Tailoring Long-Range p/n Heterojunctions: Photoconductive Nanofibers Formed by Self-Assembly of an Amphiphilic Donor-Acceptor Dyad Consisting of Oligothiophene and Perylenediimide," *Chemistry-an Asian Journal* **2010**, *5*, 1566-1572.

18. De Luca, G.; Liscio, A.; Melucci, M.; Schnitzler, T.; Pisula, W.; Clark, C. G.; Scolaro, L. M.; Palermo, V.; Mullen, K.; Samori, P., "Phase separation and affinity between a fluorinated perylene diimide dye and an alkyl-substituted hexa-peri-hexabenzocoronene," *Journal of Materials Chemistry* **2010**, *20*, 71-82.

19. Kohlmeier, A.; Nordsieck, A.; Janietz, D., "Tailoring Thermotropic Mesophase Morphologies by Molecular Recognition and Fluorophobic Effect," *Chemistry of Materials* **2009**, *21*, 491-498.

20. Dunitz, J. D., "Organic fluorine: Odd man out," *Chembiochem* **2004**, *5*, 614-621.

21. Gabriel, G. J.; Sorey, S.; Iverson, B. L., "Altering the folding patterns of naphthyl trimers," *Journal of the American Chemical Society* **2005**, *127*, 2637-2640.

22. Horiuchi, S.; Yamochi, H.; Saito, G.; Sakaguchi, K.; Kusunoki, M., "Nature and origin of stable metallic state in organic charge-transfer complexes of bis(ethylenedioxy)tetrathiafulvalene," *Journal of the American Chemical Society* **1996**, *118*, 8604-8622.

23. Lin, F.; Huang, X. M.; Qu, S. C.; Fang, Z. Y.; Huang, S.; Song, W. T.; Zhu, X.; Liu, Z. F., "Characteristics of charge density waves on the surfaces of quasi-one-dimensional charge-transfer complex layered organic crystals," *Physical Review B* **2011**, *83*.

24. Percec, V.; Glodde, M.; Bera, T. K.; Miura, Y.; Shiyanovskaya, I.; Singer, K. D.; Balagurusamy, V. S. K.; Heiney, P. A.; Schnell, I.; Rapp, A.; Spiess, H. W.; Hudson, S. D.; Duan, H., "Self-organization of supramolecular helical dendrimers into complex electronic materials," *Nature* **2002**, *419*, 384-387.

25. Scott, J. C.; Bozano, L. D., "Nonvolatile memory elements based on organic materials," *Adv. Mater.* **2007**, *19*, 1452-1463.

26. Zych, A. J.; Iverson, B. L., "Conformational modularity of an abiotic secondary-structure motif in aqueous solution," *Helv. Chim. Acta* **2002**, *85*, 3294-3300.

27. Cubberley, M. S.; Iverson, B. L., "H-1 NMR investigation of solvent effects in aromatic stacking interactions," *Journal of the American Chemical Society* **2001**, *123*, 7560-7563.

28. Horiuchi, S.; Tokura, Y., "Organic ferroelectrics," *Nature Materials* **2008**, *7*, 357-366.

29. Reczek, J. J.; Villazor, K. R.; Lynch, V.; Swager, T. M.; Iverson, B. L., "Tunable columnar mesophases utilizing C-2 symmetric aromatic donor-acceptor complexes," *Journal of the American Chemical Society* **2006**, *128*, 7995-8002.

30. Hoeben, F. J. M.; Jonkheijm, P.; Meijer, E. W.; Schenning, A., "About supramolecular assemblies of pi-conjugated systems," *Chemical Reviews* **2005**, *105*, 1491-1546.

31. Syamakumari, A.; Schenning, A.; Meijer, E. W., "Synthesis, optical properties, and aggregation behavior of a triad system based on perylene and oligo(p-phenylene vinylene) units," *Chemistry-a European Journal* **2002**, *8*, 3353-3361.

32. Dunitz, J. D.; Gavezzotti, A.; Schweizer, W. B., "Molecular shape and intermolecular liaison: Hydrocarbons and fluorocarbons," *Helv. Chim. Acta* **2003**, *86*, 4073-4092.

33. Che, Y. K.; Datar, A.; Balakrishnan, K.; Zang, L., "Ultralong nanobelts self-assembled from an asymmetric perylene tetracarboxylic diimide," *Journal of the American Chemical Society* **2007**, *129*, 7234-7235.

34. Greenfield, S. R.; Svec, W. A.; Gosztola, D.; Wasielewski, M. R., "Multistep photochemical charge separation in rod-like molecules based on aromatic imides and diimides," *Journal of the American Chemical Society* **1996**, *118*, 6767-6777.

35. Gunes, S.; Neugebauer, H.; Sariciftci, N. S., "Conjugated polymer-based organic solar cells," *Chem. Rev.* **2007**, *107*, 1324-1338.

36. Hoppe, H.; Sariciftci, N. S., "Morphology of polymer/fullerene bulk heterojunction solar cells," *J. Mater. Chem.* **2006**, *16*, 45-61.

37. Griffini, G.; Douglas, J. D.; Piliego, C.; Holcombe, T. W.; Turri, S.; Frechet, J. M. J.; Mynar, J. L., "Long-Term Thermal Stability of High-Efficiency Polymer Solar Cells Based on Photocrosslinkable Donor-Acceptor Conjugated Polymers," *Adv. Mater.* **2011**, *23*, 1660-1664.

38. Guldi, D. M., "Fullerene-porphyrin architectures; photosynthetic antenna and reaction center models," *Chem. Soc. Rev.* **2002**, *31*, 22-36.

39. Collin, J. P.; Guillerez, S.; Sauvage, J. P.; Barigelletti, F.; Decola, L.; Flamigni, L.; Balzani, V., "Photoinduced processes in dyads and triads containing a ruthenium(II) bis(terpyridine) photosensitizer covalently linked to electron-donor and acceptor groups," *Inorg. Chem.* **1991**, *30*, 4230-4238.

40. Imahori, H.; Guldi, D. M.; Tamaki, K.; Yoshida, Y.; Luo, C. P.; Sakata, Y.; Fukuzumi, S., "Charge separation in a novel artificial photosynthetic reaction center lives 380 ms," *J. Am. Chem. Soc.* **2001**, *123*, 6617-6628.

41. Imahori, H.; Tamaki, K.; Guldi, D. M.; Luo, C. P.; Fujitsuka, M.; Ito, O.; Sakata, Y.; Fukuzumi, S., "Modulating charge separation and charge recombination dynamics in porphyrin fullerene linked dyads and triads: Marcus-normal versus inverted region," *J. Am. Chem. Soc.* **2001**, *123*, 2607-2617.

42. Kuciauskas, D.; Lin, S.; Seely, G. R.; Moore, A. L.; Moore, T. A.; Gust, D.; Drovetskaya, T.; Reed, C. A.; Boyd, P. D. W., "Energy and photoinduced electron transfer in porphyrin-fullerene dyads," *J. Phys. Chem.* **1996**, *100*, 15926-15932.

43. Gawrys, P.; Boudinet, D.; Zagorska, M.; Djurado, D.; Verilhac, J. M.; Horowitz, G.; Pecaud, J.; Pouget, S.; Pron, A., "Solution processible naphthalene and perylene bisimides: Synthesis, electrochemical characterization and application to organic field effect transistors (OFETs) fabrication," *Synth. Met.* **2009**, *159*, 1478-1485.

44. Kruger, H.; Janietz, S.; Sainova, D.; Dobreva, D.; Koch, N.; Vollmer, A., "Hybrid supramolecular naphthalene diimide-thiophene structures and their application in polymer electronics," *Adv. Funct. Mater.* **2007**, *17*, 3715-3723.

45. Lee, Y. L.; Hsu, H. L.; Chen, S. Y.; Yew, T. R., "Solution-processed naphthalene diimide derivatives as conductor materials," *Journal of Physical Chemistry C* **2008**, *112*, 1694-1699.

46. See, K. C.; Landis, C.; Sarjeant, A.; Katz, H. E., "Easily synthesized naphthalene tetracarboxylic diimide semiconductors with high electron mobility in air," *Chem. Mater.* **2008**, *20*, 3609-3616.

47. Shao, H.; Nguyen, T.; Romano, N. C.; Modarelli, D. A.; Parquette, J. R., "Self-Assembly of 1-D n-Type Nanostructures Based on Naphthalene Diimide-Appended Dipeptides," *J. Am. Chem. Soc.* **2009**, *131*, 16374-16376.

48. Shukla, D.; Nelson, S. F.; Freeman, D. C.; Rajeswaran, M.; Ahearn, W. G.; Meyer, D. M.; Carey, J. T., "Thin-Film Morphology Control in Naphthalene-Diimide-Based Semiconductors: High Mobility n-Type Semiconductor for Organic Thin-Film Transistors," *Chem. Mater.* **2008**, *20*, 7486-7491.

49. Singh, T. B.; Erten, S.; Gunes, S.; Zafer, C.; Turkmen, G.; Kuban, B.; Teoman, Y.; Sariciftci, N. S.; Icli, S., "Soluble derivatives of perylene and naphthalene diimide for n-channel organic field-effect transistors," *Org. Electron.* **2006**, *7*, 480-489.

50. Liu, P.; Li, Q.; Huang, M. S.; Pan, W. Z.; Deng, W. J., "High open circuit voltage organic photovoltaic cells based on oligothiophene derivatives," *Appl. Phys. Lett.* **2006**, *89,* 213501-1-213501-3.

51. Sirringhaus, H.; Brown, P. J.; Friend, R. H.; Nielsen, M. M.; Bechgaard, K.; Langeveld-Voss, B. M. W.; Spiering, A. J. H.; Janssen, R. A. J.; Meijer, E. W.; Herwig, P.; de Leeuw, D. M., "Two-dimensional charge transport in self-organized, high-mobility conjugated polymers," *Nature* **1999**, *401*, 685-688.

52. Coakley, K. M.; McGehee, M. D., "Conjugated polymer photovoltaic cells," *Chemistry of Materials* **2004**, *16*, 4533-4542.

53. Kraabel, B.; Lee, C. H.; Mcbranch, D.; Moses, D.; Sariciftci, N. S.; Heeger, A. J., "Ultrafast Photoinduced Electron-Transfer in Conducting Polymer Buckminsterfullerene Composites," *Chem Phys Lett* **1993**, *213*, 389-394.

54. Murakami, M.; Ohkubo, K.; Fukuzumi, S., "Inter- and intramolecular photoinduced electron transfer of flavin derivatives with extremely small reorganization energies," *Chemistry* **2010**, *16*, 7820-32.

55. Sariciftci, N. S.; Smilowitz, L.; Heeger, A. J.; Wudl, F., "Photoinduced Electron-Transfer from a Conducting Polymer to Buckminsterfullerene," *Science* **1992**, *258*, 1474-1476.

56. Vivo, P.; Alekseev, A. S.; Kaunisto, K.; Pekkola, O.; Tolkki, A.; Chukharev, V.; Efimov, A.; Ihalainen, P.; Peltonen, J.; Lemmetyinen, H., "Photoinduced electron transfer in thin films of porphyrin-fullerene dyad and perylenetetracarboxidiimide," *Phys Chem Chem Phys* **2010**, *12*, 12525-12532.

57. Zenkevich, E.; von Borczyskowski, C.; Shulga, A.; Bachilo, S.; Rempel, U.; Willert, A., "Porphyrin self-assembling complexes in thin polymeric films: Stability, spectral properties, and photoinduced electron transfer dynamics.," *Abstr Pap Am Chem S* **2000**, *219*, U529-U529.

58. McDonald, N. A.; Subramani, C.; Caldwell, S. T.; Zainalabdeen, N. Y.; Cooke, G.; Rotello, V. M., "Simultaneous hydrogen bonding and [pi]-stacking interactions between flavin/porphyrin host-guest systems," *Tetrahedron Letters* **2011**, *52*, 2107-2110.

59. Closs, G. L.; Miller, J. R., "Intramolecular long-distance electron-transfer in organic-molecules," *Science* **1988**, *240*, 440-447.

60. Wasielewski, M. R., "Photoinduced electron-transfer in supramolecular systems for artificial photosynthesis," *Chemical Reviews* **1992**, *92*, 435-461.

61. Kulkarni, A. P.; Wu, P. T.; Kwon, T. W.; Jenekhe, S. A., "Phenothiazine-phenylquinoline donor-acceptor molecules: Effects of structural isomerism on charge transfer photophysics and electroluminescence," *Journal of Physical Chemistry B* **2005**, *109*, 19584-19594.

62. Kanato, H.; Takimiya, K.; Otsubo, T.; Aso, Y.; Nakamura, T.; Araki, Y.; Ito, O., "Synthesis and photophysical properties of ferrocene-oligothiophene-fullerene triads," *Journal of Organic Chemistry* **2004**, *69*, 7183-7189.

63. Hayes, R. T.; Wasielewski, M. R.; Gosztola, D., "Ultrafast photoswitched charge transmission through the bridge molecule in a donor-bridge-acceptor system," *J Am Chem Soc* **2000**, *122*, 5563-5567.

64. Tzabari, L.; Tessler, N., "Shockley-Read-Hall recombination in P3HT:PCBM solar cells as observed under ultralow light intensities," *Journal of Applied Physics* **2011**, *109*.

65. Rauh, D.; Wagenpfahl, A.; Deibel, C.; Dyakonov, V., "Relation of open circuit voltage to charge carrier density in organic bulk heterojunction solar cells," *Applied Physics Letters* **2011**, *98*.

66. Breinlinger, E. C.; Keenan, C. J.; Rotello, V. M., "Modulation of flavin recognition and redox properties through donor atom-pi interactions," *J Am Chem Soc* **1998**, *120*, 8606-8609.

67. Li, G. F.; Glusac, K. D., "The Role of Adenine in Fast Excited-State Deactivation of FAD: a Femtosecond Mid-IR Transient Absorption Study," *Journal of Physical Chemistry B* **2009**, *113*, 9059-9061.

68. Li, G. F.; Glusac, K. D., "Light-triggered proton and electron transfer in flavin cofactors," *Journal of Physical Chemistry A* **2008**, *112*, 4573-4583.

69. Caldwell, S. T.; Farrugia, L. J.; Hewage, S. G.; Kryvokhyzha, N.; Rotello, V. M.; Cooke, G., "Model systems for flavoenzyme activity: an investigation of the role functionality attached to the C(7) position of the flavin unit has on redox and molecular recognition properties," *Chem Commun* **2009**, 1350-1352.

70. Benanti, T. L., "Strategies for Directing Aromatic Packing," *Thesis* **2008**.

71. Cremer, J.; Mena-Osteritz, E. M.; Pschierer, N. G.; Mullen, K.; Bauerle, P., "Dye-functionalized head-to-tail coupled oligo(3-hexylthiophenes) - perylene-oligothiophene dyads for photovoltaic applications," *Org. Biomol. Chem.* **2005**, *3*, 985-995.